AN ABSTRACT OF THE THESIS OF

Ki-Kwang Lee for the degree of Doctor of Philosophy in Human Performance presented on November 19, 1998, Title: The Effect of Running Speed and Turning Direction on Lower Extremity Joint Moment.

Abstract approved: Redacted for Privacy

Gerald A. Smith

Fast medio-lateral movements, frequent in a number of sports activities, are associated with lower extremity injuries. These injuries may occur as a result of excessive musculoskeletal stresses on the joints and their associate structures. The purpose of this study was to investigate the effect of running speed and turning movement on the three-dimensional moments at the ankle, knee, and hip joints. Data were collected using video cameras and force plate. Eight male recreational basketball players were tested during slow (1.5 m/s), moderate (3.0 m/s), and fast running (4.5 m/s) and when cutting to the right or left (+60, +30, 0, -30, and -60°). The inverse dynamics approach was used to integrate the body segment parameter, kinematic and force plate data, and to solve the resultant joint moments. At the ankle joint, inversion/eversion, dorsi/plantar flexion, and internal/external rotation moments of the ankle joint increased with running speed ($p < .05$). At the knee joint, flexion/extension and abduction/adduction moments increased with running speed except flexion moment that decreased with running speed ($p < .05$). At the hip joint, internal/external rotation, flexion/extension, and abduction/adduction moments increased with running

speed ($p < .05$). In medial cutting movements, greater abduction moments of the ankle, adduction moments of the knee and external rotation and adduction of the hip were found ($p < .05$). In lateral cutting movements, greater inversion and adduction moments of the ankle, abduction moments of the knee and hip were found ($p < .05$). These findings reinforce the intuitive notion that fast medio-lateral turning movements produce substantially greater musculoskeletal loading on the joint structures than does straight running and consequently have greater potential for inducing lower extremity injuries such as ankle sprain or anterior cruciate ligament injury.

The Effect of Running Speed and Turning Direction on Lower Extremity Joint Moment

by

Ki-Kwang Lee

A THESIS

submitted to

Oregon State University

in partial fulfillment of
the requirements for the
degree of

Doctor of Philosophy

Completed November 19, 1998
Commencement June 1999

Doctor of Philosophy thesis of Ki-Kwang Lee presented on November 19, 1998

APPROVED:

Redacted for Privacy

Major Professor, representing Human Performance

Redacted for Privacy

Chair of Department of Exercise and Sport Science

Redacted for Privacy

Dean of Graduate School

I understand that my thesis will become part of the permanent collection of Oregon State University libraries. My signature below authorizes release of my thesis to any reader upon request.

Redacted for Privacy

Ki-Kwang Lee, Author

ACKNOWLEDGMENTS

First of all, I would like to thank my advisor, Dr. Gerald Smith, for his continued guidance, assistance, encouragement, and constructive advice during my entire doctoral program. I would also like to thank the members of my committee, Drs. Jeff McCubbin, Rod Harter, Simon Johnson, and Katharine Hunter-Zaworski for their critiques and guidance during this project.

I would also express my appreciation to Dr. Timothy White, dean of College of Health and Human Performance, for his understanding and encouragement to this study, to Dr. Terry Wood for advising on research design and statistical analysis.

All fellow graduate students and current as well as former members of the Biomechanics Laboratory have helped me throughout the course of this project. I would like to thank to Darren Dutto for his help with pilot tests.

I would like to say a special thanks to Drs. In-Sik Shin and Chul-Soo Jung and all graduate students of the Biomechanics Laboratory in Seoul National University for assistance, discussion, and great fun during data collection and analysis.

Last, I would like to express my appreciation and gratitude to my family. My lovely wife, Young-Shin Park, has supported me throughout my entire study. I am extremely happy to get two sons, Justin and Kevin, during my graduate study. I love both of you very much. I wish to thank to my parents and parents-in-law for their continued support and encouragement throughout past years.

TABLE OF CONTENTS

Page

INTRODUCTION 1

METHODS 5

Subjects and task 5

Experimental protocol and data collection 5

Data processing and calibration procedure 11

Statistical analysis 22

RESULTS 23

Ankle moments 24

Knee moments 30

Hip moments 42

DISCUSSION 53

SUMMARY 59

BIBLIOGRAPHY 63

APPENDICES 69

Appendix A Review of literature 70

Appendix B Charateristics of subjects 90

Appendix C Normalized maximum moments data 91

Appendix D Absolute maximum moments data 97

LIST OF FIGURES

Figure **Page**

1. Skin markers and anatomical landmark calibration 8
2. Experimental set-up 10
3. Data analysis 12
4. Anatomical frame of the pelvis, thigh, shank, and foot 14
5. The three Euler angles 18
6. Ensembled-average inversion/eversion moment of the ankle during stance phase of cutting motions. Moments are normalized to body weight (N) and right leg length (m) and expressed as a percentage 25
7. Running speed by turning direction interaction for ankle inversion moment 27
8. Ensembled-average dorsi/plantar flexion moment of the ankle during stance phase of cutting motions. Moments are normalized to body weight (N) and right leg length (m) and expressed as a percentage 28
9. Ensembled-average abduction/adduction moment of the ankle during stance phase of cutting motions. Moments are normalized to body weight (N) and right leg length (m) and expressed as a percentage 31
10. Running speed by turning direction interaction for ankle abduction moment 33
11. Running speed by turning direction interaction for ankle adduction moment 33
12. Ensembled-average internal/external rotation moment of the knee during stance phase of cutting motions. Moments are normalized to body weight (N) and right leg length (m) and expressed as a percentage 35

LIST OF FIGURES (Continued)

Figure **Page**

13. Ensembled-average flexion/extension moment of the knee during stance phase of cutting motions. Moments are normalized to body weight (N) and right leg length (m) and expressed as a percentage.....37

14. Running speed by turning direction interaction for knee extension moment 39

15. Ensembled-average abduction/adduction moment of the knee during stance phase of cutting motions. Moments are normalized to body weight (N) and right leg length (m) and expressed as a percentage.....40

16. Running speed by turning direction interaction for knee abduction moment 43

17. Running speed by turning direction interaction for knee adduction moment 43

18. Ensembled-average internal/external rotation moment of the hip during stance phase of cutting motions. Moments are normalized to body weight (N) and right leg length (m) and expressed as a percentage.....44

19. Running speed by turning direction interaction for hip internal rotation moment.....47

20. Running speed by turning direction interaction for hip external rotation moment.....47

21. Ensembled-average flexion/extension moment of the hip during stance phase of cutting motions. Moments are normalized to body weight (N) and right leg length (m) and expressed as a percentage.....48

LIST OF FIGURES (Continued)

Figure **Page**

22. Ensembled-average abduction/adduction moment of the hip during stance phase of cutting motions. Moments are normalized to body weight (N) and right leg length (m) and expressed as a percentage.....50

23. Running speed by turning direction interaction for hip adduction moment 52

LIST OF TABLES

Table **Page**

1. Anatomical landmarks 7
2. Inversion/eversion moment of the ankle 26
3. Dorsi/plantar flexion moment of the ankle 29
4. Abduction/adduction moment of the ankle 32
5. Internal/external rotation moment of the knee 36
6. Flexion/extension moment of the knee 38
7. Abduction/adduction moment of the knee 41
8. Internal/external rotation moment of the hip 45
9. Flexion/extension moment of the hip 49
10. Abduction/adduction moment of the hip 51

THE EFFECT OF RUNNING SPEED AND TURNING DIRECTION ON LOWER EXTREMITY JOINT MOMENTS

INTRODUCTION

During many sports a player is moving in different directions: forward, backward, to the left or right sides. Fast medio-lateral movements, frequent in a number of sports activities, such as basketball, volleyball, tennis, soccer, football, and baseball, are associated with lower extremity injuries. These injuries may occur as a result of excessive medio-lateral movement at the ankle, knee, and hip joint outside the normal ranges of motion. Several researchers (Luthi, Frederick, Hawes, & Nigg, 1986; Simpson, Shwokis, Alduwaisan, & Reeves, 1992; Stacoff, Steger, Stussi, & Reinschmidt, 1996) have focused on investigating the rear foot angle which is the medio-lateral range of motion of the shank relative the foot. They suggested that excessive movements have to be controlled and reduced to decrease the risk of injury; in other words, joint stability has to be provided.

To turn in a certain direction during running, moments must be generated to rotate the body. These moments are generated by the interaction between feet and ground during pushing on the ground and attempting to move in the desired direction. It is obvious that muscle contraction and movement of the segments play an important role during turning direction. Therefore, the joint moments, especially in the lower extremity, will be representative of the kinematic characteristics of the interaction

between the human body and environment while changing direction during running. Furthermore, during fast and sharp turning movements, high loads may act on the joint system of the lower extremity and result in pain and injuries at the joints and their associated structures. Winter (1983) has suggested that joint moments are useful indicators of the amount of physical stress placed on the musculoskeletal system. Although joint moments are used as a representation of the musculoskeletal stresses to the lower extremity and the biomechanical characteristics of changing direction during running, the effects of turning movement characteristics, such as running speed and turning direction, on moments acting on a joint, are not well known.

The resultant joint loads of a body during locomotion are calculated from the kinematics of the body, segment mass and moment of inertia and the ground reaction loads upon the feet. These loads are the sum of all structures spanning the joint. The loads cannot be directly broken into the specific forces in or on the capsule, ligaments, muscles, and articular contact surfaces. Various methods have been proposed for this decomposition process (Brand, Pederson, & Friederson, 1986; Crowninsheild & Brand, 1981; Herzog & Binding, 1993; Smith, 1975; White, Yack, & Winter, 1989), but no approach has proven to represent the true physical situation. Therefore inverse dynamics may be the only appropriate method to indirectly study joint moments during turning movement.

Like all measurements which involve human movement, joint moments are subject to a variety of sources of error. To solve the unknown joint moments in inverse dynamics problem, the parameters which must be measured or estimated include the segmental anthropometry (mass and moment of inertia), the accelerations, the lever

arms and the ground reaction forces. While the ground reaction forces make a significant contribution to the joint moments, they are also the most reliable and accurate. Segment anthropometry is notorious for its inaccuracy, but it does not make major contributions to the joint moments. The accelerations are very sensitive to marker positions during movement. Random errors are caused by the digitization of marker positions of segments. These random errors are strongly amplified by the double differentiation of position data in order to obtain segment accelerations. As a result, the noise in calculated joint loads, especially in horizontal directions may be several times as high as the actual loads. The lever arms are also very sensitive to the biomechanical model chosen to estimate joint center and segment center of mass. In the joint moment calculation, lever arms are the multipliers of ground reaction and joint forces, and so they have an important impact on the accuracy of the joint moment values. To minimize these measurement errors, three skin markers attached on each segment were used to record the movements of the body segments for estimation of the three-dimensional kinematics of segments and joint centers. The use of skin markers offers an optimal visibility and a reduction of systematic as well as random errors (Angeloni, Cappozo, Canati, & Leardini, 1993).

The purpose of this study was to investigate the effect of turning movement on the resultant joint moments of the lower extremity. More specifically, the resultant joint moments, assumed to be proportional to the musculoskeletal stresses on the joints and their associated structures, were measured and compared for identifying the effect of running speed and directions of turning motion. It was hypothesized that the torsional (internal/external rotation and abduction/adduction) moments of ankle, knee,

and hip joint would increase during turning movement with faster running speed. The results from this study may provide not only useful information of injury mechanisms caused by turning movements, but also accommodation strategies to the varied loading forces during turning movement.

METHODS

Subjects and task

Eight male recreational basketball players between the ages of 20 and to 22 were recruited for this study. Their average height was 181 cm (range, 175-188 cm), average leg length was 91 cm (range, 84-98 cm), and average weight was 710 N (ranges, 617-794 N). The procedures, risks, and benefits were explained to each subject prior to testing.

Each subject was asked to run along a runway at three different speeds (1.5, 3.0, and 4.5 m/s, respectively), and then to cut to the right or left off (+60°, +30°, 0°, -30°, and –60°) of the right foot, while wearing his own basketball shoes. Five trials were recorded at each speed and direction condition for each subject.

Experimental protocol and data collection

Anthropometric measurements proceeded the experimental trials of each subject for the purpose of estimation of segment mass, segment moments of inertia and joint centers (Verstraete, 1992; McConville, Churchill, Kaleps, Clauser, & Cuzzi, 1980; Bell, Pederson, & Brand, 1990; Vaughan, Davis, & O'Conner, 1992). These measurements included body mass, foot length, malleolus height and width, shank length and circumference, thigh length and midthigh circumference, and anterior superior liliac spine width. After anthropometric measurements, a practice session was implemented to familiarize each subject with the runway and procedures. Subjects ran using a self-determined stride length and stride frequency for each speed and direction

condition. At the cutting motion, subjects were required to contact a force plate with the right foot. The practice session concluded once the subject struck the force plate with two successful trials with the speed criterion and direction criterion met.

After the practice session, anatomical landmark calibration was performed (Cappozzo, Catani, Della Croce, & Leardini, 1995). For three-dimensional kinematic analysis, the orientation and position in space of the segment should be described with its own coordinate system. The segment anatomical frame can be defined with at least three anatomical landmarks on each segment. Anatomical landmarks were not often visible to the cameras and some anatomical landmarks were located inside the body. Therefore, skin markers and a local coordinate system defined by those markers (technical frame) were introduced to estimate the three-dimensional position of anatomical landmarks in each sampled instant of time. The position and orientation of the technical frame would be known over time relative to a global coordinate system. With information of position vectors of the anatomical landmarks and skin markers in the global coordinate system during a standing trial, it was possible to estimate the anatomical land mark positions in the global frame during movement. Twelve retro-reflective skin markers were attached to the shoe, shank, thigh, and pelvis. Three markers were glued directly to the lateral aspect of the subject's right shoe. Three markers at the shank were fixed with double-sided tape to the subject's skin. Markers at the thigh and pelvis were fixed to an elastic brace with double-sided tape (Figure 1). Anatomical landmarks in the pelvis, thigh, shank, and foot (Table 1) were determined from skin markers during an anatomical landmark calibration procedure. While subjects assumed a static posture that allowed both the anatomical and the technical

Table 1. Anatomical landmarks

Segment	Anatomical landmarks
Pelvis	ASIS (anterior superior iliac spine)
	SA (Sacrum)
Thigh	FH (center of the femoral head)
	ME (medial epicondyle)
	LE (lateral epicondyle)
Shank	HF (apex of head of the fibula)
	MM (distal apex of the medial malleolus)
	LM (distal apex of the lateral malleolus)
Foot	CA (upper ridge of the calcaneus posterior surface)
	FM (dorsal aspect of first metatarsal head)
	SM (dorsal aspect of second metatarsal head)
	VM (dorsal aspect of fifth metatarsal head)

markers to be seen by two cameras, a short video clip was recorded. The procedure were repeated for each anatomical landmark with the subject assuming different postures in order to make both the anatomical landmarks and skin markers visible to the cameras.

For determination of the location of invisible anatomical landmarks by any camera, a pointer on which two markers were mounted was used. The tip of the pointer was placed on the anatomical landmark so that the markers on the pointer and the relevant skin markers were visible to the cameras. Using known distances between

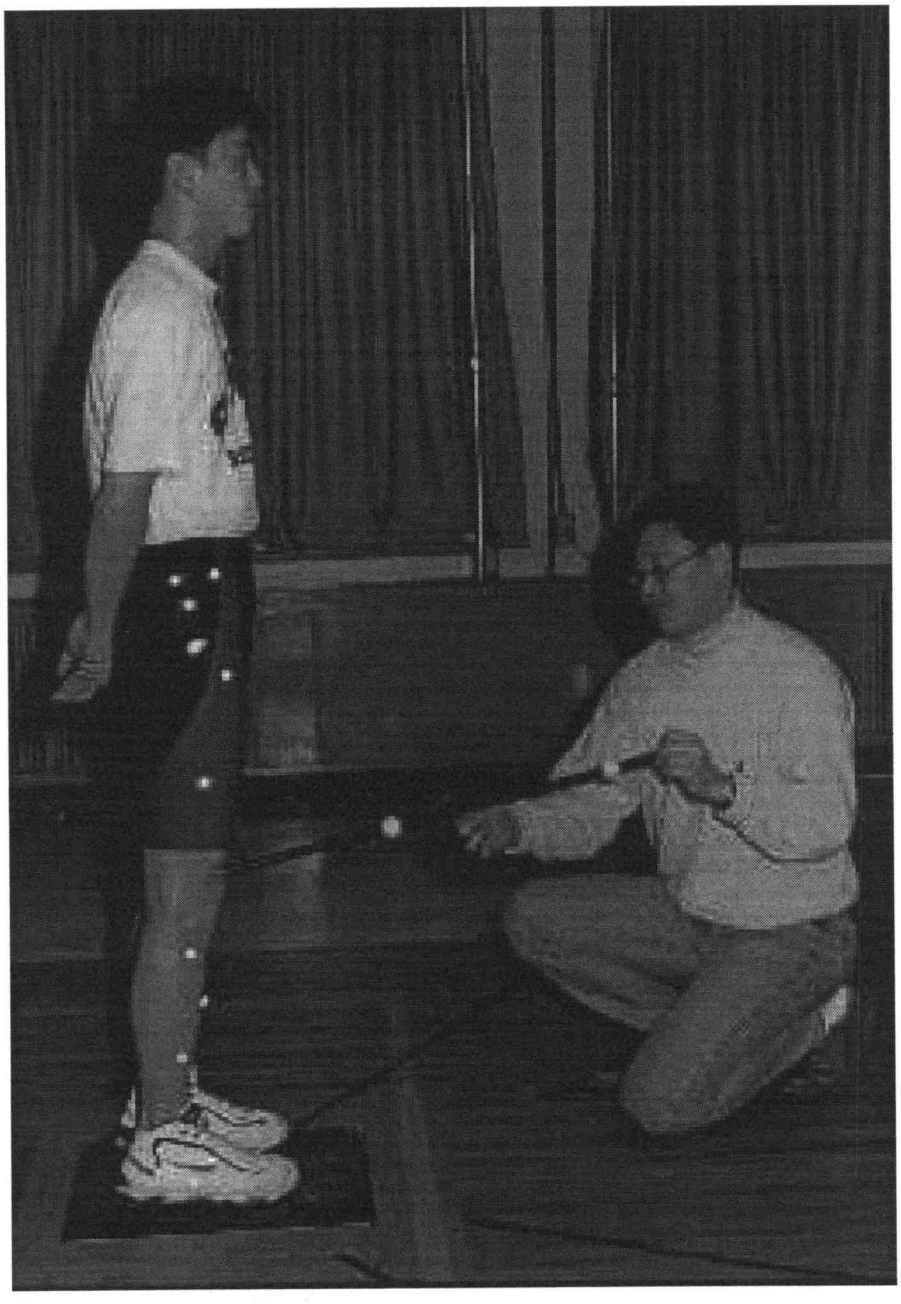

Figure 1. Skin markers and anatomical landmark calibration

each marker on the pointer and the reconstructed positions of the pointer markers, the location of the anatomical landmark (the tip of the pointer) was easily calculated. In the present study, this technique was applied to the posterior superior iliac spines and medial side of the anterior superior iliac spine, the femoral condyles and the malleoli. Markers used for the identification of the anatomical landmarks were removed before subsequent turning movement trials. After the anatomical landmark calibration procedure, the turning movement data collection was performed.

All data were collected at the Biomechanics Laboratory of the Korea Sports Science Institute, Seoul, Korea, where there was enough space to perform fast running with both medial and lateral turning movements. Five trials were recorded at each speed and direction condition for each subject. Running speed and turning direction condition were assigned randomly. All five trials were collected at one speed and direction before changing to the other condition. A protocol was accepted if the trial involved a speed within ± 0.2 m/s of the appropriate testing speed (1.5, 3.0, and 4.5 m/s) and involved a direction change within ± 3 degrees of the appropriate testing direction (60°, 30°, 0°, -30°, and –60°).

During the turning movements, positions of the markers were recorded at 60 samples per second and subsequently analyzed using 3-D automatic video-based motion recording system (KWON3D Motion Analysis System). Subjects were recorded with two video cameras (Panasonic DT 5100) and VCRs (Panasonic AG-7350). The cameras' electronic shutters were synchronized using a gen-lock adapter. Ground reaction force data were collected by a force plate (Advanced Mechanical Technology, Inc. Model OR6-5-1), mounted in the runway. Sampling frequency of the

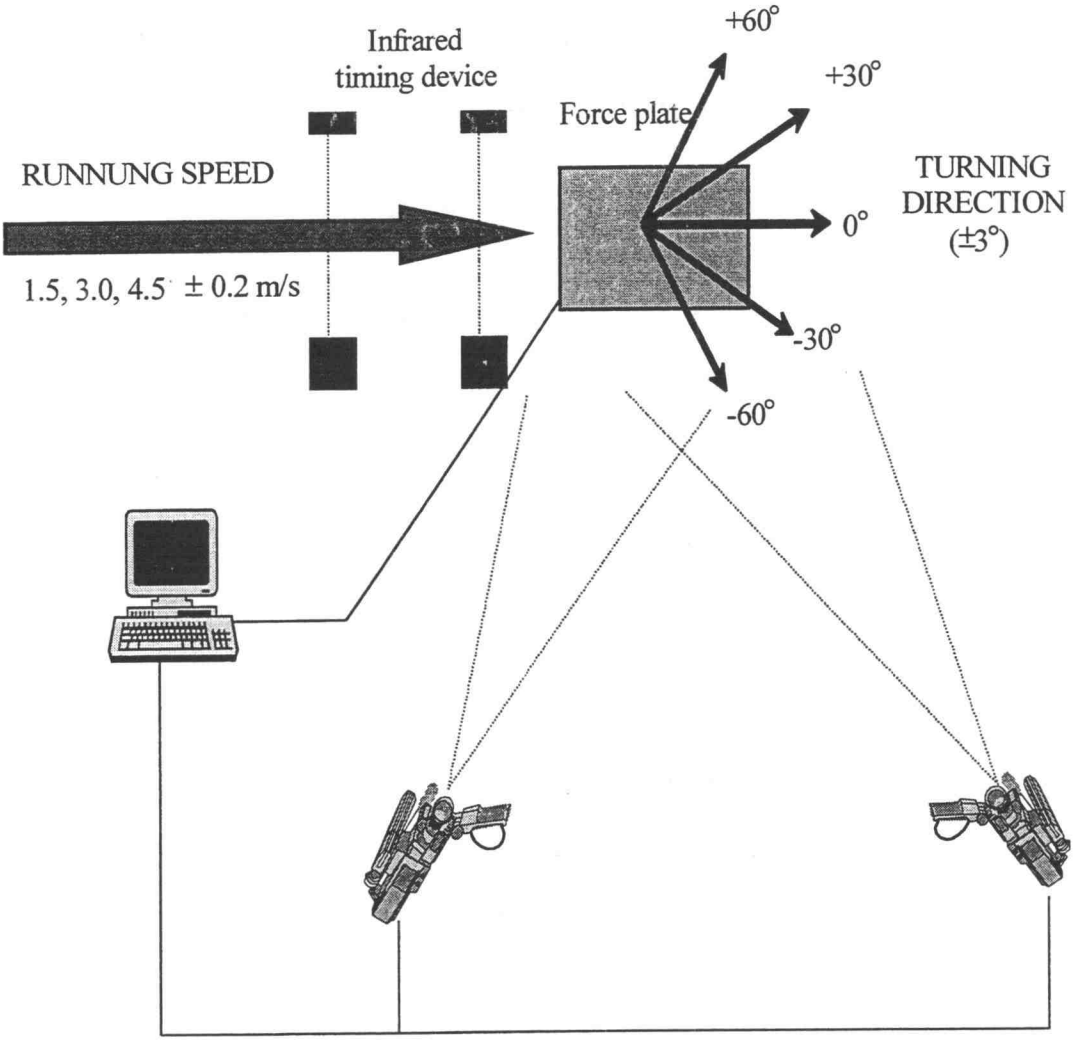

Figure 2. Experimental set-up

force plate was set as 240Hz. The video recording and force plate data were synchronized using a Peak Event Synchronization signal.

An infrared timing light (Lafayette Instrument Company Model 63501-IR) connected to a digital clock (Lafayette Instrument Company Model 54055) monitored the speed of the subject. The infrared control and the respective reflectors were positioned 2m and 1m before the center of the force plate to measure the speed of the subject when reaching the force plate.

Data processing and calculation procedure

An inverse dynamics approach was used to integrate the body segment parameter, kinematic and force plate data, and to solve for the resultant forces and moments at the ankle, knee, and hip joints. The four steps for the data analysis are illustrated in Figure 3. The goal of the first three steps was the preparation of the input of the equations of motion that are used to calculate forces and moments. Input parameters indicating the position, orientation and moment of inertia of body segments were expressed in the global coordinate system. The anthropometry computations (step 1) produced the body segment parameters in an anatomical frame. In step 2, the body segment parameters were calculated in the global coordinates system, in a 'calibration position' of the body segments. In step 3, the body segment parameters and anatomical landmarks were transformed from the technical frame coordinates to the global coordinates during the movement. In step 4, the equations of motion were applied. All calculations of each step were performed using a set of

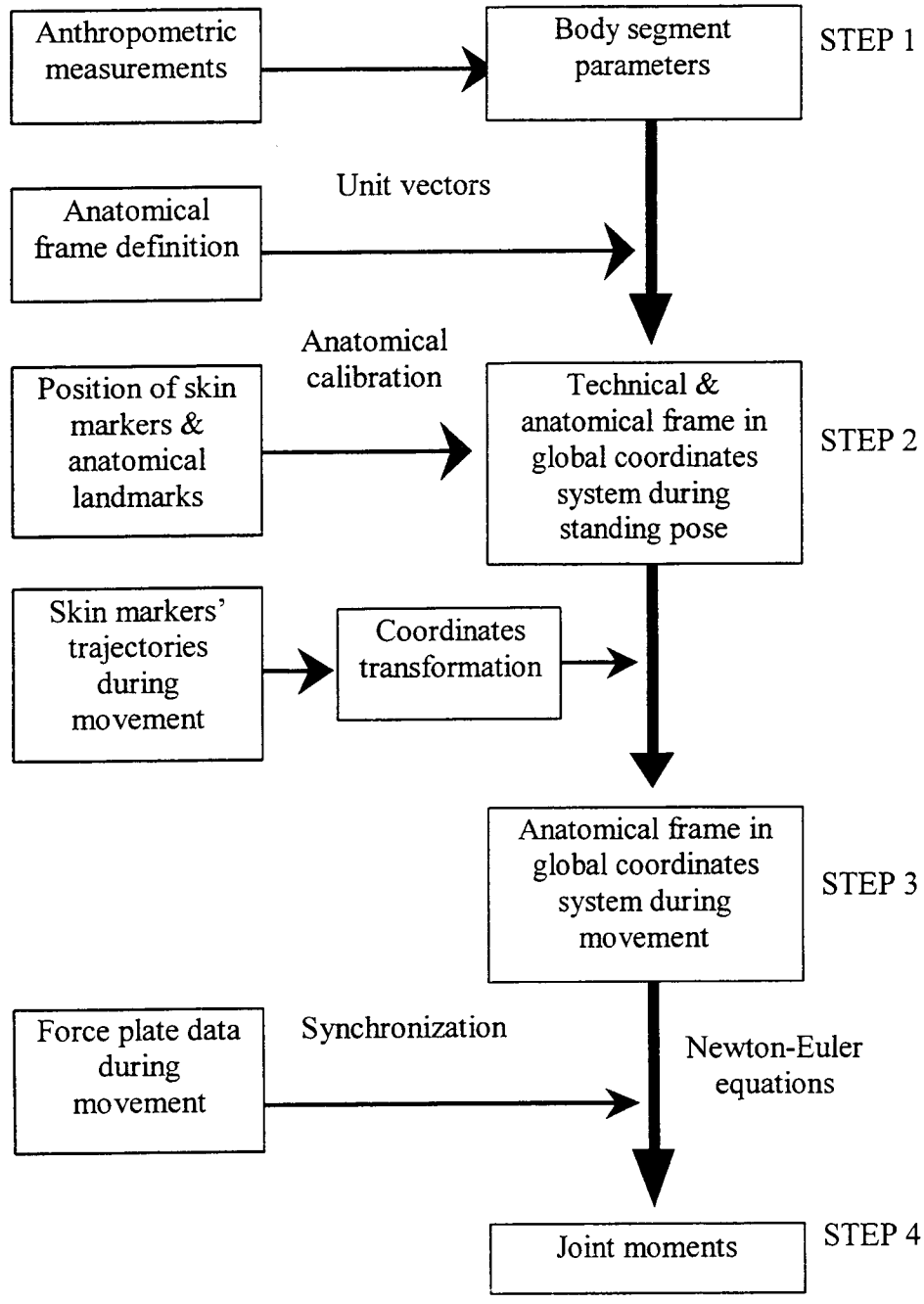

Figure 3. Data analysis

programs written in MATLAB^{TM} (MathWorks. Natick, MA) which contains a library of standard vector and matrix manipulation functions.

In step 1, segment mass and moment of inertia for the foot, shank, and thigh were estimated from anthropometric measurements and simple regression equations reported by Vaughan et al. (1992). Ankle joint center was defined at the midpoint of the line joining the tips of the malleoli (MM and LM). Knee joint center was defined as the midpoint between the lateral and medial epicondyles (LE and ME). The location of hip joint center was defined as 30% of the ASIS width superior to the ASIS; 14% of the ASIS width lateral to the midpoint of ASIS and 19% of the ASIS width posterior to the midpoint of ASIS (Bell et al., 1990). The center of mass positions were described as vectors in the anatomical frame of each segment according to Verstraete (1992) and McConville et al. (1980). Based on the anatomical landmarks listed in Table 1, the right-handed anatomical frames and unit vectors of each axis were defined for each segment in Figure 4.

In the anatomical landmarks calibration procedure, the transformation of anatomical landmarks coordinates in an anatomical frame to the same marker in a technical frame was expressed as follows:

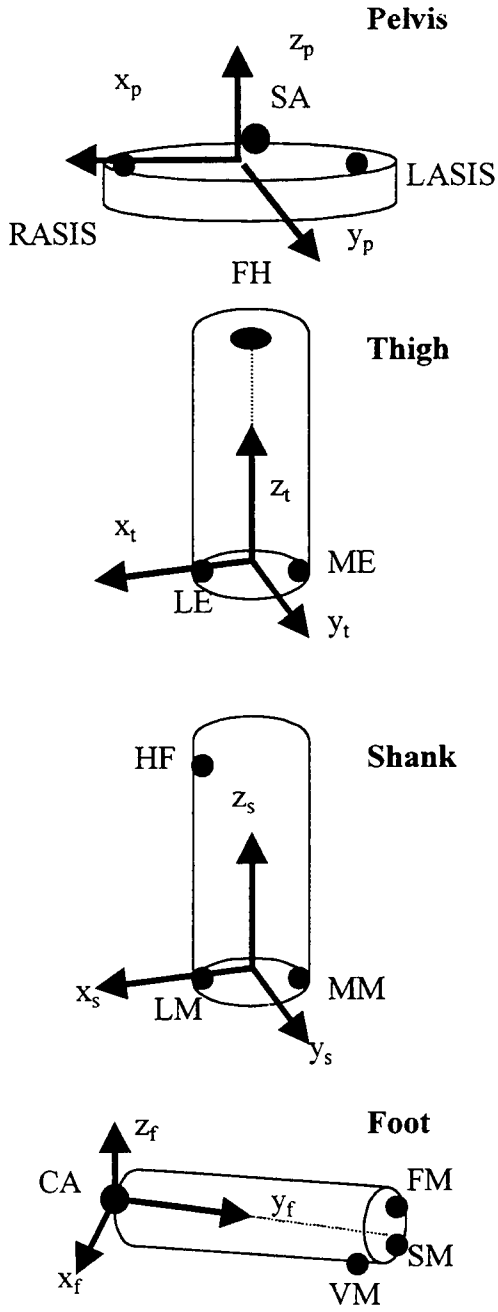

$$\mathbf{i}_p = \frac{(RASIS - LASIS)}{|(RASIS - LASIS)|}$$

$$\mathbf{k}_p = \frac{(RASIS - SA) \times (LASIS - SA)}{|(RASIS - SA) \times (LASIS - SA)|}$$

$$\mathbf{j}_p = \mathbf{k}_p \times \mathbf{i}_p$$

$$\mathbf{k}_t = \frac{(FH - (LE + ME/2))}{|(FH - (LE + ME/2))|}$$

$$\mathbf{i}_t = \frac{(LE - ME) - (((LE - ME) \cdot \mathbf{k}_t) \cdot \mathbf{k}_t)}{|(LE - ME) - (((LE - ME) \cdot \mathbf{k}_t) \cdot \mathbf{k}_t)|}$$

$$\mathbf{j}_t = \mathbf{k}_t \times \mathbf{i}_t$$

$$\mathbf{j}_s = \frac{(LM - HF) \times (MM - HF)}{|(LM - HF) \times (MM - HF)|}$$

$$\mathbf{i}_s = \frac{(LM - MM) - (((LM - MM) \cdot \mathbf{j}_s) \cdot \mathbf{j}_s)}{|(LM - MM) - (((LM - MM) \cdot \mathbf{j}_s) \cdot \mathbf{j}_s)|}$$

$$\mathbf{k}_s = \mathbf{i}_s \times \mathbf{j}_s$$

$$\mathbf{k}_f = \frac{(FM - CA) \times (VM - CA)}{|(FM - CA) \times (VM - CA)|}$$

$$\mathbf{j}_f = \frac{(CA - SM) - (((CA - SM) \cdot \mathbf{k}_f) \cdot \mathbf{k}_f)}{|(CA - SM) - (((CA - SM) \cdot \mathbf{k}_f) \cdot \mathbf{k}_f)|}$$

$$\mathbf{i}_f = \mathbf{j}_f \times \mathbf{k}_f$$

Figure 4. Anatomical frame of the pelvis, thigh, shank, and foot

$$\mathbf{r}_A = [\mathbf{T}_{A \rightarrow T}] \cdot \mathbf{r}_T$$

$$\mathbf{r}_A = \begin{bmatrix} x_A \\ y_A \\ z_A \\ 1 \end{bmatrix}, \quad \mathbf{r}_T = \begin{bmatrix} x_T \\ y_T \\ z_T \\ 1 \end{bmatrix}$$

$$[\mathbf{T}_{A \rightarrow T}] = \left[\begin{array}{c|c} [\mathbf{R}_{3\times3}] & [\mathbf{t}_{3\times1}] \\ \hline 0\ 0\ 0 & 1 \end{array}\right]$$

where, r_A, r_T = location vectors in anatomical frame and technical frame, respectively. A 4 × 4 transformation matrix T contained the 3 × 3 rotational matrix R and 3 × 1 translational matrix t.

In step 2, the transformation matrix was calculated, using a singular value decomposition method as described by Soderkvist and Wedin (1993).

$$\min \left(\sum_{i=1}^{n} \left\| [T_{A \rightarrow T}] \cdot r_{Ai} - r_{Ti} \right\|^2 \right) \quad ; n \geq 3$$

The movement trial yielded, for each body segment, the skin marker trajectories. Based on these trajectories, the transformation matrix from technical frame to global coordinate system was estimated in each sampled instant of time. Because anatomical landmarks coordinates in the technical frame determined in the standing trial were time invariant, the anatomical landmark coordinates in the global coordinate system in each time could be estimated. In step 3, joint center and center of mass positions at each time in the global coordinate system were estimated with the following:

$$\mathbf{r}^{G}_{ankle} = [T_{shanke \rightarrow G}]\mathbf{r}^{shank}_{ankle}$$
$$\mathbf{r}^{G}_{knee} = [T_{thigh \rightarrow G}]\mathbf{r}^{thigh}_{knee}$$
$$\mathbf{r}^{G}_{hip} = [T_{pelvis \rightarrow G}]\mathbf{r}^{pelvis}_{hip}$$

$$\mathbf{r}^{G}_{footcom} = [T_{foot \rightarrow G}]\mathbf{r}^{foot}_{footcom}$$
$$\mathbf{r}^{G}_{shankcom} = [T_{shank \rightarrow G}]\mathbf{r}^{shank}_{shankcom}$$
$$\mathbf{r}^{G}_{thighcom} = [T_{thigh \rightarrow G}]\mathbf{r}^{thigh}_{thighcom}$$

The recorded video images from each camera view were digitized at 60 Hz using the KWON3D Motion Analysis System interfaced with a personal computer. For each camera and subject, the videotapes containing the calibration coordinate system and the segment calibration frame were digitized manually. For the movement trials, skin markers were digitized automatically. High frequency noise in the raw digitized coordinate data for each camera was filtered prior to calculations of the 3D coordinates. Filtering was performed using a Butterworth low-pass digital filter. The cut-off frequency determined by a residual analysis as described by Winter (1990). Typical cut-off frequencies were 6-8 Hz. The spatial reconstruction was performed using a standard direct linear transformation (DLT) approach. The 3D coordinates of skin marker data and the force plate data were then interpolated to 100 Hz.

Linear velocities and accelerations for the ankle, knee, hip, $foot_{COM}$, $shank_{COM}$, and $thigh_{COM}$ were calculated using the central difference theorem. This technique allows for calculation of instantaneous velocities and accelerations.

Angular kinematic parameters for kinetic analysis consisted of segment angular velocities and segment angular accelerations. The segment Euler angles that described how one segment was oriented relative to the fixed global reference

coordinate system were used in this study. The segment Euler angles are important because they are needed to define the angular velocities and angular accelerations of the segments. The Euler angles of the segments were computed from the unit vectors of the anatomical frames. Figure 5 shows three successive rotations of the axes which bring global frame to anatomical frame in three dimensions. The first rotation occurred about the global X-axis by ϕ, the second rotation occurred about the contemporary y_1-axis by θ, and the third rotation occurred about the contemporary z_2-axis by ψ. These three rotation angles were the orientation angles of the segment to global coordinate system. The rotation matrix between global coordinate system and local anatomical frame could be expressed as follows:

$$R_{GA} = \begin{bmatrix} \cos\psi & \sin\psi & 0 \\ -\sin\psi & \cos\psi & 0 \\ 0 & 0 & 1 \end{bmatrix} \begin{bmatrix} \cos\theta & 0 & -\sin\theta \\ 0 & 1 & 0 \\ \sin\theta & 0 & \cos\theta \end{bmatrix} \begin{bmatrix} 1 & 0 & 0 \\ 0 & \cos\phi & \sin\phi \\ 0 & -\sin\phi & \cos\phi \end{bmatrix}$$

$$= \begin{bmatrix} \cos\theta\cos\psi & \sin\phi\sin\theta\cos\psi & -\cos\phi\sin\theta\cos\psi + \sin\phi\sin\psi \\ -\cos\theta\sin\psi & -\sin\phi\sin\theta\sin\psi + \cos\phi\cos\psi & \cos\phi\sin\theta\sin\psi + \sin\phi\cos\psi \\ \sin\theta & -\sin\phi\cos\theta & \cos\phi\cos\theta \end{bmatrix}$$

The Euler angles were calculated as follows:

$$\phi = \sin^{-1}[\mathbf{R}_{31}]$$
$$\theta = \tan^{-1}[(-\mathbf{R}_{32})/\mathbf{R}_{33})]$$
$$\psi = \tan^{-1}[(-\mathbf{R}_{21})/\mathbf{R}_{11})]$$

where, R_{ij} are the elements of the rotation matrix.

The segment angular velocities were obtained from the Euler angle and its time derivatives as follows:

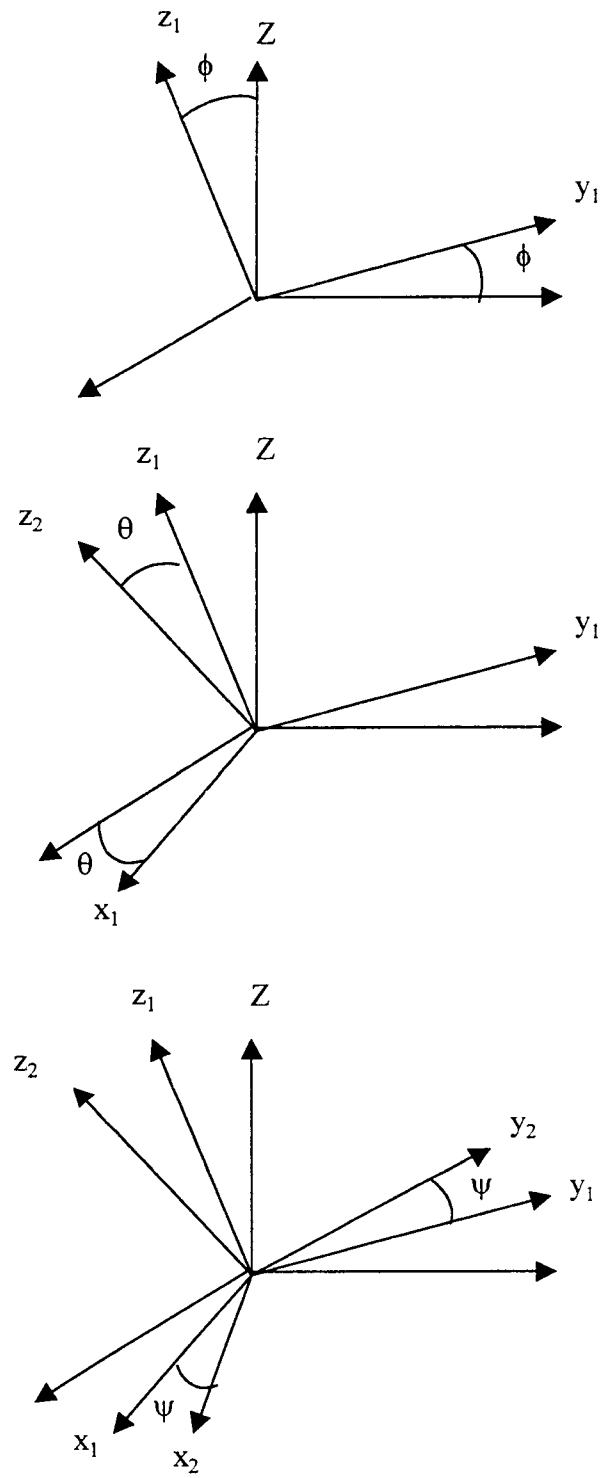

Figure 5. The three Euler angles

$$\begin{bmatrix} \omega_x \\ \omega_y \\ \omega_z \end{bmatrix} = \begin{bmatrix} \dot{\phi} + \dot{\psi}\sin\theta \\ \dot{\theta}\cos\phi - \dot{\psi}\sin\phi\cos\theta \\ \dot{\theta}\sin\phi + \dot{\psi}\cos\phi\cos\theta \end{bmatrix}$$

where, the dot above the Euler angles indicates the first derivative with respect to time.

By taking the first derivative of above equations, the segment angular accelerations in segment anatomical frame were determined as follows:

$$\begin{bmatrix} \dot{\omega}_x \\ \dot{\omega}_y \\ \dot{\omega}_z \end{bmatrix} = \begin{bmatrix} \ddot{\phi} + \ddot{\psi}\sin\theta + \dot{\phi}\dot{\psi}\cos\theta \\ \ddot{\theta}\cos\phi - \dot{\theta}\dot{\phi}\sin\phi - \ddot{\psi}\sin\phi\cos\theta - \dot{\phi}\dot{\psi}\cos\phi\cos\theta + \dot{\psi}\dot{\theta}\sin\phi\sin\theta \\ \ddot{\theta}\sin\phi + \dot{\theta}\dot{\phi}\cos\phi + \ddot{\psi}\cos\phi\cos\theta - \dot{\psi}\dot{\phi}\sin\phi\cos\theta - \dot{\psi}\dot{\theta}\cos\phi\sin\theta \end{bmatrix}$$

where, the double dot above the Euler angles indicates the second derivative with respect to time.

Forces and moments acting on the joints were calculated using Newton-Euler equations of motion. The calculation of forces and moments required the calculation of body segment parameters, segment center of mass and joint center positions, segmental linear accelerations, segmental angular velocities and accelerations and external forces acting on the body. The ankle resultant load was calculated with the equations of motion of the foot. The foot equations accounted for the inertial and gravitational effects as well as a joint connected to it proximally (ankle) and an external load applied to it on the sole (ground reaction load). The vector form of the translational dynamics equation of the foot is

$$\vec{F}_{ankle} = m_f \vec{a}_f - m_f \vec{g} - \vec{F}_{gr}$$

where, F_{ankle}: ankle joint force vector

m_f: foot mass

a_f: linear acceleration of foot mass center

g: gravity vector

f_{gr}: ground reaction force vector

The expanded three-dimensional form of the equation is

$$\begin{bmatrix} F_{anklex} \\ F_{ankley} \\ F_{anklez} \end{bmatrix} = m_f \begin{bmatrix} a_{fx} \\ a_{fy} \\ a_{fz} \end{bmatrix} - m_f \begin{bmatrix} 0 \\ 0 \\ g \end{bmatrix} - \begin{bmatrix} F_{grx} \\ F_{gry} \\ F_{grz} \end{bmatrix}$$

The vector form of the rotational dynamics equation of the foot is

$$\vec{M}_{ankle} = \vec{J}_f - \vec{M}_{gr} - \vec{p}_{gr} \times \vec{F}_{gr} - \vec{p}_{ankle} \times \vec{F}_{ankle}$$

where, M_{ankle}: ankle joint moment vector

m_f: foot mass

J_f: change of angular momentum of foot

M_{gr}: moment vector of ground reaction forces

p_{gr}: position vector from foot mass center to center of pressure

p_{ankle}: position vector from foot mass center to ankle joint

The expanded three-dimensional form of the equation is

$$\begin{bmatrix} M_{anklex} \\ M_{ankley} \\ M_{anklez} \end{bmatrix} = \begin{bmatrix} I_{xx}\alpha_x + (I_{zz} - I_{yy})\omega_y\omega_z \\ I_{yy}\alpha_y + (I_{xx} - I_{zz})\omega_x\omega_z \\ I_{zz}\alpha_z + (I_{xx} - I_{yy})\omega_x\omega_y \end{bmatrix} - \begin{bmatrix} 0 \\ 0 \\ M_{grz} \end{bmatrix} - \begin{bmatrix} P_{gry}F_{grz} - P_{grz}F_{gry} \\ P_{grz}F_{grx} - P_{grx}F_{grz} \\ P_{grx}F_{gry} - P_{gry}F_{grx} \end{bmatrix} - \begin{bmatrix} P_{ankley}F_{anklez} - P_{anklez}F_{ankley} \\ P_{anklez}F_{anklex} - P_{anklex}F_{anklez} \\ P_{anklex}F_{ankley} - P_{ankley}F_{anklex} \end{bmatrix}$$

In a similar fashion, the vector moment equilibrium equation of the shank rearranged to solve for the knee moment is

$$\bar{M}_{knee} = \bar{J}_s - \bar{M}_{ankle} - \bar{p}_{ankle} \times \bar{F}_{ankle} - \bar{p}_{knee} \times \bar{F}_{knee}$$

The equations of motion of the hip have an identical form to the knee equations except that the knee terms are replaced with hip terms, and the ankle terms are replaced with knee terms.

The resultant joint forces and moments from the above calculations were three-dimensional vectors in the global coordinate system. However, it is difficult to relate these laboratory-based components to human subjects, who may moving at an angle to the global axes. A more easily understood approach is to express the force and moments in terms of body-based coordinate systems that have anatomical significance. Therefore, instead of the global joint moments, anatomically meaningful axes were used (flexion/extension, a mediolateral axis of the proximal segment; internal/external rotation, a longitudinal axis of the distal segment; abduction/adduction, a floating axis perpendicular to the mediolateral and longitudinal axes). These were determined from the global joint moment data and segmental positions as a function of time.

Statistical analysis

To minimize variability due to body differences, the joint moments were normalized to body weight times leg length. The statistical analysis of the study used the mean of five trials for each speed and direction to characterize a subject's performance. A two-way within-subjects analysis of variance (ANOVA) was conducted to evaluate the effect of running speeds and turning directions on maximum joint moments. The dependent variable was the maximum value of each joint moment. The within-subjects factors were running speeds with three levels (slow, moderate, and fast) and turning directions with five levels (+60°, +30°, 0°, -30°, and -60°). The speed and direction main effects were tested using the multivariate criterion of Wilks' lambda (Λ). Because of insufficient residual degrees of freedom, the speed × direction interaction effect was tested using the two-way within-subjects ANOVA.

Additionally, statistical significance in the running speed and turning direction main effects and the speed × direction interaction effect were further assessed using paired-sample t-tests, controlling for Type I error by Holm's sequential Bonferroni procedure.

RESULTS

Results of this study for flexion-extension moments during straight running corresponded well with joint moment patterns for running in the literature (Buczek & Cavanagh, 1990; Gordon & Robertson, 1985; Simpson & Bates, 1990; Winter, 1983). Overall, similar to other studies, the maximum flexion/extension moments were found to increase with increasing speed. The pattern of ankle dorsi/plantar flexion moment closely resembled the joint moment pattern of runners reported by Buczek and Cavanagh (1990) and Gordon and Robertson (1985). They have reported an initial dorsiflexion moment while others have observed only plantar flexion dominance (Simpson & Bates, 1990; Winter, 1983). The knee flexion/extension moment pattern also resembled patterns in the literature, the initial flexor moments shifted to extensor moments that reached maximum values during midstance. The hip flexion/extension moments were predominantly extensor and displayed two maxima which were similar to the results reported by other researchers (Simpson & Bates, 1990; Winter, 1983).

The ensemble-average three-dimensional moments about the ankle, knee, and hip joint representing the effect of running speed and turning direction are shown in figures in following sections. In those figures, moments have been normalized to body weight and right leg length and expressed as a percentage. Moments in Nm can be estimated by multiplying the normalized value by subjects' average weight (710 N) and leg length (0.91 m), and dividing by 100.

Ankle moments

Inversion/eversion, dorsi/plantarflexion, and internal/external rotation moments of the ankle joint increased with running speed. Turning direction was also significant for the moments of the ankle except dorsi/plantar flexion moments (Tables 2-4). The ankle inversion moment predominated during the entire stance period with maximum values occurring at midstance during moderate and fast speed, while, eversion moment appeared in late stance during medial turning (Figure 6). For the maximum inversion moment, the speed and direction main effects were significant ($p < .001$ and $p = .006$), as well as the speed × direction interaction effect ($p < .001$). As running speed increased, the maximum inversion moment increased. There was a 65% (24 Nm) increase during moderate running compared to slow running, as well as 29% (18 Nm) increase during fast running compared to moderate running. The maximum inversion moments during lateral turning were greater than those during medial turning and straight running. There was a 30% (18 Nm) increase during –30° turning and 36% (22 Nm) increase during –60° compared to straight running. Furthermore, there were only small increases during medial turning by the speed effect, this effect increased to 145% (66 Nm) during -60° turning (Figure 7).

The ankle dorsiflexion moments were generated during impact phase except during fast lateral turning (Figure 8). These initial dorsiflexion moments shifted to plantar flexion moments. While any effect was not significant for the maximum dorsiflexion moment of ankle, the maximum plantar flexion moment increased with speed ($p = .003$). This resulted in 25% (17 Nm) and 37% (23 Nm) increases during moderate and fast running compared to slow running.

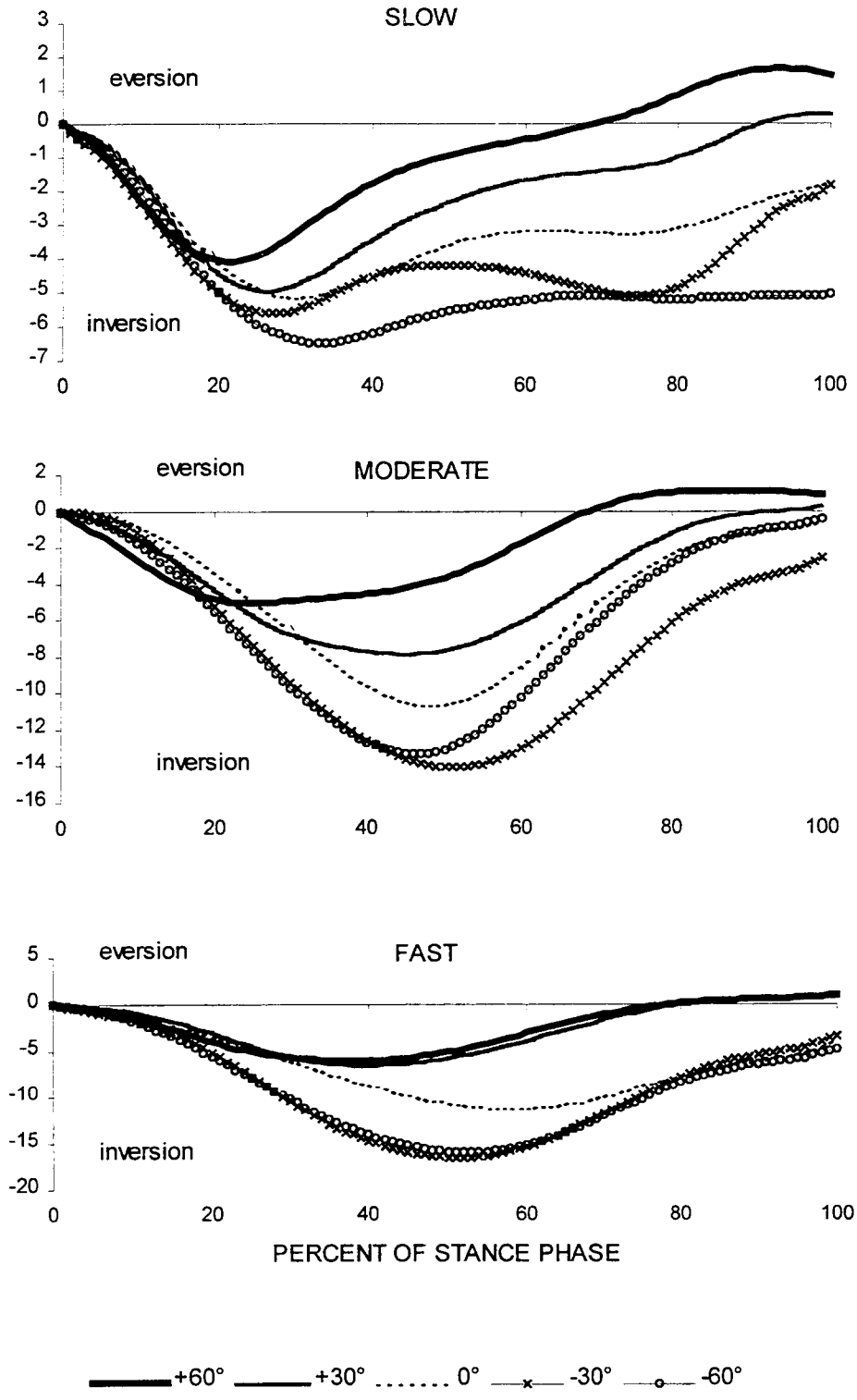

Figure 6. Ensembled-average inversion/eversion moment of the ankle during stance phase of cutting motions. Moments are normalized to body weight (N) and right leg length (m) and expressed as a percentage.

Table 2. Inversion/eversion moment of the ankle

		Inversion			
		slow	**moderate**	**fast**	
+60	**M**	**-4.67** [A,B,C]	**-5.89** [A,D]	**-7.38** [B,C,D]	**-5.98** [0,-30,-60]
	SD	2.95	2.43	2.54	2.18
+30	**M**	**-5.50** [E,F,G,H,I]	**-8.50** [E,F,H]	**-7.10** [G,I]	**-7.03** [0,-30,-60]
	SD	1.36	3.24	2.72	2.13
0	**M**	**-5.57** [A,E,F,G]	**-11.24** [A,E,F]	**-12.09** [G]	**-9.63** [+60,+30,-30,-60]
	SD	1.13	2.03	3.03	1.54
-30	**M**	**-6.13** [B]	**-13.62** [D]	**-17.53** [B,D]	**-12.43** [+60,+30, 0]
	SD	1.00	3.82	4.87	2.77
-60	**M**	**-7.04** [C,H,I]	**-15.05** [H]	**-17.22** [C,I]	**-13.10** [+60,+30, 0]
	SD	1.45	2.55	3.25	1.33
	M	**-5.78** [m,f]	**-9.51** [s,f]	**-12.26** [s,m]	
	SD	1.18	1.47	1.49	
		Eversion			
		slow	**moderate**	**fast**	
+60	**M**	**2.42**	**1.82**	**2.74**	**2.33**
	SD	2.79	1.66	2.77	2.02
+30	**M**	**1.14**	**0.69**	**2.08**	**1.30**
	SD	1.35	1.35	2.31	1.39
0	**M**	**0.04**	**0.12**	**0.12**	**0.09**
	SD	0.11	0.13	0.15	0.07
-30	**M**	**0.03**	**0.08**	**0.14**	**0.08**
	SD	0.08	0.09	0.13	0.06
-60	**M**	**0.00**	**0.06**	**0.14**	**0.07**
	SD	0.00	0.08	0.21	0.09
	M	**0.73**	**0.40**	**1.04**	
	SD	0.82	0.35	0.96	

*Superscript digits indicate significant difference by turning direction effect.

**Superscript s,m,f indicate significant difference by running speed effect.

***Superscript capitals indicate significant difference by interaction effect.
Difference (A-A) of a pair which have the same letter (A, B, C, ...) in the same direction was significantly different from the difference (A-A) of another pair in a different direction.

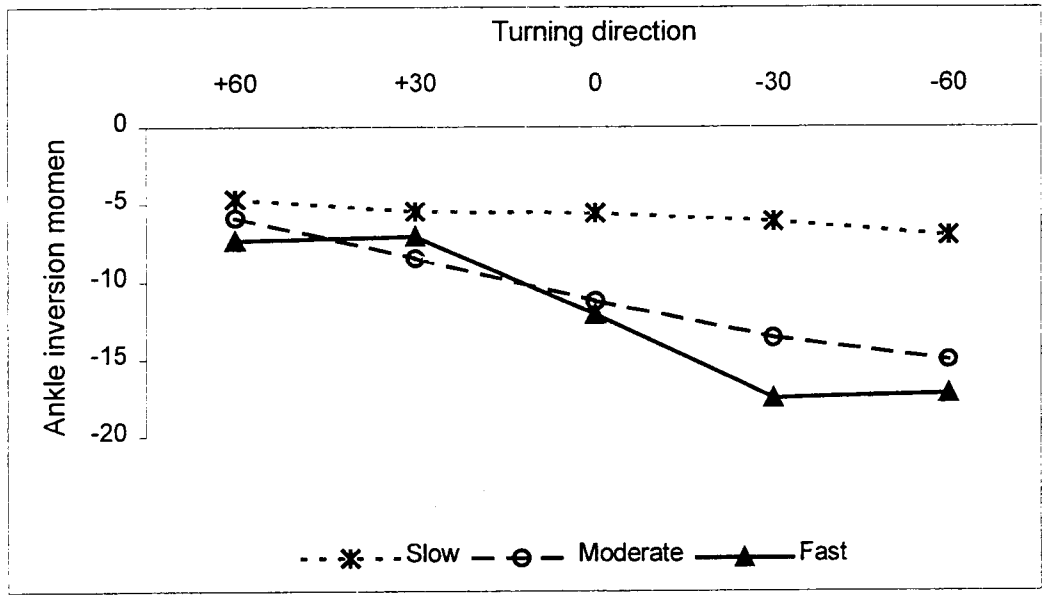

Figure 7. Running speed by turning direction interaction for ankle inversion moment

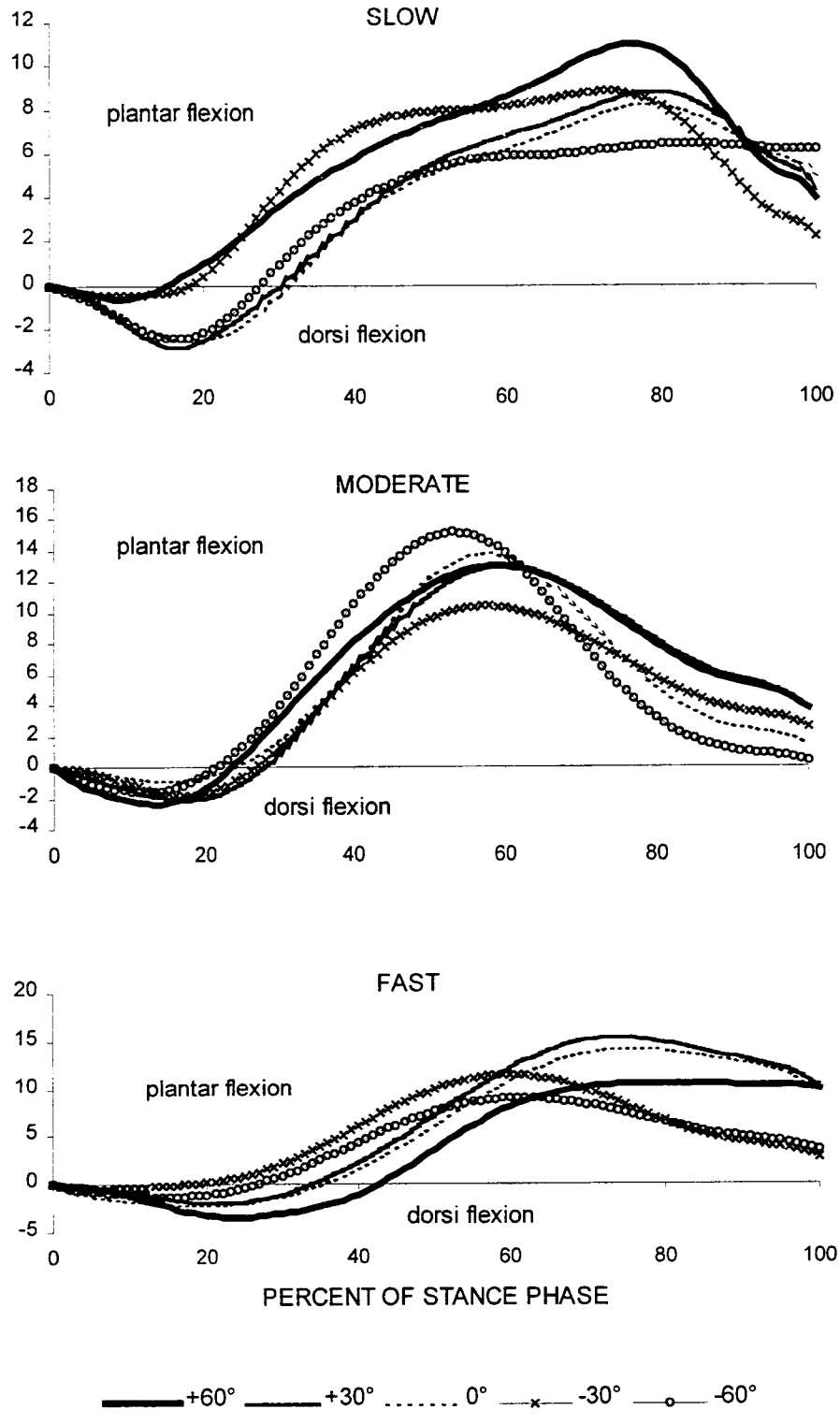

Figure 8. Ensembled-average dorsi/plantar flexion moment of the ankle during stance phase of cutting motions. Moments are normalized to body weight (N) and right leg length (m) and expressed as a percentage.

Table 3. Dorsi/plantar flexion moment of the ankle

		Dorsiflexion			
		slow	**moderate**	**fast**	
+60	**M**	**-2.24**	**-2.83**	**-5.93**	**-3.67**
	SD	1.98	2.23	4.63	2.28
+30	**M**	**-3.33**	**-2.85**	**-3.26**	**-3.15**
	SD	2.14	1.74	2.26	1.31
0	**M**	**-2.98**	**-1.76**	**-3.50**	**-2.75**
	SD	1.07	1.19	3.65	1.66
-30	**M**	**-1.98**	**-3.13**	**-2.64**	**-2.58**
	SD	1.55	2.03	3.37	1.61
-60	**M**	**-2.97**	**-2.30**	**-2.11**	**-2.46**
	SD	1.36	1.07	1.68	0.77
	M	**-2.70**	**-2.40**	**-3.49**	
	SD	1.27	1.20	2.23	
		Plantarflexion			
		slow	**moderate**	**fast**	
+60	**M**	**12.77**	**13.71**	**15.01**	**13.83**
	SD	3.89	2.52	3.87	2.42
+30	**M**	**10.71**	**13.61**	**17.29**	**13.87**
	SD	2.29	2.41	5.72	2.83
0	**M**	**9.72**	**15.01**	**15.54**	**13.42**
	SD	1.78	2.93	4.27	2.36
-30	**M**	**11.03**	**15.84**	**13.64**	**13.51**
	SD	5.94	7.82	4.24	4.82
-60	**M**	**8.53**	**11.61**	**10.54**	**10.23**
	SD	1.47	2.82	4.97	2.79
	M	**10.55** [m,f]	**13.12** [s]	**14.40** [s]	
	SD	2.62	3.30	3.04	

*Superscript s,m,f indicate significant difference by running speed effect.

The ankle adduction moments predominated during lateral turning. However, during medial turning, initial adduction moments shifted to abduction moments that reached maximum values late stance (Figure 9). For the maximum abduction moment of ankle, the main effect associated with direction and the interaction effect were significant ($p = .024$ and $p < .001$). Maximum abduction moments significantly increased with medial turning. There were a 198% (22 Nm) increase during +30° turning and a 268% (29 Nm) increases during +60° turning compared to straight running. Additionally, while there was no difference by the speed effect during straight running, this effect increased to 88% (23 Nm) during +30° turning (Figure 10).

For the maximum adduction moment of ankle, the main effect associated with speed factor and the interaction effect were significant ($p = .003$ and $p < .001$). There were a 39% (5 Nm) increase during moderate running compared to slow running, as well as 88% (16 Nm) increase during fast running compared to moderate running. While there was only a 62% (7 Nm) increase by the speed effect during straight running, this effect increased to 194% (35 Nm) during -60° turning (Figure 11).

Knee moments

Flexion/extension and abduction/adduction moments of the knee joint increased with running speed except flexion moment that decreased with running speed. Turning direction was also significant for the extension and abduction/adduction moments of the knee (Tables 5-7). The knee internal rotation moments occurred early in the stance period, while external rotation moments

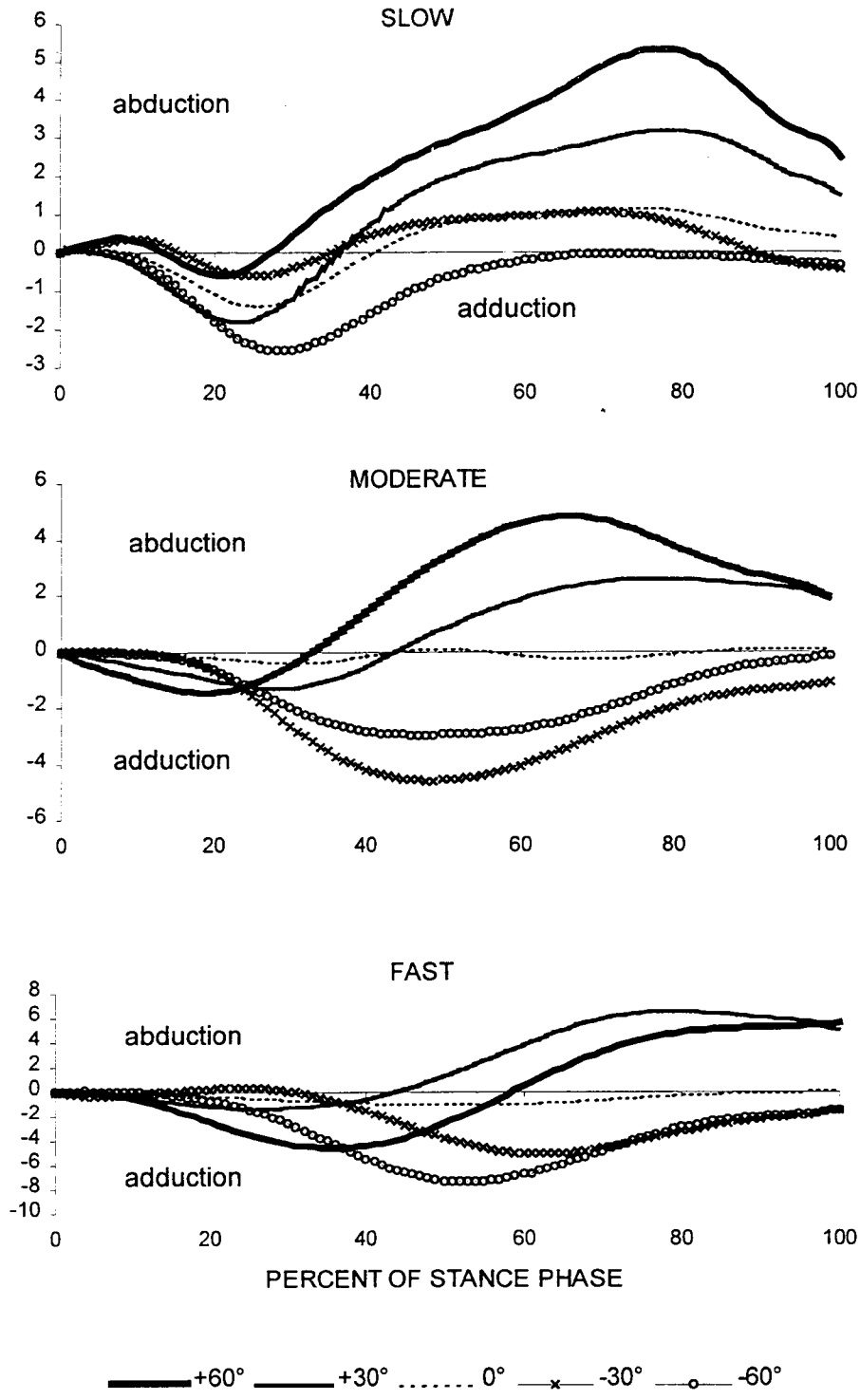

Figure 9. Ensembled-average abduction/adduction moment of the ankle during stance phase of cutting motions. Moments are normalized to body weight (N) and right leg length (m) and expressed as a percentage.

Table 4. Abduction/adduction moment of the ankle

		Abduction			
		slow	**moderate**	**fast**	
+60	**M**	**5.99**	**5.58**	**7.09**	**6.22** [0,-30,-60]
	SD	3.02	2.52	2.67	2.30
+30	**M**	**3.94** [A]	**3.74** [B,C]	**7.42** [A,B,C]	**5.03** [0,-30,-60]
	SD	1.89	2.88	2.20	2.13
0	**M**	**1.71** [A]	**1.66** [B]	**1.71** [A,B]	**1.69** [+60,+30]
	SD	1.16	1.46	1.36	1.25
-30	**M**	**1.99**	**1.07**	**1.63**	**1.56** [+60,+30]
	SD	2.43	2.19	1.49	1.24
-60	**M**	**0.65**	**0.66** [C]	**0.66** [C]	**0.66** [+60,+30]
	SD	0.58	0.64	1.16	0.45
	M	**2.86**	**2.39**	**3.70**	
	SD	1.64	1.67	1.20	
		Adduction			
		slow	**moderate**	**fast**	
+60	**M**	**-1.77**	**-1.86**	**-6.19**	**-3.27**
	SD	1.50	1.34	3.35	1.55
+30	**M**	**-2.11**	**-2.44**	**-2.53**	**-2.36**
	SD	1.29	1.30	2.17	0.67
0	**M**	**-1.68** [A,B,C,D]	**-1.74** [A,C]	**-2.72** [B,D]	**-2.05**
	SD	0.90	1.40	3.14	1.36
-30	**M**	**-1.49** [A,B]	**-4.26** [A]	**-6.00** [B]	**-3.92**
	SD	0.98	2.12	3.37	1.82
-60	**M**	**-2.80** [C,D]	**-5.80** [C]	**-8.22** [D]	**-5.61**
	SD	1.47	2.75	3.77	2.02
	M	**-1.97** [m,f]	**-2.73** [s,f]	**-5.13** [s,m]	
	SD	0.88	1.15	2.00	

*Superscript digits indicate significant difference by turning direction effect.

**Superscript s,m,f indicate significant difference by running speed effect.

***Superscript capitals indicate significant difference by interaction effect.
Difference (A-A) of a pair which have the same letter (A, B, C, ...) in the same direction was significantly different from the difference (A-A) of another pair in a different direction.

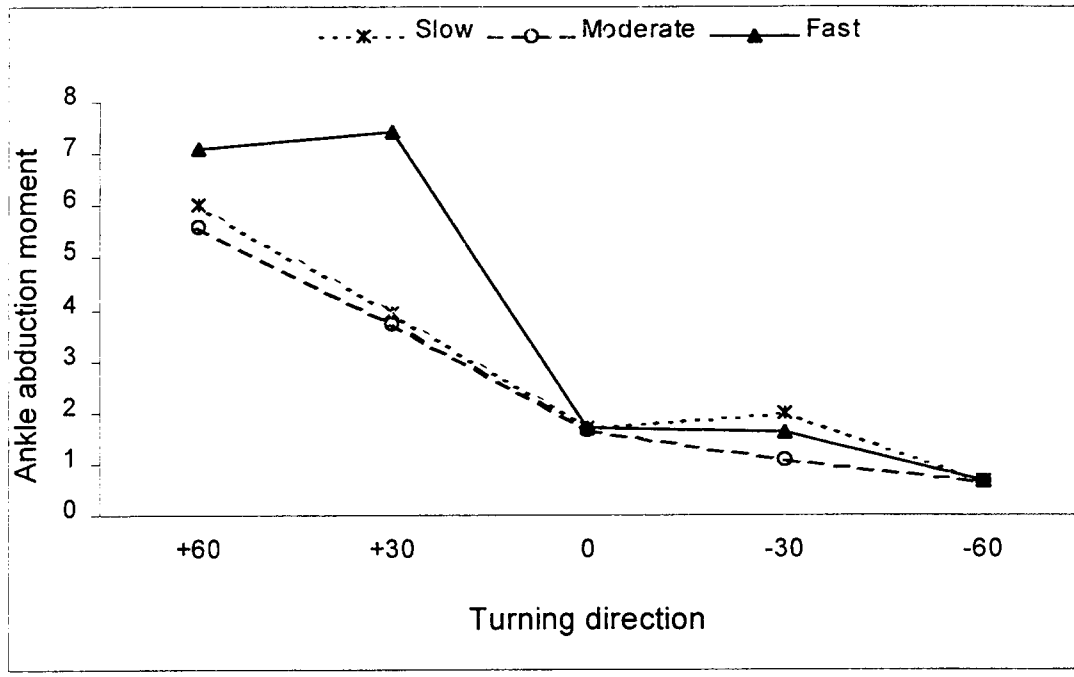

Figure 10. Running speed by turning direction interaction for ankle abduction moment

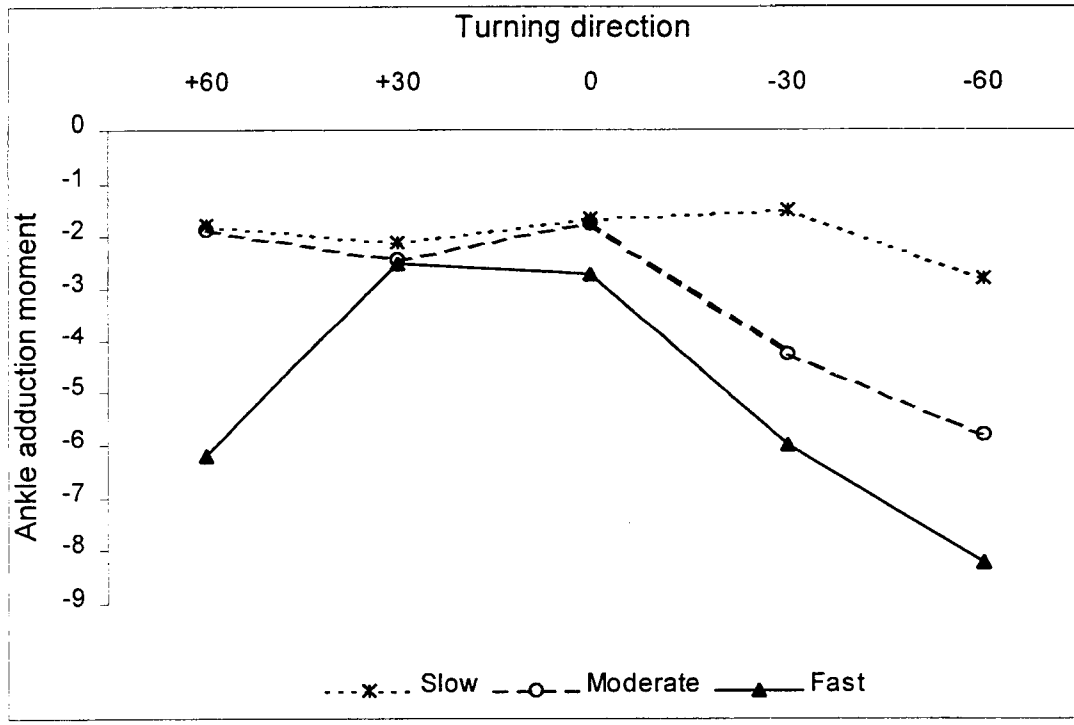

Figure 11. Running speed by turning direction interaction for ankle adduction moment

appeared late in the stance period (Figure 12). Any effect was not significant for the maximum internal/external rotation moment.

The knee extension moments predominated except for slow running, where flexion moments appeared late in the stance period (Figure 13). The maximum flexion moment decreased with running speed ($p = .011$). This resulted in a 62% (14 Nm) decrease during moderate running compared to slow running. For the maximum extension moments, the main effect associated with speed and direction and the interaction effect were all significant ($p < .001$, $p = .021$, and $p = .006$, respectively). The maximum extension moment increased with running speed. There was a 94% (51 Nm) increase during moderate running compared to slow running, as well as 84% (88 Nm) increase during fast running compared to moderate running. As runner turned medially, maximum extension moments increased (147 Nm during +60° turning vs. 102 Nm during -30° turning). Additionally, while there was small decrease between moderate and fast speed during -60° turning, this decrease reversed to a 56% (86 Nm) increase during +60° turning (Figure 14).

For all turning direction, the knee abduction moments predominated during slow running. However, adduction moments predominated during fast medial turning (Figure 15). For the maximum abduction moments, the main effect associated with speed and direction and the interaction effect were all significant ($p = .001$, $p = .008$, and $p < .001$, respectively). There was a 28% (9 Nm) increase during fast running compared to slow running. As runner turned laterally, maximum abduction moments significantly increased. There was a 126% (35 Nm) increase during -60° turning

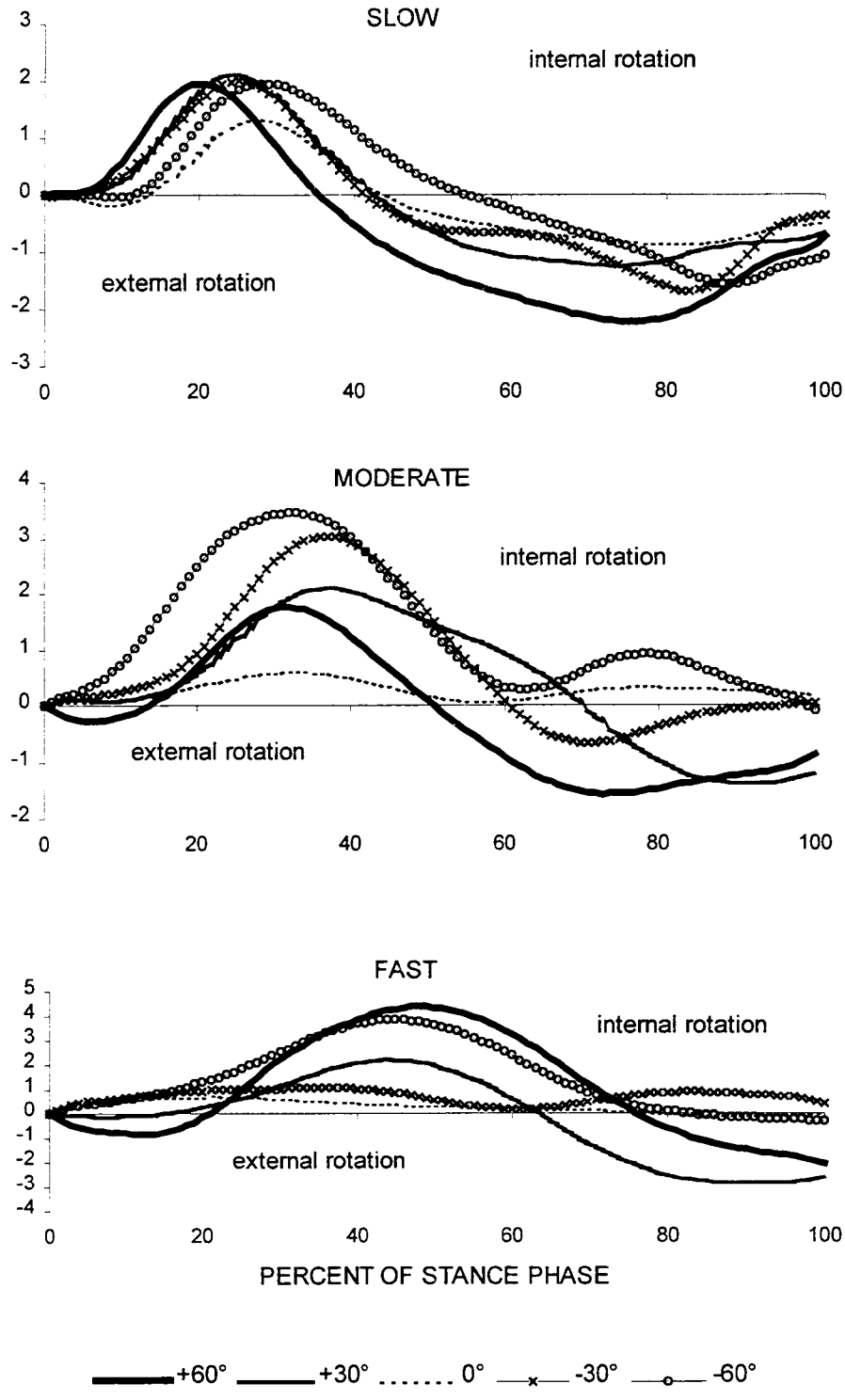

Figure 12. Ensembled-average internal/external rotation moment of the knee during stance phase of cutting motions. Moments are normalized to body weight (N) and right leg length (m) and expressed as a percentage.

Table 5. Internal/external rotation moment of the knee

			Internal rotation		
		slow	moderate	fast	
+60	**M**	**2.50**	**2.53**	**5.99**	**3.67**
	SD	1.23	1.47	2.48	1.21
+30	**M**	**2.86**	**3.26**	**3.10**	**3.07**
	SD	1.46	2.18	2.03	1.25
0	**M**	**1.58**	**2.07**	**3.18**	**2.28**
	SD	0.82	1.98	2.56	1.35
-30	**M**	**2.18**	**4.09**	**3.04**	**3.11**
	SD	2.21	2.79	2.59	2.29
-60	**M**	**2.16**	**3.20**	**4.03**	**3.13**
	SD	1.28	1.62	2.18	1.33
	M	**2.26**	**2.79**	**3.87**	
	SD	1.10	1.40	1.51	
			External rotation		
		slow	**moderate**	**fast**	
+60	**M**	**-3.06**	**-3.19**	**-4.56**	**-3.60**
	SD	2.44	4.79	7.05	4.33
+30	**M**	**-2.48**	**-2.03**	**-3.86**	**-2.79**
	SD	2.06	2.98	5.30	3.37
0	**M**	**-1.75**	**-1.77**	**-2.46**	**-1.99**
	SD	1.64	2.41	3.62	2.52
-30	**M**	**-2.58**	**-0.89**	**-1.88**	**-1.78**
	SD	1.35	1.02	2.52	1.34
-60	**M**	**-2.16**	**-1.47**	**-0.69**	**-1.44**
	SD	1.96	1.74	0.96	1.25
	M	**-2.40**	**-2.07**	**-2.69**	
	SD	1.37	1.75	3.55	

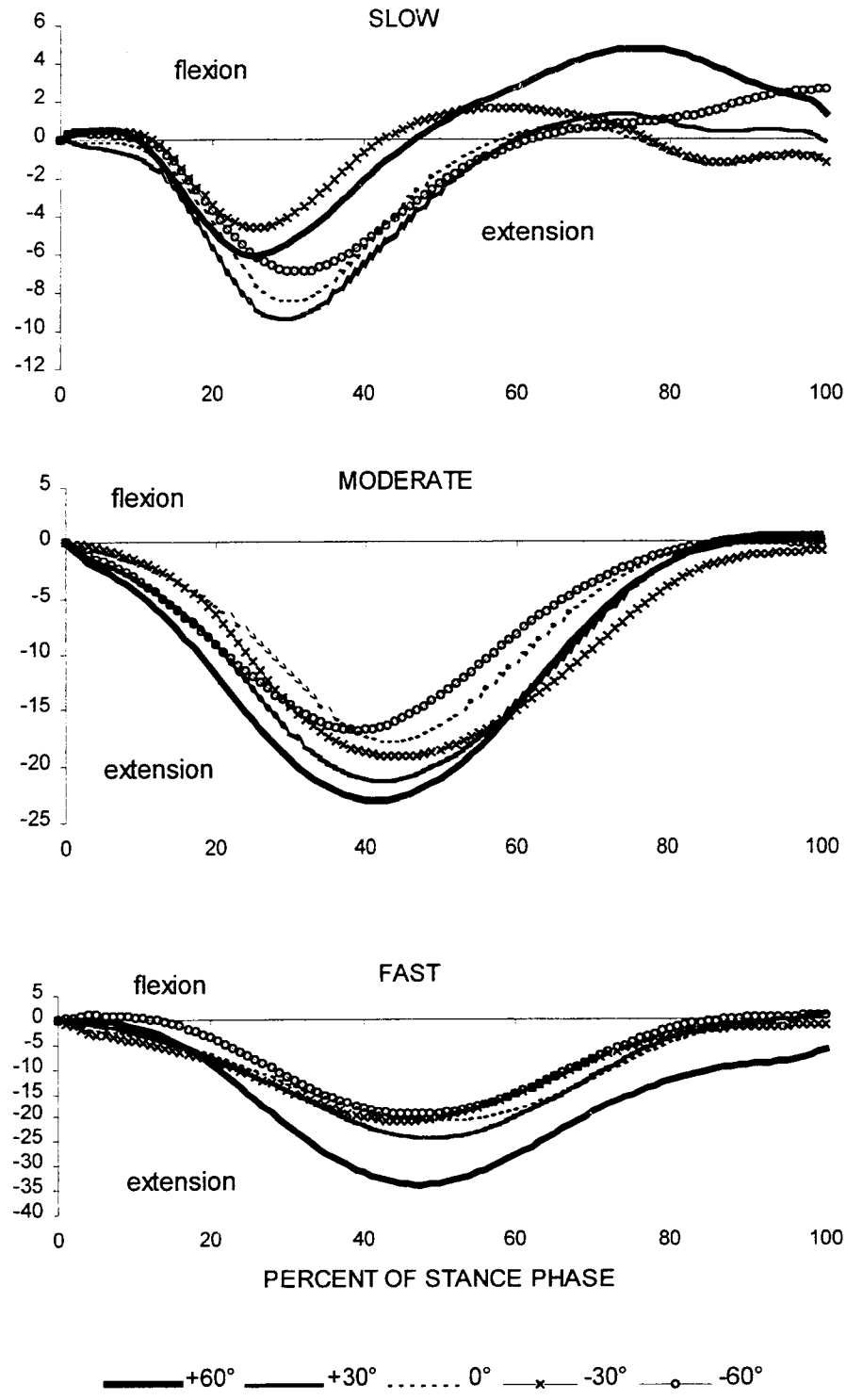

Figure 13. Ensembled-average flexion/extension moment of the knee during stance phase of cutting motions. Moments are normalized to body weight (N) and right leg length (m) and expressed as a percentage.

Table 6. Flexion/extension moment of the knee

		Flexion			
		slow	**moderate**	**fast**	
+60	**M**	**5.67**	**1.52**	**1.35**	**2.84**
	SD	4.85	1.98	1.57	2.37
+30	**M**	**3.18**	**1.33**	**2.17**	**2.22**
	SD	2.88	1.85	1.98	1.77
0	**M**	**2.29**	**0.75**	**1.13**	**1.39**
	SD	2.04	1.38	0.96	1.17
-30	**M**	**2.39**	**0.30**	**3.05**	**1.91**
	SD	2.39	0.49	4.53	2.03
-60	**M**	**3.79**	**0.67**	**2.17**	**2.21**
	SD	1.66	1.12	2.51	1.41
	M	**3.46** [m]	**1.33** [s]	**1.97**	
	SD	2.46	1.37	1.54	
		Extension			
		slow	**moderate**	**fast**	
+60	**M**	**-7.56**	**-23.73** [A]	**-37.10** [A]	**-22.80** [-30]
	SD	6.76	5.85	10.44	5.99
+30	**M**	**-11.39**	**-22.05**	**-26.08**	**-19.84**
	SD	8.52	5.51	12.76	7.94
0	**M**	**-9.26**	**-18.50**	**-22.83**	**-16.86**
	SD	8.37	8.33	10.80	8.20
-30	**M**	**-5.49**	**-18.30**	**-23.60**	**-15.80** [-60]
	SD	3.99	6.60	16.87	6.59
-60	**M**	**-8.35**	**-20.64** [A]	**-20.14** [A]	**-16.38**
	SD	7.61	7.23	8.51	6.97
	M	**-8.41** [m,f]	**-16.32** [s,f]	**-25.95** [s,m]	
	SD	5.30	3.64	10.15	

*Superscript digits indicate significant difference by turning direction effect.

**Superscript s,m,f indicate significant difference by running speed effect.

***Superscript capitals indicate significant difference by interaction effect.
Difference (A-A) of a pair which have the same letter (A, B, C, ...) in the same direction was significantly different from the difference (A-A) of another pair in a different direction.

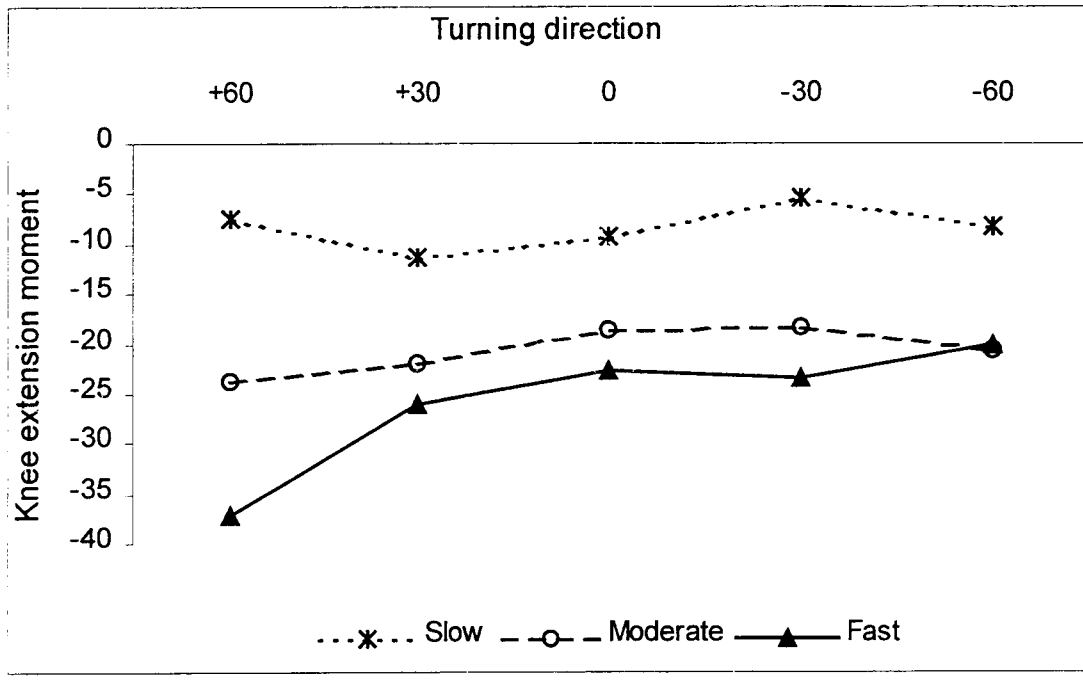

Figure 14. Running speed by turning direction interaction for knee extension moment

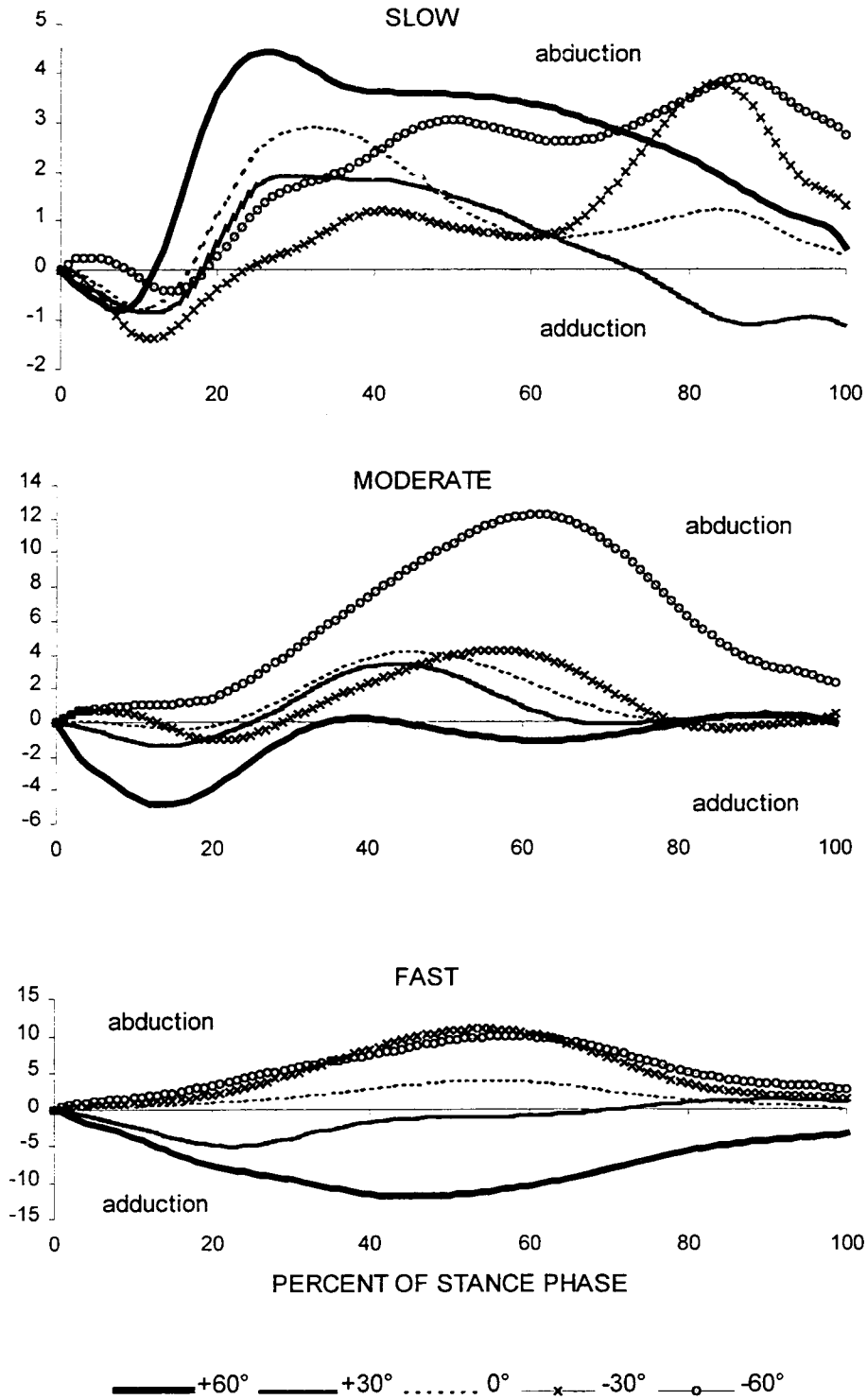

Figure 15. Ensembled-average abduction/adduction moment of the knee during stance phase of cutting motions. Moments are normalized to body weight (N) and right leg length (m) and expressed as a percentage.

Table 7. Abduction/adduction moment of the knee

		Abduction			
		slow	moderate	fast	
+60	M	6.19 A	1.97 B	0.27 A,B	2.81 -60
	SD	4.30	3.35	0.52	2.03
+30	M	3.58	4.36	2.92	3.62 -60
	SD	2.73	3.59	4.11	2.92
0	M	3.48 D	4.83 C,D	4.74 C	4.35 -60
	SD	1.49	2.86	5.16	3.06
-30	M	4.73 E	4.92 B,C,E	11.29 A,B,C	6.98 -60
	SD	2.18	3.11	5.60	3.37
-60	M	5.49 D,E	13.18 D,E	10.75	9.81 +60,+30, 0,-30
	SD	3.25	5.93	2.79	2.82
	M	4.69 f	5.53	6.00 s	
	SD	1.22	2.10	2.26	
		Adduction			
		slow	moderate	fast	
+60	M	-2.39 A,C,E	-5.50 B,D,E	-14.74 A,B	-7.54 +30, 0,-30,-60
	SD	2.27	1.87	4.84	2.43
+30	M	-2.47	-3.03	-6.28	-3.93 +60
	SD	1.96	2.45	4.51	2.52
0	M	-1.14 D	-1.11 C,D	-1.73 C	-1.33 +60
	SD	0.98	1.00	1.47	0.93
-30	M	-2.23 A	-2.57 B,C	-0.95 A,B,C	-1.91 +60
	SD	2.43	3.35	1.41	2.34
-60	M	-1.33 D,E	-0.66 D,E	-0.52	-0.84 +60,+30
	SD	1.34	1.15	1.31	0.92
	M	-1.91 f	-2.48 f	-4.84 s,m	
	SD	1.42	1.61	1.76	

*Superscript digits indicate significant difference by turning direction effect.

**Superscript s,m,f indicate significant difference by running speed effect.

***Superscript capitals indicate significant difference by interaction effect.
Difference (A-A) of a pair which have the same letter (A, B, C, ...) in the same direction was significantly different from the difference (A-A) of another pair in a different direction.

compared to straight running. Additionally, while there were small increases by the speed effect during straight running or medial turning, this effect increased to 140% (50 Nm) during -60° turning (Figure 16). For the maximum adduction moment of knee, the main effect associated with speed and direction and the interaction effect were all significant ($p = .001$, $p = .026$, and $p < .001$, respectively). There was a 153% (19 Nm) increase during fast running compared to slow running. Maximum adduction moments significantly increased with medial turning. There were a 467% (40 Nm) increase during -60° turning compared to straight running. Additionally, while there were small increases or decreases by the speed effect during straight running or lateral turning, this effect increased to 517% (80 Nm) during +60° turning (Figure 17).

Hip moments

Internal/external rotation, flexion/extension abduction/adduction moments of the hip joint increased with running speed. Turning direction was also found to significantly affect internal/external rotation and abduction/adduction moments (Tables 8-10). The hip internal rotation moments predominated for medial turning, while external rotation moments predominated for lateral turning (Figure 18). For the maximum internal rotation moment, only the interaction effect was significant ($p <$ .001). While there were small increase or decrease by the speed effect during straight running or medial turning, this speed effect resulted in a 208% (43 Nm) increase during -60° turning (Figure 19). For the maximum external rotation moments, the main effect associated with speed and direction and the interaction effect were all

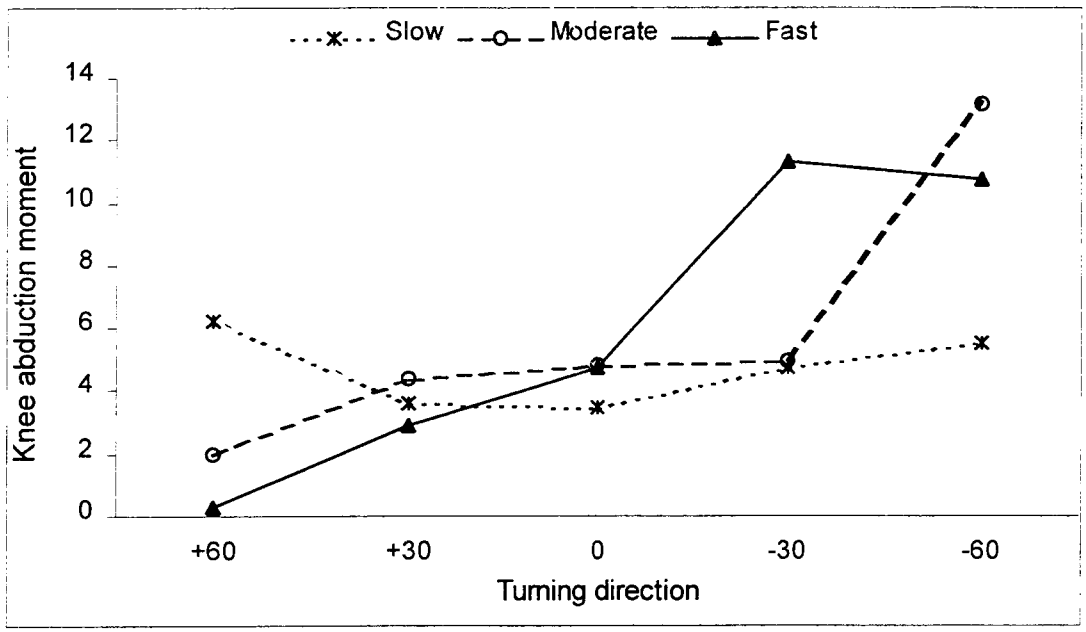

Figure 16. Running speed by turning direction interaction for knee abduction moment

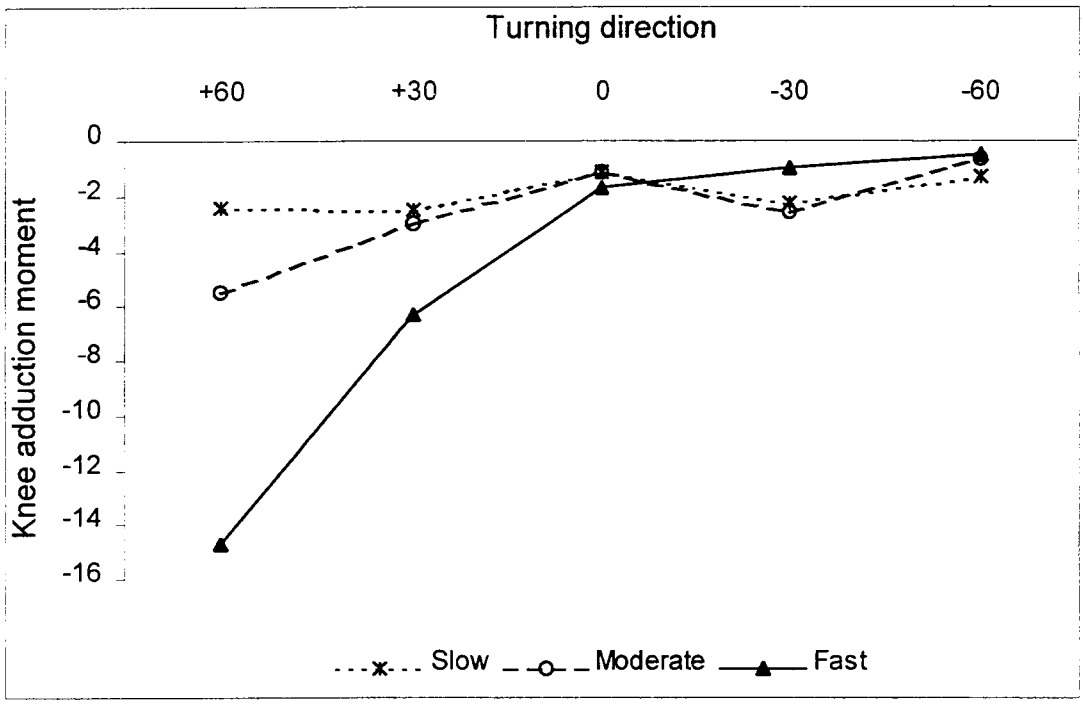

Figure 17. Running speed by turning direction interaction for knee adduction moment

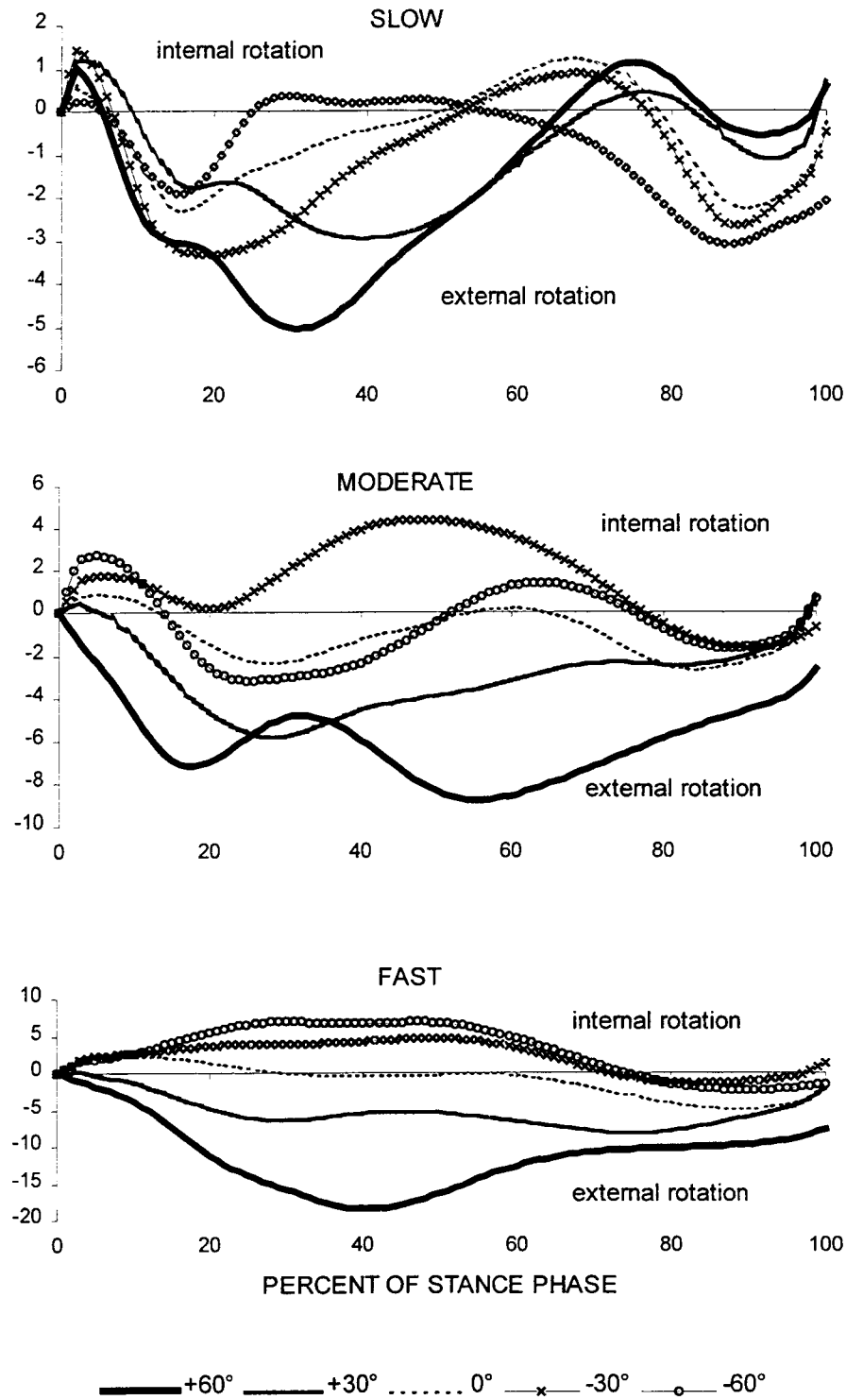

Figure 18. Ensembled-average internal/external rotation moment of the hip during stance phase of cutting motions. Moments are normalized to body weight (N) and right leg length (m) and expressed as a percentage.

Table 8. Internal/external rotation moment of the hip

		Internal rotation			
		slow	moderate	fast	
+60	**M**	**3.41** [A]	**1.11**	**0.71** [A]	**1.74**
	SD	2.22	1.20	1.06	1.25
+30	**M**	**3.79**	**1.41**	**2.24**	**2.48**
	SD	2.34	1.82	2.22	1.85
0	**M**	**3.06**	**2.60**	**4.18**	**3.28**
	SD	2.45	2.12	3.16	2.13
-30	**M**	**4.64**	**5.72**	**7.13**	**5.83**
	SD	4.22	2.85	3.28	2.67
-60	**M**	**3.23** [A]	**6.89**	**9.95** [A]	**6.69**
	SD	2.79	4.63	7.13	4.31
	M	**3.63**	**3.86**	**4.84**	
	SD	1.92	1.68	1.21	
		External rotation			
		slow	**moderate**	**fast**	
+60	**M**	**-7.19** [A]	**-11.53** [B]	**-24.26** [A,B]	**-14.33** [+30, 0,-30,-60]
	SD	9.25	5.41	9.20	4.48
+30	**M**	**-5.23**	**-7.36**	**-14.04**	**-8.88** [+60, 0,-60]
	SD	4.61	2.24	8.31	4.24
0	**M**	**-4.19**	**-4.13**	**-6.41**	**-4.91** [+60,+30]
	SD	2.77	4.00	8.54	4.86
-30	**M**	**-7.72** [A]	**-6.54** [B]	**-3.08** [A,B]	**-5.78** [+60]
	SD	7.80	11.87	5.23	7.92
-60	**M**	**-4.92**	**-2.71**	**-4.32**	**-3.98** [+60,+30]
	SD	3.82	4.04	7.46	4.80
	M	**-5.85** [f]	**-6.82**	**-10.42** [s]	
	SD	4.75	5.29	5.32	

*Superscript digits indicate significant difference by turning direction effect.

**Superscript s,m,f indicate significant difference by running speed effect.

***Superscript capitals indicate significant difference by interaction effect.
Difference (A-A) of a pair which have the same letter (A, B, C, ...) in the same direction was significantly different from the difference (A-A) of another pair in a different direction.

significant ($p = .037$, $p = .007$, and $p < .001$, respectively). The external rotation moments increased with speed, a 78% (30 Nm) increase during fast running compared to slow running. Maximum external rotation moments significantly increased with medial turning. There was a 81% (26 Nm) increase during +30° turning and a 192% (61 Nm) increase during +60° turning compared to straight running. Additionally, while there were only small increases or decreases by the speed effect during straight running and lateral turning, this effect increased to 237% (110 Nm) during +60° turning (Figure 20).

The hip flexion/extension moments were predominantly extensor and displayed two peaks (Figure 21). While any effect was not significant for the maximum flexion moment, The maximum extension moment increased with running speed ($p = .050$). There were 73% (55 Nm) and 47% (42 Nm) increases during fast running compared to slow and moderate running.

As similar to the knee abduction/adduction moments pattern, the hip abduction moments predominated for lateral turning, while adduction moments predominated for medial turning (Figure 22). The maximum abduction moments increased with lateral turning ($p = .006$). There were a 148% (51 Nm) increase during -30° turning and a 264% (91 Nm) increases during -60° turning compared to straight running. For the maximum adduction moment, the main effect associated with speed and direction and the interaction effect were all significant ($p = .027$, $p = .001$, and $p < .001$, respectively). There was an 86% (39 Nm) increase during fast running compared to

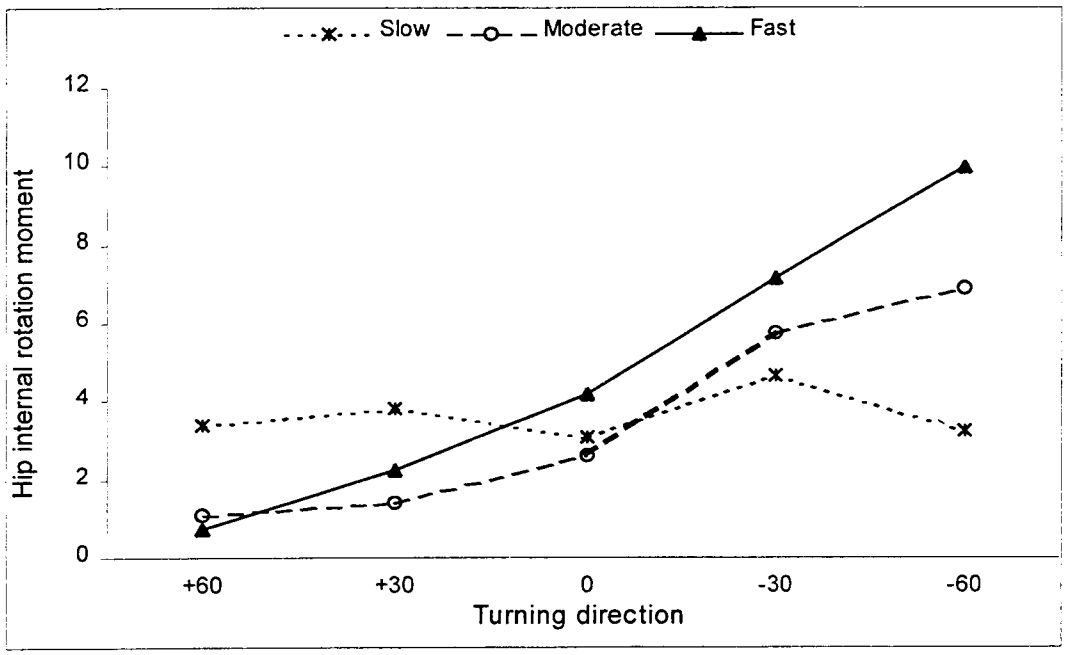

Figure 19. Running speed by turning direction interaction for hip internal rotation moment

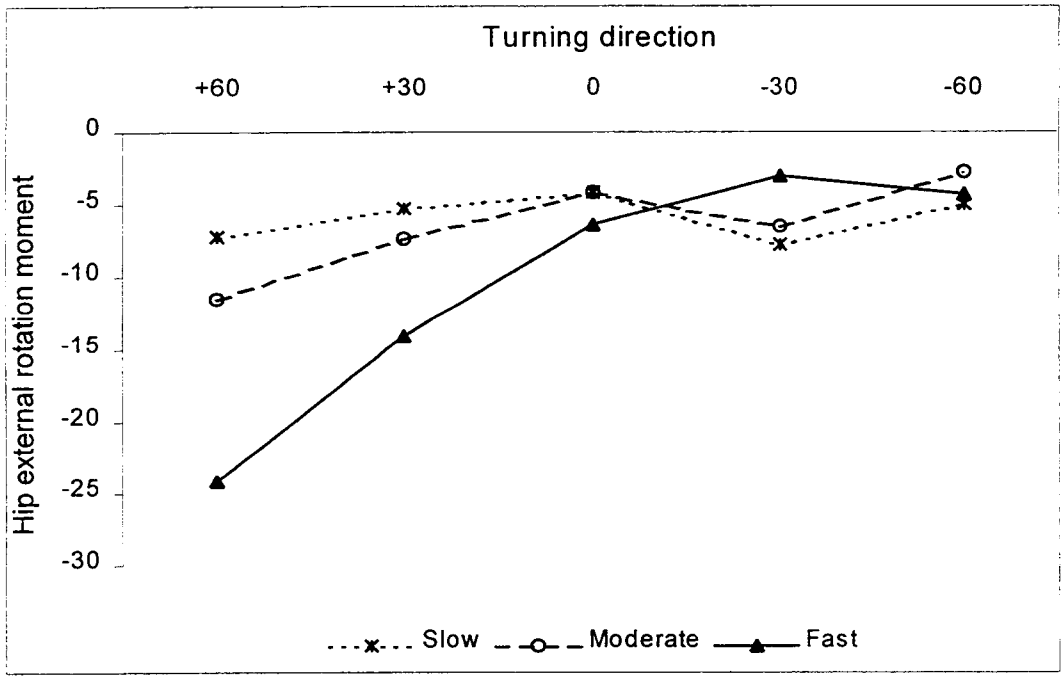

Figure 20. Running speed by turning direction interaction for hip external rotation moment

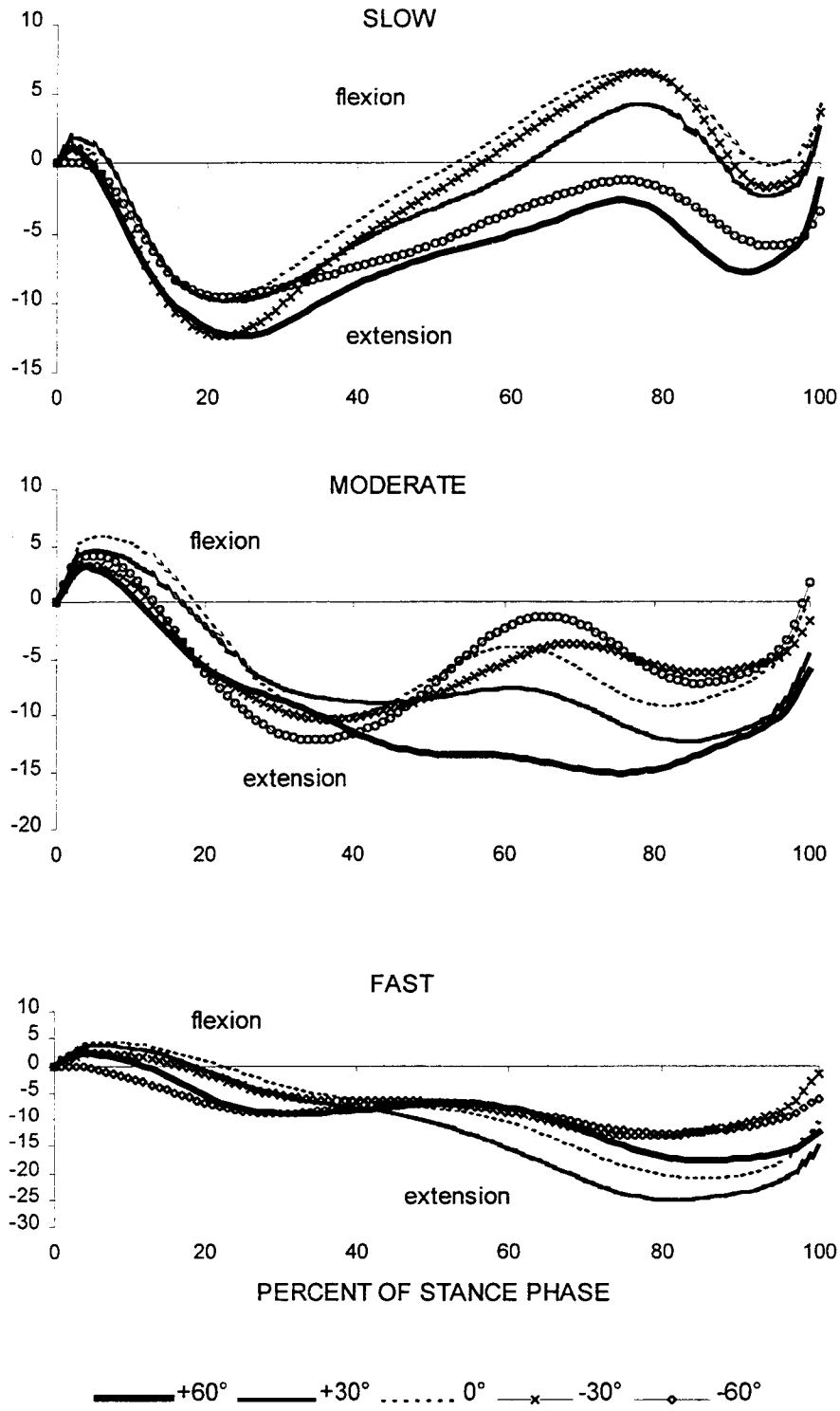

Figure 21. Ensembled-average flexion/extension moment of the hip during stance phase of cutting motions. Moments are normalized to body weight (N) and right leg length (m) and expressed as a percentage.

Table 9. Flexion/extension moment of the hip

		Flexion			
		slow	**moderate**	**fast**	
+60	**M**	**2.22**	**3.39**	**2.44**	**2.68**
	SD	2.65	3.24	2.20	1.69
+30	**M**	**6.06**	**5.02**	**4.63**	**5.24**
	SD	4.75	2.32	3.05	2.87
0	**M**	**7.69**	**6.14**	**7.30**	**7.04**
	SD	4.24	5.10	7.46	4.17
-30	**M**	**7.60**	**5.83**	**7.54**	**6.99**
	SD	4.86	4.95	5.70	3.71
-60	**M**	**2.67**	**3.45**	**1.01**	**2.38**
	SD	4.45	2.58	1.64	2.47
	M	**5.25**	**5.58**	**4.59**	
	SD	3.23	2.97	2.92	
		Extension			
		slow	**moderate**	**fast**	
+60	**M**	**-13.75**	**-17.99**	**-18.74**	**-16.83**
	SD	6.42	9.55	8.30	5.57
+30	**M**	**-10.79**	**-13.51**	**-26.56**	**-16.95**
	SD	4.78	4.81	13.17	5.54
0	**M**	**-9.97**	**-12.59**	**-22.77**	**-15.11**
	SD	3.16	3.80	10.58	5.04
-30	**M**	**-13.00**	**-14.03**	**-18.32**	**-15.12**
	SD	6.47	8.96	13.96	7.00
-60	**M**	**-10.71**	**-11.69**	**-14.09**	**-12.16**
	SD	2.72	3.61	4.30	2.15
	M	**-11.65** [f]	**-13.69** [f]	**-20.10** [s,m]	
	SD	3.02	3.96	8.52	

*Superscript s,m,f indicate significant difference by running speed effect.

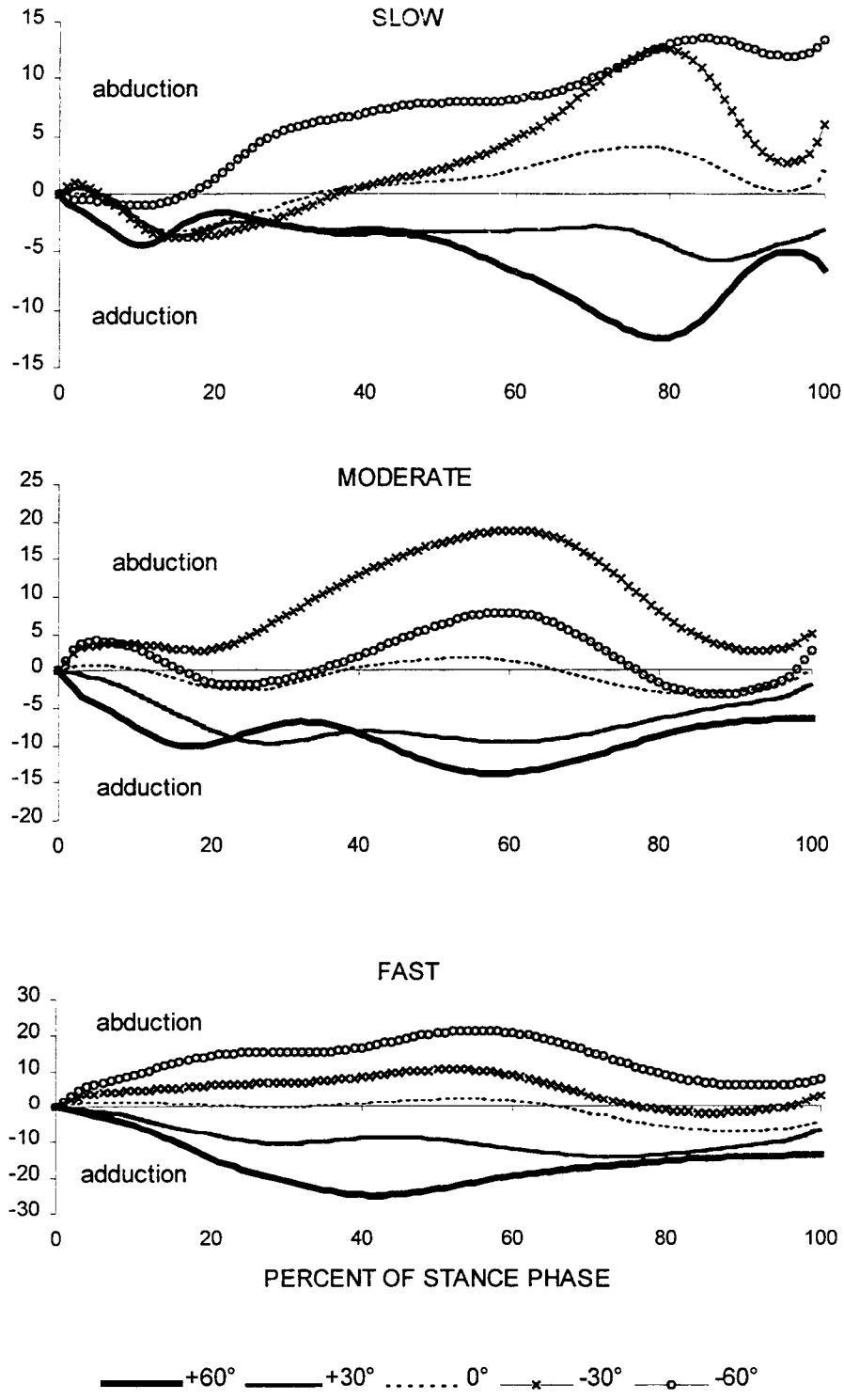

Figure 22. Ensembled-average abduction/adduction moment of the hip during stance phase of cutting motions. Moments are normalized to body weight (N) and right leg length (m) and expressed as a percentage.

Table 10. Abduction/adduction moment of the hip

		Abduction			
		slow	moderate	fast	
+60	M	1.07	1.10	0.73	0.97 -30,-60
	SD	1.72	1.42	1.04	1.27
+30	M	2.56	1.12	1.95	1.87 -30,-60
	SD	2.40	1.97	2.38	2.06
0	M	5.59	4.60	5.75	5.31 -30,-60
	SD	1.36	3.21	3.38	1.60
-30	M	13.69	11.69	14.19	13.19 +60,+30, 0,-60
	SD	3.71	5.80	8.82	5.56
-60	M	15.91	19.18	22.90	19.33 +60,+30, 0,-30
	SD	6.64	10.28	5.33	6.58
	M	7.76	9.30	9.10	
	SD	2.26	3.37	2.74	
		Adduction			
		slow	moderate	fast	
+60	M	-13.32 A	-15.96	-31.20 A	-20.16 +30, 0,-30,-60
	SD	3.14	3.67	13.26	4.60
+30	M	-7.92 B,C	-12.93	-21.13 B,C	-13.99 +60, 0,-30,-60
	SD	3.70	6.09	9.27	3.58
0	M	-4.47	-4.66	-7.77	-5.63 +30,+60
	SD	2.11	3.76	7.89	4.45
-30	M	-6.50 A,C	-7.47	-5.00 A,C	-6.32 +30,+60
	SD	8.21	11.40	4.92	7.64
-60	M	-1.44 B	-0.93	-0.33 B	-0.90 +30,+60
	SD	1.57	1.51	0.82	0.86
	M	-6.73 f	-7.85 f	-13.08 s,m	
	SD	2.44	4.28	2.97	

*Superscript digits indicate significant difference by turning direction effect.

**Superscript s,m,f indicate significant difference by running speed effect.

***Superscript capitals indicate significant difference by interaction effect.
Difference (A-A) of a pair which have the same letter (A, B, C, ...) in the same direction was significantly different from the difference (A-A) of another pair in a different direction.

slow running. Maximum adduction moments increased with medial turning. There were a 148% (54 Nm) increase during +30° turning and a 258% (94 Nm) increase during +60° turning compared to straight running. Additionally, while there were small increases or decreases by the speed effect during straight running or lateral turning, this effect increased to 134% (116 Nm) during +60° turning (Figure 23).

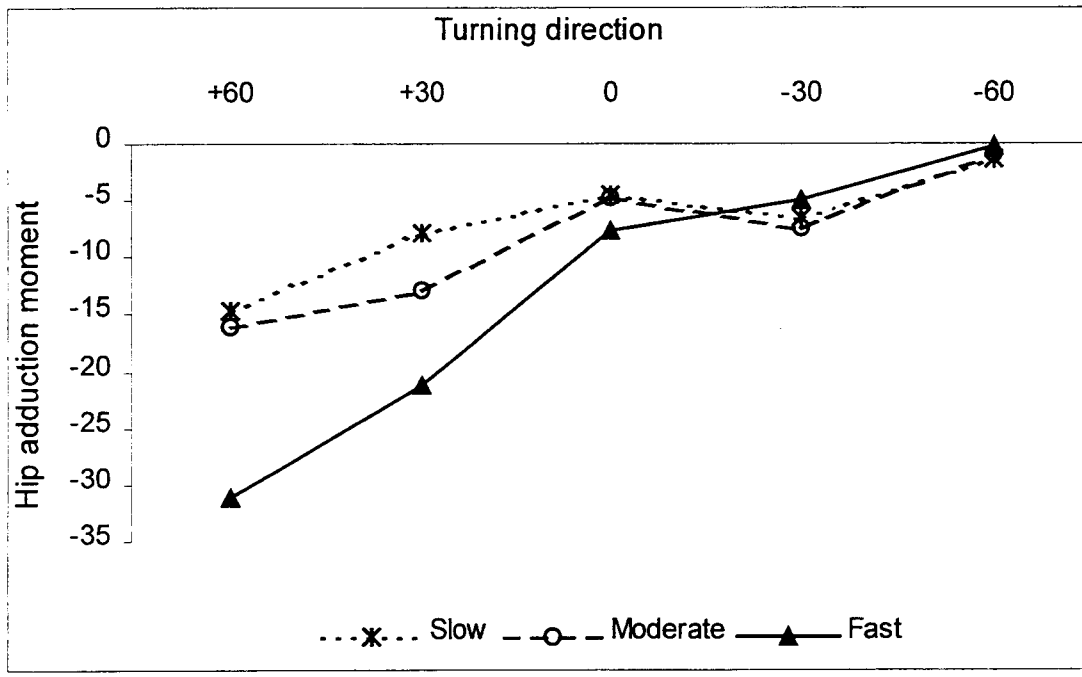

Figure 23. Running speed by turning direction interaction for hip adduction moment

DISCUSSION

Comparison of the current data from the straight running (0°) trials can be made with other results in the literature serving to validate the computational methods which were used here. Results of flexion-extension moments during straight running corresponded well with joint moment patterns for running in the literature (Buczek & Cavanagh, 1990; Gordon & Robertson, 1985; Harrison, Lees, McCullagh, & Rowe, 1986; Simpson & Bates, 1990; Winter, 1983). The pattern of ankle dorsi/plantar flexion moment resembled the joint moment pattern of runners reported by Buczek and Cavanagh (1990) and Gordon and Robertson (1985). The knee flexion/extension moment pattern also resembled patterns in the literature: the initial flexor moments shifted to extensor moments that reached maximum values during midstance. The hip flexion/extension moments were predominantly extensor and displayed two maxima which were similar to the results reported by other researchers (Simpson & Bates, 1990; Winter, 1983). The maximum extension joint moments during running have been reported for a variety of running velocities: 2.7 m/s by Winter (1983), 4.09 m/s by Simpson and Bates (1990), 4.5 m/s by Harrison et al. (1986) and Buczeck and Cavanagh (1990), and 5-6 m/s by Gordon and Robertson (1985). In this study, the maximum extension moment of the ankle, knee, and hip during fast straight running were approximately 100 Nm, 150 Nm, and 150 Nm, respectively. These values were generally lower than maximum extension moments presented by other authors which ranged from 160-220 Nm for the ankle, 150-300 Nm for the knee, and 80-250 Nm for

the hip, respectively. That this study resulted in an apparently low value for maximum extension moment may be explained by the difference in running speeds from other experimental settings. Additionally, runners in this study were not asked to maintain constant speed as in jogging or sprinting. During cutting movements directional change rather velocity is the primary characteristic. Therefore runners in this study may have diminished propulsive force later in stance, consequently producing smaller extension moments compared to other studies.

Furthermore, the moment in the frontal plane, such as inversion/eversion moment of the ankle and abduction/adduction moments of the knee and hip, were most affected by the turning direction. However, the calculation of this moment is most sensitive to the errors from defining joint center and anatomical axes and measurement of the point of application for the ground reaction force. For example, when the ground reaction force is 1000 N, a 1 cm error in the point of application of the ground reaction force from the joint axis can cause an error of 10 Nm. In this study, the maximum ankle inversion moment during slow (1.5 m/s) straight running was approximately 35 Nm. Since the most dominant external force for the ankle inversion moment is the vertical ground reaction force and the center of pressure is limited to excursion of about 4 cm within the medio-lateral side of the ankle joint, the maximum possible inversion moment would be between 30 and 40 Nm. This is in good agreement with the 35 Nm mean value observed.

In medial cutting movements, greater abduction moments of the ankle, adduction moments of the knee and external rotation and adduction moments of the

hip were found compared to values for straight running. Greater ankle abduction (external rotation) moments may help enable decelerating external rotation of the upper body and opposite leg. A potential explanation for greater adduction moments of the knee and hip is that these moments may support the weight of the body which is medial to the knee and hip, respectively. These moments provide the needed moments to keep the body from moving toward the stance leg during medial turning. Greater hip external rotation moments may serve to slow external rotations of the pelvis and opposite leg.

In lateral cutting movements, greater inversion and adduction moments of the ankle, abduction moments of the knee and hip were found compared to values for straight running. Greater ankle adduction (internal rotation) moments may help enable rotating of the upper body and opposite leg externally. During fast lateral turning there was a greater movement of the upper body and opposite leg to the pivot leg producing larger translations of the whole body center of mass. With this movement, the inversion movement at the ankle joint was produced by structures such as muscles (foot invertors) and ligaments. Although there was greater ankle inversion moment during fast lateral running, the ankle was still stable by the external eversion moment by the vertical ground reaction force and shifted center of pressure to the right side of the foot and lateral ground reaction force. One of the most common injuries of the foot is an ankle sprain that occurs in the lateral complex of the ankle during inversion. Parenteau, Viano, and Petit (1998) reported that ankle joint injury occurred at 34.1 ± 14.5 Nm and 34.3 ± 7.5° in inversion during quasi-static loading condition, while

Begeman, Balakrishnan, and King (1993) reported 35.1 ± 15.6 Nm and 60.5 ± 6.0° during dynamic loading conditions. Therefore, in unstable conditions, such as slipping or an uneven surface, which might result in excessive inversion, maximum value of inversion moment (≈ 110 Nm) during fast lateral turning movement in this study shows the great potential of ankle sprain.

An explanation for greater abduction moments of the knee and hip compared to values for straight running is that these moments may support the weight of the body which is lateral to the knee and hip, respectively. These moments provide the needed moments to keep the body from moving to the right during lateral turning.

The maximum torsional moment in cadaver knees without ligament damage is 35-80 Nm in internal/external rotation, and the ultimate strength in abduction/adduction is 125-210 Nm (Piziali, Nagel, Koogle, & Whalen, 1982). The maximum torsional moment supported by the knee in this study was 40 Nm in internal/external rotation and 95 Nm for abduction/adduction moment during fast medio-lateral turning. Although these values are within the range of the ultimate strength of the knee, it could be suggested that the faster and sharper cutting movements have a greater potential for knee injury. Especially, anterior cruiciate ligament (ACL) injury is usually caused by a twisting action while the knee is fixed and in an internally rotated and abduction position while supporting weight. If the trunk and thigh rotated over a lower extremity while supporting weight, the ACL can be sprained or torn as the lateral femoral condyle moves posterior in external rotation. Noyes, Butler, Grood, and Zernicke (1984) suggested that during fast cutting, tensile

load for the ACL reached to 1000 N and resulted in isolated fiber damages. Although turning direction was not significant for the maximum internal/external rotation moments of the knee, the maximum abduction/adduction moments increased during medial/lateral turning especially at fast running speed. Therefore excessive abduction/adduction moments during fast medial/lateral turning may affect hamstring activity that provides dynamic stability to the knee and lead ACL injury in non-contact situation.

Injuries to the hip joint account for a small percentage of total injuries in the lower extremity, because of the strong ligamentous and muscular support, and solid structural characteristics. Greater internal/external rotation and abduction/adduction moments of the hip during fast medial/lateral turning compared with straight running may result in imbalance of the lower extremity that might produce excessive loads to the knee and ankle joint.

Although much care was taken, three-dimensional inverse dynamics approach for human movement includes several sources of error. The most important parameters affecting the accuracy of the joint moment estimation are the vectors defining the flexion/extension and abduction/adduction moments axes, and measurements of the joint centers and center of pressure. Anatomical landmark calibration method is effective in identifying the joint centers and invisible bony markers and therefore improves the accuracy in defining three-dimensional axes of moments. It is obvious that large abduction/adduction and internal/external rotation moments should be produced for both propulsion and medio-lateral stability during cutting movements,

because the ground reaction force passes medial or lateral to the lower extremity joint centers. Although results in this study are in good agreement with this idea and other literature, a careful consideration is required to interpret absolute magnitude of moments, because moment calculation is very sensitive to various sources of error.

SUMMARY

During fast turning movements, high loads act on the joint system of the lower extremity for propulsion in the desired direction and for stabilization of the body. Consequently, high loads which are related to net muscle force and internal joint reaction forces may result in pain and injuries at the joints and their associated structures.

The objectives of this study were to determine the three-dimensional moments of ankle, knee, and hip joint during stance phase of various turning movements, and through comparisons to identify the effect of running speed and direction of cutting motion. Eight male subjects ran along a runway at three speeds (1.5, 3.0, and 4.5 m/s) and then to cut to the right or left (+60, +30, 0, -30, and -60°) of the right foot. Five trials at each speed and direction condition were recorded using video cameras and force plate. The inverse dynamics approach was used to integrate the body segment parameters, kinematics of segments and ground reaction forces data, and to solve the resultant joint moments.

Running speed was the major factor influencing the magnitude of the joint moments with this speed effect found at the ankle, knee, and hip joint. Knee extension moment showed the greatest increase by running speed, exhibiting an approximately threefold increase. The only moment component that did not substantially change with speed was the internal/external rotation moment of the knee joint. Turning direction also significantly affected the magnitude of the joint moments. In medial turning

movements, greater abduction moments of the ankle, adduction moments of the knee and external rotation and adduction moments of the hip were found. These results suggest that greater abduction moments of the ankle and external rotation moments of the hip helped enable decelerating external rotation of the upper body and swing leg, consequently these moments provided the stability of the interlimb coordination and the propulsion of body to the medial direction. Greater adduction moments of the knee and hip were primarily due to the medial offset of the body's center of mass and medial and lateral acceleration and deceleration of the center of mass during medial turning. In lateral turning movements, greater inversion moments of the ankle, abduction moments of the knee and hip were found. To move to lateral direction, the whole body center of mass may be translated by movement of the upper body and swing leg to the pivot leg. During this movement, to maintain stability and to shift the body to the right, greater inversion moment about the ankle joint is generated. Also, by the ground reaction force vector and moment arms, greater abduction moment about knee and hip joints is generated to support body weight and keep the body moving to the right.

Based on results of this study, during fast medio-lateral turning movements, higher torsional loads (internal/external rotation and abduction/adduction) were found to act on the lower extremity joint system. Contraction of the muscles crossing the joint probably reduces the potential for injury. The stiffness of the joint has been shown to increase under contraction of the muscles crossing the joint (Louie & Mote, 1987; Olmstread, Wever, Bryant, & Gouw, 1986). If the stiffness increases, the

resulting translations and rotations across the joint decrease for the same applied load, and the strain is reduced in the ligaments crossing the joint. Therefore, to improve performance and reduce the risk of joint injuries during fast turning movements, not only flexor/extensor but also abductor/adductor and rotator structures of the musculoskeletal system should be well strengthened through appropriate training. Furthermore, to decrease the risk of injuries which resulted from both high mechanical loads and excessive rotation of joint system, joint stability *may* be enhanced by various devices such as braces, taping, or specially designed sport shoes. The effectiveness of such devices has been a matter of considerable research effort (Anderson, Wojtys, Loubert, & Miller; 1992; Luethi et al.; 1986) without general agreement.

After completion of this study several suggestions can be made which might enhance future research. Characteristics of the muscle contraction pattern with respect to movement and joint moment pattern are important for the development of methods for training, evaluation and treatment of individuals with musculoskeletal injuries. Hence, measurement of muscle activation during cutting movements would add to the current findings. Analysis of joint moment, velocity of anatomical joint angles and power patterns could be used to determine an appropriation of the roles played by muscle groups in producing motion of the lower extremity.

Future research should probably include movement analysis of the whole body including swing leg and upper body during cutting movements. By evaluating both the kinematics and kinetics of whole body movement, researchers can get a clearer understanding of various movement strategies. Future study of other factors affecting

joint loads, such as braces, shoes and playing surfaces might clarify these devices affect cutting movements. Relationship between loading pattern and these factors may provide useful information for designing optimal equipment to improve performance and reduce injury.

BIBLIOGRAPHY

Anderson, K., Wojtys, E. M., Loubert, P. V., & Miller, R. E. (1992). A biomechanical evaluation of taping and bracing in reducing knee joint translation and rotation. American Journal of Sports Medicine, 20, 416-421.

Andrews, J. G., & Mish, S. P. (1996). Methods for investigating the sensitivity of joint resultants to body parameter variations. Journal of Biomechanics, 29, 651-654.

Angeloni, C., Cappozo, A., Catani, F., & Leardini, A. (1993). Quantification of relative displacement of skin- and plate-mounted markers with respect to bones. Journal of Biomechanics, 26, 864.

Apkarian, J., Naumann, S., & Cairnst, B. (1989). A three dimensional kinematic and dynamic model of the lower limb. Journal of Biomechanics, 22, 143-155.

Baumann, W. (1981). On mechanical loads on the human body during sports activities. In A. Morechi, K. Fidelus, K. Kedzior, & A. Wit (Eds.), Biomechanics VII-B (pp. 79-87). Baltimore, MD: University Park Press.

Begeman, P., Balakrishnan, P., & King, A. I. (1993). Dynamic human ankle response to inversion and eversion. Symposium Proceedings-Centers for Disease Control, 121-132.

Bell, A. L., Pederson, D. R., & Brand, R. A. (1990). A comparison of the accuracy of several hip center location methods. Journal of Biomechanics, 23, 617-621.

Blankevoort, L., Huiskes, R., & Lange, A. (1990). Helical axes of passive knee joint motions. Journal of Biomechanics, 23, 1219-1229.

Bogert, A. J. van den. (1994). Analysis and simulation of loads in the human musculoskeletal system, a methodological overview. Exercise and Sports Science Review, 22, 23-51.

Bogert, A. J. van den, Smith, G. D., & Nigg, B. M. (1994). In vivo determination of anatomical axes of the ankle joint complex: An optimization approach. Journal of Biomechanics, 27, 1477-1488.

Bogert, A. J. van den, Read, L., & Nigg, B. M. (1996). A method for inverse dynamic analysis using accelerometry. Journal of Biomechanics, 29, 949-954.

Bogert, A. J. van den, & Koning, J. J. de (1996). On optimal filtering for inverse dynamics analysis. Paper presented in Congress of Canadian Society of Biomechanics, Vancouver.

Brand, R. A., Pederson, D. R., & Friederson, J. A. (1986). The sensitivity of muscle force predictions to changes in physiologic cross-sectional area. Journal of Biomechanics, 19, 589-596.

Buczeck, F. L., & Cavanagh, P. R. (1990). Stance phase knee and ankle kinematics and kinetics during level and downhill running. Medicine and Science in Sports and Exercise, 22, 669-677.

Cappelo A., Cappozzo, A., Palombara, P. F., Lucchetti, L., & Leardini, A. (1997). Multiple anatomical landmark calibration for optimal bone pose estimation. Human Movement Science, 16, 259-274.

Cappozzo, A., Catani, F., Della Croce, U., & Leardini, A. (1995). Position and orientation in space of bones during movement: Anatomical frame definition and determination. Clinical Biomechanics, 10, 171-178.

Cappozzo, A., Catani, F., Leardini, A., Benedetti, M. G. & Della Croce, U. (1996). Position and orientation in space of bones during movement: Experimental artefacts. Clinical Biomechanics, 11, 90-100.

Challis, J. H. (1996). Accuracy of human limb movement of inertia estimations and their influence on resultant joint moments. Journal of Applied Biomechanics, 12, 517-530.

Cheze, L., Fregly, B. J., & Dimnet, J. (1995). A solidification procedure to facilitative kinematic analysis based on video motion. Journal of Biomechanics, 28, 879-884.

Colby, S., Francisco, A., Finch, M., Beutter, A., & Garrerr, W. (1997). Electromyographic and kinematic analysis of cutting maneuvers: Implications for anterior cruciate ligament injury. Proceedings of the 21st conference of the American Society of Biomechanics. Clemson University, SC.

Cole, G. K., Nigg, B. M., Ronsky, J. L., & Yeadon, M. R. (1993). Application of the joint coordinate system to three-dimensional joint attitude and movement representation: A standard proposal. Journal of Biomechanical Engineering, 115, 344-349.

Craig, J. J. (1989). Introduction to robotics: Mechanics and control. Realing, MA: Addison-Wesley.

Crowninshield, R. D., & Brand, R. A. (1981). A physiologically based criterion of muscle force prediction in locomotion. Journal of Biomechanics, 14, 793-801.

Dempster, W. T., & Gaugran, R. L. (1955). Properties of body segments based on size and weight. American Journal of Anatomy, 120, 33-54.

Engsberg, J. R., & Andrews, J. G. (1987). Kinematic analysis of the talocalcaneal/talocrural joint during running support. Medicine and Science in Sports and Exercise, 19, 275-284.

Gordon, D., & Robertson, E. (1985). Functions of the leg muscle during the stance phase of running. In B. Jonsson (Ed.), Biomechanincs X-B (pp. 1021-1027). Champaign, IL: Human Kinetics.

Grood, E. W., & Suntay, W. J. (1983). A joint coordinate system for the clinical description of the three-dimensional motion: Applications of the knee. Journal of Biomechanical Engineering, 105, 136-144.

Harrison, R. N., Lees, A., McCullagh, P. J. J., & Rowe, W. B. (1986). A bioengineering analysis of human muscle and joint forces in the lower limbs during running. Journal of Sports Science, 4, 201-218.

Herzog, W., & Binding, P. (1993). Co-contraction of pairs of antagonistic muscles-anatomical solution for planar-static optimization approaches. Mathematical Bioscience, 118, 83-95.

Hinrichs, R. N. (1985). Regression equations to predict segmental moments of inertia from anthropometric measurements: An extension of data of Chandler et al. (1975). Journal of Biomechanics, 18, 621-624.

Jensen, R. K. (1989). Changes in segment inertia proportions between 4 and 20 years. Journal of Biomechanics, 22, 529-536.

Kingma, I., Toussaint, H. M., Loose, M. P. de, & Dieen, J. H. (1996). Segment inertia parameter evaluation in two anthropometric models by application of a dynamic linked segment model. Journal of Biomechanics, 29, 693-704.

Ladin, Z., & Wu, G. (1991). Combining position and acceleration measurements for joint force estimation. Journal of Biomechanics, 24, 1173-1187.

Leva, P. (1996). Joint center longitudinal positions computed from a selected subset of Chandler's data. Journal of Biomechanics, 29, 1231-1233.

Luethi, S. M., Frederick, E. C., Hawes, M. R., & Nigg, B. M. (1986). Influence of shoe construction on lower extremity kinematics and load during lateral movements in tennis. International Journal of Sport Biomechanics, 2, 166-174.

Louie, J. K., & Mote, C. D. (1987). Contribution of the musculature to rotatory laxity and torsional stiffness at the knee. Journal of Biomechanics, 20, 281-300.

Mann, R. V., & Sprague, P. (1980). A kinetic analysis of the ground leg during sprint running. Research quarterly for Exercise and Sport, 51, 334-350.

Mann, R. V. (1981). A kinetic analysis of sprinting. Medicine and Science in Sports and Exercise, 13, 325-330.

McCaw, S. T., & DeVita, P. (1995). Errors in alignment of center of pressure and foot coordinates affect predicted lower extremity torques. Journal of Biomechanics, 28, 985-988.

McConville, J. T., Churchill, T. D., Kaleps, I., Clauser, C. E., & Cuzzi, I. (1980). Anthropometric relationships of body and body segment moments of inertia. United States Air Force Aerospace Medical Research Laboratory, AFAMRL-TP-80-119.

Nigg, B. M., & Cole, G. K. (1995). Measuring technique: Optical methods. In B. M. Nigg, & W.Herzog (Eds.), Biomechanics of the musculo-skeletal system (pp.254-286). New York, NY: John Wiley & Sons.

Nissan, M. (1980). Review of some basic assumptions in knee biomechanics. Journal of Biomechanics, 13, 375-381.

Noyes, F. R., Butler, D. L., Grood, E. S., Zernicke, R. F., & Hefzy, M. S. (1984). Biomechanical analysis of human ligament graft used in knee ligament repairs and reconstruction. Journal of Bone and Joint Surgery, 66A, 344-352.

O'Coner, B., Yack, H. J., & White, S. C. (1995). Reducing errors in kinetic calculations: Improved synchronization of video and ground reaction force records. Journal of Applied Biomechanics, 11, 216-223.

Olmstead, T. G., Wevers, H. W., Bryant, J. T., & Gouw, G. J. (1986). Effect of muscular activity on the valgus/varus laxity and stiffness of the knee. Journal of Biomechanics, 19, 565-577.

Parenteau, C. S., Viano, D. C., Petit, P. Y. (1998). Biomechanical properties of human cadaveric ankle-subtalar joints in quasi-static loading. Journal of Biomechanical Engineering, 120, 105-111.

Pearsall, D. J., & Costigan, P. A. (1996). The effect of segment parameter error on gait analysis. In proceedings of the 20th annual conference of the American society of Biomechanics (pp. 211-212). Atlanta, GA.

Piziali, R. L., Nagel, D. A., Koogle, T., & Whalen, R. (1982). Knee and tibia strength in snow skiing. In R. J. Johnson, W. Hauser, & M. Magi (Eds.), In Ski Trauma and Skiing Safety IV (pp.24-31). Munich: TUV Publication Series.

Simpson, K. J., & Bates, T. (1990). The effect of running speed on lower extremity joint moments generated during the support phase. International Journal of Sport Biomechanics, 6, 309-324.

Simpson, K. J., Shwokis, P. A., Alduwaisan, S., & Reeves, K. T. (1992). Factors influencing rearfoot kinematics during a rapid lateral braking movement. Medicine and Science in Sports and Exercise, 24, 586-594.

Smith, A. J. (1975). Estimates of muscle and joint forces at the knee and ankle during a jumping activity. Journal of Human Movement Studies, 1, 78-86.

Soderkvist, I., & Wedin, P. A. (1993). Determining the movements of the skeleton using well-configured markers. Journal of Biomechanics, 26, 1473-1477.

Soutas-Little, R. W., Beavis, G. C., Vertraete, M. C., & Markus, T. L. (1987). Analysis of foot motion during running using joint coordinate system. Medicine and Science in Sports and exercise, 19, 285-293.

Spoor, C., & Veldpaus, F. (1980). Rigid body motion calculated from spatial coordinates of markers. Journal of Biomechanics, 21, 45-54.

Stacoff, A., Steger, J., Stussi, E., & Reinschmidt, C. (1996). Lateral stability in sideward cutting movements. Medicine and Science in Sports and Exercise, 28, 350-358.

Vaughan, C. L., Davis, B. L., & O'Conner, J. C. (1992). Dynamics of human gait. Champaign, IL: Human Kinetics.

Verstraete, M. C. (1992). A technique for locating the center of mass and principal axes of the lower limb. Medicine and Science in Sports and Exercise, 24, 825-831.

White, S. C., Yack, H. J., & Winter, D. A. (1989). A three-dimensional musculoskeletal model for gait analysis: Anatomical variability estimates. Journal of Biomechanics, 22, 885-893.

Winter, D. A. (1983). Moments of force and mechanical power in jogging. Journal of Biomechanics, 16, 91-100.

Winter, D. A. (1990). Biomechanics and motor control of human movement. New York, NY: John Wiley & Sons.

Woltring, H. J. (1985). On optimal smoothing and derivative estimation from noisy displacement data in biomechanics. Human Movement Science, 4, 229-245.

Young, J. M., Chandler, R. F., Snow, C. C., Robinette, K. M., Zehner, G. F., & Lofberg, M. S. (1983). Anthropometric and mass distribution characteristics of the adult female. Federal Aviation Administration, FAA-AM-83-16.

Zarrugh, M. Y. (1981). Kinematic prediction of intersegment loads and power at the leg in walking. Journal of Biomechanics, 14, 713-725.

APPENDICES

APPENDIX A
Review of literature

This chapter is divided into four parts. In the first section, the current knowledge regarding lower extremity motion during medio-lateral movement is summarized. The second part deals with studies about joint loads during locomotion. The third part deals with the methodology concerning the determination of three-dimensional joint loads. The last part of this literature review presents and discusses problems associated with inverse dynamics and methods to improve the joint load estimation.

Lower extremity motion during medio-lateral movements

There are not many studies that investigate medio-lateral movement. Most studies have been limited to kinematics such as rearfoot angle during lateral movement. The rearfoot motion parameters, maximum rearfoot angle and maximum rearfoot velocity, as well as their corresponding times, may be used as indirect measures of stress to the lower leg and foot tissues. Determining the etiology of injuries and performance characteristics may also require understanding the biomechanical characteristics that influence rearfoot motion during lateral movements.

Lueti et al. (1986) investigated the influence of different kinds of tennis shoe construction on the kinematics of the foot and leg during fast lateral movement

(sideways shuffle) and the influence of the kinematic differences on the internal loading conditions. After wearing either a soft or stiff shoe for 3 months, each of 229 players was filmed performing a maximal effort lateral movement. Greater inversion values and internal resistance forces were reported for the soft-shoe condition. The authors observed wide intersubject variability for the execution of lateral movement, maximum vertical, and medio-lateral force values, and velocity of the foot at touchdown. These factors also could affect the magnitude of the rearfoot motion and loading forces, therefore predisposing certain players to pain. For instance, the players reporting pain also displayed greater velocity of the foot at touchdown. Because they used a simple model to compare loading patterns, they did not calculate actual internal forces on the lower extremity.

Simpson et al. (1992) studied the factors related to rearfoot kinematics during lateral braking movement. Seven highly skilled male tennis players performed side shuffle movement at four speeds (70, 80, 90, and 100% maximum speed). A rear view of the right leg performing a brake step onto a force plate was filmed. After analyzing various characteristics using statistical methods, they reported that average movement velocity, foot velocity at touchdown, and body mass demonstrated weak or nonsignificant correlation with the rearfoot parameters. Although inversion was correlated significantly with the maximum rearfoot angle and velocity, the results were affected by movement speed and sample size. They concluded that the biomechanical characteristics (force and temporal factors) were the most useful parameters for prediction of changes in rearfoot kinematics.

Stacoff et al. (1996) studied the effect of different shoe sole properties (hardness, thickness, and stiffness) and designs on the lateral stability during sideward cutting movement. Twelve subjects performed a cutting movement barefoot and with five different pairs of shoes, each filmed in the frontal plane. After analyzing various parameters such as the range of motion in inversion and angular velocity of the rearfoot, they concluded that inversion immediately after touchdown within the first 40 ms of the stance phase should be reduced to decrease the risk of injury in lateral cutting movements. Shoe sole properties and designs may affect the lateral stability by increasing or reducing the leverage about the subtalar joint.

Colby, Francisco, Finch, Beutter, and Garrerr (1997) investigated the muscle activation of the quadriceps and hamstrings and knee flexion angle during cutting motions. They assumed that the mechanism of anterior cruciate ligament (ACL) injury during non-contact situations might involve internal forces that are generated by the leg muscle of the athlete. EMG and two-dimensional kinematic data were collected while fifteen subjects performed sidestep cutting and crosscutting movements. Results of EMG and the corresponding knee flexion angle indicated that quadriceps activation began just before heel strike and peaked in mid eccentric motion while the minimum hamstring activation occurred just after heel strike. The maximum difference between quadriceps and hamstring muscle activation occurred after the minimum hamstring activation, but prior to the peak quadriceps activation. Heel strike occurred at an average of 22 degrees of knee flexion. They suggested that coupled with insufficient levels of hamstring activity that may not prevent anterior tibial displacement, forces

generated by the quadriceps muscles at the knee could produce significant anterior force to tear the ACL.

Joint loads studies during locomotion

Due to the invasive nature of direct measurements, the loads at the joints of the support lower extremity have been determined through models of the human body with inverse dynamics. In the following section, joint loads patterns during the stance phase of running and their corresponding muscle function with knowledge of resultant joint moments and joint kinematics will be discussed.

To relate joint moments and muscle function during movement, joint moment curves can be expressed with joint and/or segment angular velocity curves. When a joint moment is in the same direction as the angular velocity of the joint, it is sometimes referred to as a concentric moment, whereas if directions are opposite, it is referred to as an eccentric moment (Mann & Sprague, 1980). Muscle function patterns can be also derived by power which is calculated by product of moment and joint angular velocity (Winter, 1983). Positive and negative power values imply concentric and eccentric muscular dominance, respectively. Therefore analysis of joint moment, joint angular velocity, and power patterns may lead to an appreciation of the roles played by muscle groups in producing motion of the lower extremity.

The joint moments curves reported in the literature have been reasonably consistent between subjects and across running speeds (Baumann, 1981; Mann & Sprague, 1982; Winter, 1983; Simpson & Bates, 1990). Increased between subject

variability from the ankle to the hip has been reported by Mann (1981) and Winter. Winter reported large coefficient of variability magnitudes of 36.2, 45.5 and 77.5% for the ankle, knee and hip moments, respectively. Simpson and Bates found the joint moment parameters (peak joint moments and the relative and absolute times for various temporal events) increased with increases in running speed (3.06 to 4.60 m/s). However, the pattern of the increases was joint and subject dependent. The hip joint moment parameters exhibited the greatest number of significant increases with speed, averaging 59.0 % differences compared to 25.0% and 27.1 % differences for the ankle and knee joint moment parameters, respectively.

Just before and during the initial part of foot strike, very inconsistent patterns of ankle moment curve are generated. This variability may attribute to difficulties in smoothing joint coordinates through foot contact or locating the center of pressure of the ground reaction forces. After the initial impact phase, plantar flexor moment dominates for the entire stance phase. This moment is initially eccentric and helps to absorb the shock of landing and control the forward rotation of the tibia over the ankle, and is later concentric as it aids in propelling the body forward and upward (Mann & Sprague, 1980). The decrease in magnitude of this propulsive moment as toe-off is approached, may be due to the rapid rate of shortening of the plantar flexors.

Concentric knee flexor moments are generated during the impact phase (Mann & Sprague, 1980; Winter, 1983; Simpson & Bates, 1990). This moment could attenuate the impact and assist the hip extensor to reduce the horizontal velocity during ground contact. After initial concentric flexor moments, extensor moments act that

reach maximum value during midstance. These moments would allow for the storage of elastic energy in extensor muscles. However, high magnitudes of these moments might implicate hamstring injury (Mann & Sprague). Increased concentric knee extensor moments also serve directly to propel the body forward and upward (Mann & Sprague; Simpson & Bates).

Simpson and Bates (1990) have observed that hip joint moments were predominantly extensor and the appearance of flexor moment late in the stance phase, while other researchers (Mann & Sprague, 1980; Winter, 1983) have reported that the transition to flexor occurred during the midstance. Increased hip extensor moments can be interpreted as an attempt to minimize the braking effects and to dampen the impact shock to the trunk (Mann & Sprague; Simpson & Bates). The eccentric hip flexor moment may help to rotate the trunk forward for take-off (Mann & Sprague) or slow down thigh rotation in preparation for the swing phase (Winter).

Joint loads estimation

Transducers have been developed that can be implanted surgically to measure the force exerted by a muscle at the tendon. However, this direct measurement of forces has only applications in animal experiments, because it is invasive and requires sophisticated instrumentation and recording techniques (Bogert, 1994). Usually internal forces of the human body are calculated indirectly. With a full kinematic description, accurate anthropometric measures, and the external forces, it is possible to calculate the joint reaction forces and muscle moments (Winter, 1990).

The resultant joint loads are the sum of all structures spanning the joint. The loads cannot be directly broken into the specific forces in or on the capsule, ligaments, muscles, and articular contact surfaces. Various methods have been proposed for this decomposition process (Brand et al., 1986; Crowninshield & Brand, 1981; Herzog & Binding, 1993; Smith, 1975; White et al., 1989), but no approach has proven to represent the true physical situation.

To estimate muscle forces, which is extremely problematic, EMG can be used. However this technique requires a complex model that involves knowledge of the lengths, contraction velocities and stiffness of the muscles, and connective tissues at any given moment (Brand et al., 1986; Crowninshield & Brand, 1981). The other approach for deriving muscle forces is to estimate the physiological cross-sectional area (PCA) of all muscles that produce a similar action. The total stress of all the muscle may allow the determination of muscle forces by partitioning the individual muscle stresses (Winter, 1990). Muscle force estimates also are dependent on muscle moment arm lengths (Smith, 1975), which in turn, are sensitive to the accuracy of the muscle attachment coordinates (White et al., 1989).

Optimization is a method to select a unique solution from infinite number of solutions of an underdetermined system of equations. Herzog and Binding (1993) applied optimization theory to predict individual muscle force. However, this method is difficult to validate because the actual forces for human movement cannot be easily measured nor has the optimization criterion for impact movements been identified with certainty. These problems demonstrate that there are limitations to any practical

model of determining internal forces. Thus, inverse dynamics is the most widely used method for estimating internal loads as a validated method.

Generally net resultant loads in the human joints are estimated through the chain calculation process. The process begins with the ankle load that is evaluated from the ground reaction load on the foot and the foot kinematic state and mass/inertia parameters (kinematic refers to the position and orientation of the foot as well as the rotational and translation velocity and acceleration). After this the knee load is calculated from the ankle load and the calf kinematic state and mass/inertia. Last, the hip load is calculated from the knee load and the thigh kinematic state and mass/inertia. Thus, the evaluation proceeds from joint to joint, distal to proximal along the chain of body segments that compose the leg.

Other methods have been proposed for calculation of joint resultant loads (Zarrugh, 1981; Apkarian, Naumann, & Cairnst, 1989; Craig, 1989). Zarrugh used matrix methods to determine all the joint loads simultaneously. Apkarian et al. applied an alternate chain calculation that uses the joint kinematic state rather than segment kinematic state. This last approach, known as the Newton-Euler recursive inverse dynamics formulation, is commonly used in robotics to calculate the required torque in the motors at joints (Craig).

Early studies of locomotion analysis were limited to two-dimensional dynamics equations for the sagittal plane only because of limitations in available computational equipment. In addition, for normal human locomotion, the contribution of the nonsagittal joint dynamics to locomotion was significantly less than that in the

sagittal plane. Currently, however, with the wide availability of inexpensive powerful computers and the emphasis on pathological locomotion analysis, most computer software packages to evaluate joint kinetics during locomotion use fully three-dimensional equations.

In the analysis of three-dimensional dynamics, methodology concerning the determination of three-dimensional kinematics should be considered. In two-dimensions, segment and joint movement is well defined and unambiguous in the plane of interest. However, this is not the case for the determination of the three-dimensional kinematics. Joint attitude and movement in three-dimension can be expressed by several different ways. They include joint coordinate systems calculating Cardanic (or Euler) angles and respective translations, helical angles, finite helical axes, and instantaneous helical axes. All of these concepts have advantage and disadvantages, and depending on the research question, one or the other concept may be most appropriate (Nigg & Cole, 1994).

For locomotion studies, Cardan angles are most commonly used because they provide a representation of joint orientation based on an anatomical coordinate system. Typically, the position of three or more markers attached to the segments of interest is calculated using automatic video systems. These segmental markers can then be used to measure movement of a segmental anatomical coordinate system. Anatomical coordinate systems can be defined based on established relationships between bone embedded reference coordinate systems and external markers placed on anatomical landmarks (Cappozzo, Catani, Della Croce, & Leardini, 1995).

In this procedure, coordinate transformations are typically required which can be calculated using different methods (Spoor and Veldpaus, 1980; Soderkvist and Wedin, 1993). Having established two coordinate systems, the attitude and translations of one coordinate system relative to the other coordinate system is typically expressed by a 3×3 rotation matrix (direction cosine matrix) and a 3×1 translation vector, which can conveniently be represented together by a 4×4 matrix. From this matrix, a set of three independent angles (Cardan angles), and translations can be extracted by decomposition into an ordered sequence of rotations about and translations along three axes.

The magnitudes of rotational and translational components change depending on the rotational sequence. Therefore, the sequence of ordered rotations should be chosen so that the anatomical definitions are satisfied. For instance, the first joint axis is fixed to the proximal, the second joint axis is fixed to the distal segment, and the axis, typically referred to as the floating axis, is normal to the other two body fixed axes (Grood and Suntay, 1983). For the knee joint, Goody and Suntay proposed the sequence (1) flexion/extension occurs around the medio-lateral femur fixed axis, (2) abduction/adduction around the floating axis and (3) internal/external knee rotation around tibia fixed proximal-distal (longitudinal) axis to conform to the anatomical definitions of segment rotations.

For the foot motion at the ankle joint, Cole et al. (1993) proposed that plantar/dorsiflexion be calculated around the medio-lateral axis fixed in the shank, abduction/adduction around the floating axis, and in/eversion around the foot fixed

longitudinal axis. The proposal by Cole et al. was in contrast to the sequences used in earlier studies calculating the abduction/adduction around the foot fixed proximal-distal axis and the in/eversion around the floating axis (Soutas-Little, Beavis, Vertraete, & Markus, 1987; Engsberg & Andrews, 1987).

Methods to improve joint loads calculation

In the following paragraphs, several disadvantages of inverse dynamics analysis and methods that have been proposed to overcome these problems are presented.

Accurate estimation of body segment parameters

The reliability of inverse dynamics may depend on the degree of accuracy of body segment parameter (BSP). BSPs include segment mass, segment moment of inertia, location of the center of mass, orientation of the principal inertia axes of the segment, and the location of the joint center connecting the segments.

The mass of a segment is the integral over the segment volume of the differential volume times the density of this differential volume. The moment of inertia of the segment is a means of expressing mathematically how the mass of the segment is distributed relative to some coordinate system. The moments of inertia of body segments are commonly estimated in terms of principal inertia axes which are assumed to coincide with the anterior-posterior, medial-lateral, and proximal-distal axes of the segment (Hinrichs, 1985). Typically the segment mass and moments of

inertia are calculated from regression equations requiring anthropometric measurements as input or modeling the segments as geometric solids of known density (Kingma, Toussaint, Loose, & Dieen, 1996). Regression equations have been based on cadaver measurements or in vivo assessments of BSPs. Data exist for younger males (McConville et al., 1980) and females (Young, Chandler, Snow, Robinette, Zehner, & Lofberg, 1983) as well as children (Jensen, 1989). For geometric modeling, the dimensions of shape of the body segments are based on measurements on the experimental subjects.

Location of center of mass must be expressed relative to some objectively defined location or coordinate system on the segment. Typically in two dimensional kinetic analyses, this has been from the end of the segment along a line passing through the joints on either end of the segment and has been expressed as a percent of segment length (Dempster and Gaugran, 1955). In three-dimensional analyses, the same approach has been used and the center assumed to lie along the centerline of a segment (Hinrichs, 1985). More recently, methods have been developed to objectively estimate the three dimensional location of the mass center relative to coordinate systems generated from anatomical landmarks (McConville et al., 1980; Verstraete, 1992).

Studies evaluating the effects of error in the estimation of the segment inertial parameters, such as mass, moments of inertia, and center of mass, on calculated joint loads have been published (Challis, 1996; Andrews and Mish, 1996; Pearsall and Costigan, 1996). These have shown that the influence of errors in inertial parameters

when computing joint loads was small. Only if the accuracy of the joint resultant loads is a critical concern, a careful selection of inertial parameters estimation method will be required (Andrews and Mish, 1996). It is difficult to select best method for estimation of inertial parameters and that may be depend on the type of movement (Kingma et al., 1996). According to Pearsall and Costigan (1996), the effect of error in the estimation of the inertial parameters is minimal when the segment accelerations are low, such as during the stance phase of walking. However, the effect of error in the estimation of the inertial parameters will increase with high acceleration and small external loads such as during the swing phase of running.

The location of the joint center must be known relative to the coordinate systems of the segments being joined. Typically, human joints are assumed to be in a fixed position relative to each coordinate system and to be perfect hinges or ball-and-socket joints. When joint center positions are properly selected to the theoretical positions, the consequent position errors are considered to be negligible. It is recommended to use more accurate joint models, especially when joint center are utilized as reference points for determining segment inertial parameters (Leva, 1996). Although several sophisticated models exist for knee joint (Blankevoort, Huiskes, & Lange, 1990) and ankle joint (Bogert, Smith, & Nigg, 1994), the large amount of work is required to build such sophisticated models. The effects of error in the estimation of the joint centers on calculated kinetic quantities have not been well characterized. Nissan (1980) reported that the calculated knee joint moment was sensitive to the identified location of the joint center. A 1cm shift in the anterior-

posterior location of the knee joint center caused a 15% change in the magnitude of the knee joint moment during the stance phase of walking.

Reduction of skin movement artefact

External markers typically used in kinematic analyses of human movements may not give an accurate representation of the motion of the underlying bone that is actually being measured. This error, typically referred to as the skin movement artefact, is believed to be the major error source in human movement analyses (Cappozzo et al., 1996). There are several non-invasive methods proposed to reduce the skin movement artefact.

Cheze, Fregly, and Dimnet (1995) suggested a solidification model to reduce the skin movement artefact. Their model is based on geometrical considerations for a best rigid model. The solidification method is applied to each segment to which more than three markers are attached, and consists of the following procedure. First, the three markers defining the least perturbed triangle over time are identified. Second, from these three markers, the dimension of the triangle which best fits the triangle over time is calculate. Finally, the position of the "solid" triangle is fitted to the measured triangle throughout the motion. The measured marker positions are then replaced by the positions of the fitted "solid" triangle, and these new coordinates are then used for all further calculations. The solidification method may mainly reduce the relative movement of the skin markers with respect to each other. However, the three markers

yielding the best rigid model may still move as one unit with respect to the underlying bone.

The use of redundant number of skin markers (>3 markers) may also help to reduce the skin movement artefact. The algorithm presented by Soderkvist and Wedin (1993) may be applied to different combinations of skin markers. The marker combination providing the smallest norm of residuals, and thus providing the best rigid model may then be used for further calculations. However, the high number of markers at each segment may present a problem for automatic spatial tracking systems. Many cameras may be required so that every marker can be viewed during the entire motion.

The use of "technical frames' and the concept of "anatomical landmark calibration", introduced by Cappozzo et al. (1995) may provide the solution of the above problems. Using technical frames that are in an arbitrary position, the location of the anatomical landmarks in the relevant technical frame (calibration parameters) can be estimated. In the procedure described as a "anatomical landmark calibration", calibration parameters may be easily obtained using a pointer on which a minimum of two markers have been mounted at an adequate and known distance from its tip. Cappelo, Cappozzo, Palombara, Lucchetti, and Leardini (1997) proposed a modified protocol involving a multiple anatomical landmark calibration of all the selected anatomical landmarks for different poses of the body segment in the range of the movement under analysis to minimize skin movement artefact.

Treatments of kinematic data associated with high-frequency loading

The processing of kinematic data requires numerical differentiation, which tends to amplify noise in the measurements. This can be avoided by low-pass filtering (Woltring, 1985). The Butterworth digital filtering method is most widely used to remove noise. However, Woltring reported that higher order spline smoothing appeared to have superior performance compared with digital filters or Fourier analysis in boundary conditions. Boundary conditions are important when low cutoff frequencies are used and the data record is short.

Inverse dynamics analysis becomes increasingly inaccurate for high frequency loading, such as impact in running. In this case filtering is a major source of error. High-frequency peaks in the acceleration may be removed by filtering process. The severity of this problem depends on the segment mass, because acceleration is multiplied by segment mass in the inverse dynamics analysis.

In order to overcome this problem, two different approaches have been proposed; optimal filtering (Bogert & Koning, 1996) and use of accelerometers (Ladin & Wu, 1991; Bogert, Read, & Nigg, 1996). Bogert and Koning (1996) found optimal combination of cut-off frequencies for kinematic and force variables for typical running movement. They also suggested that optimal filer procedure could overcome problems associated with impact and inverse dynamics should be done twice: once to obtain moments and once to obtain force.

The use of accelerometers and angular rate sensors allows direct measurement of the linear acceleration and the angular velocity, and only one differentiation is

required for the angular acceleration. According to Bogert et al. (1996), the accelerometry method systematically underestimated the joint force and moment at the hip by about 20%, because forces generated by the swing leg were neglected. They also pointed out that the accelerometry analysis was not reliable during the impact phase of running, when the upper body and accelerometer did not behave as a rigid body.

Alignment of kinetic and kinematic data

The center of pressure represents the origin of the resultant ground reaction force vector. Error in accurately locating center of pressure on the foot arises because the ground reaction force and kinematic data are collected using independent measurement systems, often at different sampling rates. The kinematic and kinetic data must be aligned both spatially and temporally in the analysis. Operationally, spatial alignment refers to accurately digitizing the position of the human in relation to the force platform. Inaccurate alignment of the coordinate systems defining the point of application of the external ground reaction forces (center of pressure) and the segment endpoint coordinates may be potential sources of error when calculating joint moments.

McCaw and DeVita (1995) reported that the calculated joint torque was sensitive to the location of the center of pressure. The +0.5 and +1.0 cm shifts in the location of the center of pressure caused, on average, 7 and 14 % changes, respectively, in maximum joint torque and angular impulse values.

Minimizing temporal alignment error may result in greater accuracy and reliability in calculations used to determine joint kinetics. If the signal for synchronization comes on after the video image is captured, this signal will not be seen until the next video image. A one field synchronization error (1/60 s) may produce a 59% (30.07 Nm) difference in the maximum knee extension moment. O'Coner, Yack, and White (1995) provided a strategy of choosing sampling rate for synchronization of video and ground reaction force data. They recommended that use of an A/D sampling rate of 598 Hz with algorithm for vertical blanking pulse in video signal would enable video and analog data to be synchronized to within 1/1196 s.

Summary

There are not many studies that investigate medio-lateral movement. Most studies have been limited to kinematics such as rearfoot angle during lateral movement. Although the rearfoot angle and velocity is a one of indirect measures of stress to the lower leg and foot tissues, to determine the injury mechanism and turning movements strategy, kinematic measurements to show how the moments about joints are effected are required.

Due to the invasive nature of direct measurements, the loads at the joints of the support lower extremity have been determined through models of the human body with inverse dynamics. The resultant joint loads from inverse dynamics approach are the sum of all structures spanning the joint. The loads cannot be directly broken into the specific forces in or on the capsule, ligaments, muscles, and articular contact

surfaces. Various methods have been proposed for this decomposition process but no approach has proven to represent the true physical situation.

Early studies of locomotion analysis were limited to two-dimensional dynamics equations for the sagittal plane only because of limitations in available computational equipment. In addition, for normal human locomotion, the contribution of the nonsagittal joint dynamics to locomotion was significantly less than that in the sagittal plane. Currently, however, with the wide availability of inexpensive powerful computers and the emphasis on pathological locomotion analysis, most computer software packages to evaluate joint kinetics during locomotion use fully three-dimensional equations.

The reliability of inverse dynamics may depend on the degree of accuracy of body segment parameter. Typically the segment mass and moments of inertia are calculated from regression equations. Recently, methods have been developed to objectively estimate the three dimensional location of the mass center and joint center relative to coordinate systems generated from anatomical landmarks. The skin movement artefact is the major error source in human movement analyses. The use of "technical frames' and the concept of "anatomical landmark calibration" may provide the solution of the skin movement artefact problems. Inverse dynamics analysis becomes increasingly inaccurate for high frequency loading, such as impact in running. In this case filtering is a major source of error. High-frequency peaks in the acceleration may be removed by filtering process. To overcome this problem, optimal filtering and use of accelerometers have been proposed. Minimizing spatial and

temporal alignment error also result in greater accuracy and reliability in calculations used to determine joint kinetics.

APPENDIX B

Characteristics of subjects

Subject Number	Age	Weight (kg)	Leg length (m)
1	21	72	0.95
2	21	75	0.89
3	20	69	0.93
4	23	71	0.89
5	21	63	0.84
6	20	76	0.85
7	20	81	0.95
8	20	73	0.98
Average	**20.8**	**72.5**	**0.91**

APPENDIX C

Normalized maximum moments data

Ankle moment	Turning direction	Running speed	Subject							
			1	2	3	4	5	6	7	8
AINV	+60	1.5	-2.75	-0.02	-4.37	-5.30	-4.52	-9.72	-7.42	-3.23
AINV	+60	3.0	-3.48	-5.03	-5.61	-7.57	-2.03	-6.32	-9.70	-7.39
AINV	+60	4.5	-4.38	-7.90	-7.29	-6.54	-6.29	-9.48	-12.23	-4.92
AINV	+30	1.5	-5.58	-3.96	-5.22	-6.68	-4.17	-5.32	-8.14	-4.95
AINV	+30	3.0	-12.51	-6.37	-8.38	-10.04	-2.00	-9.54	-11.13	-8.03
AINV	+30	4.5	-8.38	-8.12	-3.26	-6.55	-3.68	-9.41	-11.15	-6.30
AINV	0	1.5	-3.71	-6.65	-5.42	-5.66	-4.99	-4.76	-7.32	-6.04
AINV	0	3.0	-10.14	-9.21	-11.48	-11.59	-11.76	-10.09	-15.73	-9.95
AINV	0	4.5	-15.43	-6.93	-15.26	-10.99	-12.63	-9.09	-14.52	-11.84
AINV	-30	1.5	-4.94	-5.74	-5.27	-6.01	-5.56	-7.43	-7.76	-6.37
AINV	-30	3.0	-13.64	-7.63	-12.04	-18.02	-16.92	-11.09	-18.31	-11.33
AINV	-30	4.5	-16.96	-10.41	-17.35	-20.21	-27.04	-13.88	-18.63	-15.77
AINV	-60	1.5	-5.06	-8.02	-6.49	-8.10	-4.75	-7.47	-8.61	-7.82
AINV	-60	3.0	-12.41	-13.67	-11.92	-14.22	-15.33	-17.78	-15.76	-19.31
AINV	-60	4.5	-14.94	-17.12	-24.00	-13.26	-18.51	-15.15	-16.59	-18.18
AEVE	+60	1.5	2.10	8.36	1.31	0.46	0.66	1.85	0.00	4.61
AEVE	+60	3.0	4.70	3.22	2.01	0.36	2.39	0.00	0.00	1.88
AEVE	+60	4.5	4.64	5.59	1.33	0.21	7.03	0.00	0.00	3.14
AEVE	+30	1.5	0.00	4.05	0.00	1.40	0.94	1.08	0.00	1.68
AEVE	+30	3.0	0.00	1.01	0.18	0.00	3.94	0.05	0.25	0.12
AEVE	+30	4.5	0.84	5.74	2.68	1.61	5.33	0.25	0.00	0.18
AEVE	0	1.5	0.00	0.32	0.00	0.00	0.00	0.00	0.00	0.00
AEVE	0	3.0	0.00	0.00	0.16	0.16	0.28	0.03	0.31	0.00
AEVE	0	4.5	0.18	0.37	0.29	0.00	0.00	0.15	0.00	0.00
AEVE	-30	1.5	0.24	0.00	0.00	0.00	0.00	0.00	0.00	0.00
AEVE	-30	3.0	0.14	0.03	0.24	0.04	0.00	0.16	0.00	0.00
AEVE	-30	4.5	0.07	0.00	0.32	0.00	0.14	0.07	0.34	0.18
AEVE	-60	1.5	0.00	0.00	0.00	0.00	0.00	0.00	0.00	0.00
AEVE	-60	3.0	0.00	0.03	0.05	0.00	0.21	0.14	0.00	0.09
AEVE	-60	4.5	0.00	0.00	0.55	0.00	0.38	0.18	0.01	0.00
AFLEX	+60	1.5	-2.15	0.00	-4.66	-0.46	-4.77	-0.46	-4.02	-1.42
AFLEX	+60	3.0	-2.03	-0.94	-5.54	-0.72	-0.98	-4.84	-1.62	-5.98
AFLEX	+60	4.5	-2.71	-3.90	-16.65	-6.30	-4.58	-7.26	-2.67	-3.38
AFLEX	+30	1.5	-1.24	-1.06	-5.07	-3.14	-7.12	-1.27	-4.20	-3.56
AFLEX	+30	3.0	-1.60	-3.15	-4.73	-2.59	-0.09	-2.30	-2.67	-5.67
AFLEX	+30	4.5	-0.20	-4.94	-5.93	-0.85	-4.29	-5.24	-0.94	-3.70
AFLEX	0	1.5	-1.68	-3.13	-3.23	-1.66	-4.87	-2.75	-2.69	-3.86
AFLEX	0	3.0	-1.84	-0.54	-3.42	-0.82	-0.96	-0.68	-2.56	-3.28
AFLEX	0	4.5	-1.97	-3.21	-5.89	-1.17	-0.25	-1.40	-2.62	-11.49
AFLEX	-30	1.5	-2.42	0.00	-2.67	-0.27	-3.72	-0.28	-3.62	-2.86

AFLEX	-30	3.0	-1.64	0.00	-3.96	-0.99	-3.94	-5.58	-3.64	-5.30
AFLEX	-30	4.5	-1.53	-3.24	-10.23	-0.32	-1.33	0.00	-3.94	-0.52
AFLEX	-60	1.5	-2.08	-3.32	-1.27	-3.78	-5.58	-2.83	-1.69	-3.22
AFLEX	-60	3.0	-1.90	-1.44	-4.05	-0.68	-1.94	-3.23	-2.24	-2.94
AFLEX	-60	4.5	-1.38	-0.87	-3.49	-1.25	-2.24	0.00	-2.34	-5.33
AEXTN	+60	1.5	10.98	21.15	9.12	11.22	13.38	14.34	9.03	12.98
AEXTN	+60	3.0	19.13	14.66	10.66	12.94	13.28	14.30	12.28	12.43
AEXTN	+60	4.5	20.27	11.89	11.44	13.08	15.81	21.44	13.92	12.24
AEXTN	+30	1.5	12.91	11.21	8.01	7.45	11.33	13.97	9.27	11.55
AEXTN	+30	3.0	11.86	14.04	12.60	15.12	17.36	16.02	11.06	10.84
AEXTN	+30	4.5	21.94	9.41	14.13	14.93	27.25	21.35	14.81	14.48
AEXTN	0	1.5	10.61	10.94	8.06	6.23	11.73	10.27	9.49	10.43
AEXTN	0	3.0	14.56	13.79	13.23	16.65	18.27	19.61	10.85	13.13
AEXTN	0	4.5	19.98	10.75	9.82	18.03	21.11	17.68	14.55	12.43
AEXTN	-30	1.5	9.45	25.45	8.04	7.25	9.32	10.37	7.91	10.43
AEXTN	-30	3.0	14.43	34.14	10.43	15.62	17.69	12.30	10.51	11.62
AEXTN	-30	4.5	13.52	12.93	11.06	20.98	18.82	10.42	8.40	13.03
AEXTN	-60	1.5	9.05	11.38	7.54	6.38	8.10	9.32	8.43	8.06
AEXTN	-60	3.0	9.31	15.18	8.83	14.09	11.24	15.36	9.22	9.63
AEXTN	-60	4.5	4.78	17.07	8.46	13.19	10.28	17.41	4.75	8.37
AABD	+60	1.5	3.74	12.36	2.56	7.87	4.96	6.17	4.77	5.52
AABD	+60	3.0	8.10	9.55	3.03	7.25	5.41	2.69	5.22	3.42
AABD	+60	4.5	9.50	8.75	3.46	8.72	10.37	4.03	7.12	4.78
AABD	+30	1.5	2.89	6.87	0.97	5.68	2.96	5.29	3.74	3.15
AABD	+30	3.0	0.51	8.09	0.97	7.19	5.54	3.12	3.11	1.44
AABD	+30	4.5	7.26	8.72	4.77	10.64	9.39	7.51	6.92	4.13
AABD	0	1.5	1.08	3.84	0.20	1.85	2.24	1.70	2.33	0.45
AABD	0	3.0	2.30	4.43	0.29	2.55	0.73	1.97	1.04	0.00
AABD	0	4.5	2.39	4.19	0.21	2.41	2.07	1.14	1.24	0.00
AABD	-30	1.5	0.75	6.14	0.09	2.02	0.74	5.45	0.72	0.00
AABD	-30	3.0	1.43	6.37	0.48	0.15	0.00	0.14	0.00	0.00
AABD	-30	4.5	2.31	0.04	1.82	2.51	4.49	0.56	0.15	1.19
AABD	-60	1.5	0.77	1.26	0.07	0.76	1.63	0.62	0.13	0.00
AABD	-60	3.0	0.72	0.39	0.83	1.71	0.09	1.45	0.06	0.04
AABD	-60	4.5	1.01	0.00	3.41	0.01	0.38	0.28	0.12	0.07
AADD	+60	1.5	-0.27	0.00	-2.20	-1.28	-1.78	-3.68	-4.10	-0.87
AADD	+60	3.0	-0.31	-1.78	-2.51	-0.64	-0.16	-3.59	-2.93	-2.98
AADD	+60	4.5	-1.33	-6.69	-9.96	-5.88	-10.33	-5.39	-8.10	-1.85
AADD	+30	1.5	-0.02	-1.23	-1.89	-4.20	-2.56	-2.13	-3.33	-1.51
AADD	+30	3.0	-4.56	-2.93	-2.00	-1.99	-0.13	-1.75	-3.19	-3.01
AADD	+30	4.5	0.00	-6.91	-2.41	-0.29	-2.92	-3.82	-2.03	-1.88
AADD	0	1.5	0.00	-2.90	-1.13	-2.45	-1.52	-1.46	-2.35	-1.62
AADD	0	3.0	-1.55	-1.11	-2.73	-1.00	-0.35	-0.04	-3.81	-3.36
AADD	0	4.5	-1.80	-3.50	-9.48	-0.30	0.00	-0.40	-2.00	-4.31
AADD	-30	1.5	-1.02	0.00	-1.60	-2.06	-1.74	-0.30	-2.36	-2.82
AADD	-30	3.0	-4.87	-0.01	-4.95	-3.98	-3.19	-4.23	-5.40	-7.43
AADD	-30	4.5	-6.81	-4.96	-9.18	-0.74	-2.00	-5.57	-8.82	-9.95
AADD	-60	1.5	-0.73	-2.52	-0.96	-4.86	-2.26	-4.07	-3.26	-3.77
AADD	-60	3.0	-4.73	-2.18	-5.13	-4.14	-6.36	-5.93	-6.25	-11.71
AADD	-60	4.5	-4.99	-4.11	-14.40	-7.53	-8.81	-4.91	-8.09	-12.90

Knee moment	Turning direction	Running speed	Subject							
			1	2	3	4	5	6	7	8
KINTR	+60	1.5	0.87	4.73	2.56	1.48	3.09	3.41	2.12	1.73
KINTR	+60	3.0	0.90	3.64	4.05	1.55	0.16	3.22	3.87	2.87
KINTR	+60	4.5	6.90	6.57	8.08	3.16	7.91	4.83	8.67	1.82
KINTR	+30	1.5	0.79	3.34	5.08	4.69	2.68	2.56	1.79	1.92
KINTR	+30	3.0	0.97	3.25	5.81	1.61	0.85	6.73	4.16	2.73
KINTR	+30	4.5	1.71	7.58	1.37	2.15	2.84	3.76	3.70	1.68
KINTR	0	1.5	0.24	3.12	1.39	1.89	1.90	1.14	1.36	1.61
KINTR	0	3.0	1.99	2.95	2.41	1.26	0.32	0.18	6.36	1.08
KINTR	0	4.5	3.42	3.06	8.07	3.52	0.11	0.00	4.64	2.65
KINTR	-30	1.5	0.60	7.58	1.68	1.63	1.39	1.44	1.47	1.66
KINTR	-30	3.0	0.82	9.85	2.16	2.01	4.39	4.22	5.61	3.69
KINTR	-30	4.5	0.36	6.57	4.13	1.12	0.53	2.73	6.91	2.00
KINTR	-60	1.5	0.65	3.31	1.51	4.58	2.35	1.59	1.02	2.30
KINTR	-60	3.0	0.50	3.17	1.77	3.33	5.27	2.75	5.32	3.51
KINTR	-60	4.5	1.09	5.42	3.93	1.97	7.77	2.36	5.30	4.44
KEXTR	+60	1.5	-1.39	-7.42	-0.32	-3.73	-5.08	-2.39	-0.44	-3.67
KEXTR	+60	3.0	-0.61	-0.92	-0.57	-6.56	-13.92	-1.34	-0.39	-1.22
KEXTR	+60	4.5	-0.92	-1.02	-0.69	-7.56	-21.06	-2.01	-0.46	-2.77
KEXTR	+30	1.5	-1.23	-2.07	-0.16	-5.42	-5.90	-1.93	-1.16	-1.94
KEXTR	+30	3.0	-0.70	-0.10	-0.09	-7.12	-6.52	-0.94	-0.28	-0.49
KEXTR	+30	4.5	-0.73	-0.48	-2.47	-9.80	-14.38	-0.67	0.00	-2.33
KEXTR	0	1.5	-1.71	-0.87	-0.15	-4.83	-3.68	-0.72	-0.89	-1.12
KEXTR	0	3.0	-1.15	-0.04	-0.33	-6.63	-4.17	-1.71	-0.17	0.00
KEXTR	0	4.5	-0.33	-0.17	-0.18	-9.04	-7.08	-2.88	0.00	0.00
KEXTR	-30	1.5	-4.31	-4.12	-3.14	-2.87	-2.96	-1.47	-0.81	-0.98
KEXTR	-30	3.0	-0.85	-0.80	-1.50	-0.76	-3.06	-0.16	0.00	0.00
KEXTR	-30	4.5	-1.88	0.00	-0.65	-3.85	-7.27	-0.36	-0.11	-0.94
KEXTR	-60	1.5	-1.87	-1.23	-1.78	-0.94	-6.94	-1.72	-1.19	-1.57
KEXTR	-60	3.0	-1.53	-1.53	-3.35	-0.12	-4.75	-0.25	-0.24	0.00
KEXTR	-60	4.5	-2.89	-0.37	0.00	-0.49	-0.86	-0.91	0.00	0.00
KFLEX	+60	1.5	0.77	0.85	0.69	7.23	10.64	13.31	4.05	0.03
KFLEX	+60	3.0	1.30	0.01	0.35	0.19	0.00	2.89	1.70	5.72
KFLEX	+60	4.5	0.00	0.79	0.80	0.82	0.00	4.33	0.78	3.25
KFLEX	+30	1.5	2.51	0.00	0.28	2.25	3.27	9.20	3.31	4.59
KFLEX	+30	3.0	0.00	0.00	0.00	1.49	0.00	3.93	0.74	4.46
KFLEX	+30	4.5	4.06	0.00	1.41	4.62	0.00	1.44	1.13	4.69
KFLEX	0	1.5	0.24	0.00	0.53	1.45	3.56	3.88	3.06	5.61
KFLEX	0	3.0	0.07	0.00	0.00	0.00	0.17	3.70	0.00	2.02
KFLEX	0	4.5	1.94	0.00	1.10	0.55	1.34	0.15	1.01	2.92
KFLEX	-30	1.5	0.00	0.00	0.43	3.42	4.73	6.60	1.89	2.06
KFLEX	-30	3.0	0.00	0.00	0.17	0.91	0.00	1.25	0.00	0.05
KFLEX	-30	4.5	0.71	0.00	0.18	12.55	0.93	2.89	0.00	7.10
KFLEX	-60	1.5	4.39	0.00	4.02	4.37	3.94	5.61	4.57	3.40
KFLEX	-60	3.0	0.00	0.00	0.00	0.05	0.00	2.65	0.37	2.29
KFLEX	-60	4.5	0.37	2.29	1.77	1.30	0.95	8.11	0.39	2.17
KEXTN	+60	1.5	-14.35	-4.53	-19.92	-2.05	-3.49	-6.19	-9.96	-7.82

KEXTN	+60	3.0	-25.31	-29.74	-27.88	-20.00	-15.60	-31.69	-21.99	-17.64
KEXTN	+60	4.5	-39.72	-48.73	-32.74	-32.20	-41.05	-47.54	-38.89	-15.89
KEXTN	+30	1.5	-12.40	-25.49	-20.48	-9.61	-12.85	-1.62	-7.87	-0.80
KEXTN	+30	3.0	-22.55	-30.54	-27.62	-16.47	-15.38	-22.93	-24.21	-16.71
KEXTN	+30	4.5	-20.08	-50.24	-33.27	-11.41	-20.59	-36.14	-19.97	-16.93
KEXTN	0	1.5	-11.76	-27.02	-12.90	-7.22	-7.82	-4.76	-2.08	-0.48
KEXTN	0	3.0	-20.55	-32.81	-22.90	-13.46	-13.74	-5.74	-24.13	-14.71
KEXTN	0	4.5	-28.71	-42.77	-27.72	-8.58	-11.63	-24.29	-17.61	-21.35
KEXTN	-30	1.5	-11.26	-3.56	-11.46	-2.42	-5.59	-0.18	-5.03	-4.45
KEXTN	-30	3.0	-24.87	-5.90	-23.09	-12.21	-19.10	-25.11	-18.52	-17.63
KEXTN	-30	4.5	-27.88	-49.97	-39.71	0.00	-14.28	-25.98	-26.36	-4.58
KEXTN	-60	1.5	-6.43	-25.57	-4.97	-10.31	-8.74	-7.28	-0.89	-2.62
KEXTN	-60	3.0	-22.87	-35.36	-22.09	-17.95	-18.83	-21.11	-17.24	-9.69
KEXTN	-60	4.5	-9.98	-34.07	-18.41	-14.88	-29.85	-20.61	-22.13	-11.17
KABD	+60	1.5	4.27	7.55	0.06	12.17	3.52	11.31	2.50	8.15
KABD	+60	3.0	0.60	2.42	0.26	0.00	0.00	0.00	2.65	9.81
KABD	+60	4.5	0.00	0.89	0.00	0.00	0.00	0.00	0.00	1.31
KABD	+30	1.5	4.09	1.90	2.30	1.33	1.33	8.37	2.22	7.14
KABD	+30	3.0	7.84	2.94	2.80	3.75	3.75	0.92	1.33	11.56
KABD	+30	4.5	1.65	0.00	3.64	1.10	1.10	0.63	2.58	12.70
KABD	0	1.5	3.13	2.15	3.93	2.81	4.99	4.18	1.06	5.57
KABD	0	3.0	5.08	2.72	3.95	3.66	7.01	6.97	0.07	9.16
KABD	0	4.5	0.84	1.76	1.99	0.48	10.85	9.89	0.16	11.93
KABD	-30	1.5	8.77	4.16	6.49	5.39	4.85	2.82	1.95	3.38
KABD	-30	3.0	6.58	1.05	8.68	5.29	7.93	2.46	0.72	6.69
KABD	-30	4.5	13.09	6.21	18.07	12.15	19.49	8.20	3.21	9.92
KABD	-60	1.5	3.81	7.04	9.41	6.10	10.21	1.55	1.92	3.90
KABD	-60	3.0	12.85	16.15	21.49	16.58	16.01	10.78	1.68	9.94
KABD	-60	4.5	12.21	5.07	13.75	9.97	8.92	12.94	12.22	10.93
KADD	+60	1.5	-2.37	-6.17	-5.66	-0.87	-1.27	-0.72	-1.76	-0.33
KADD	+60	3.0	-4.04	-7.25	-6.40	-5.63	-5.63	-8.40	-3.90	-2.75
KADD	+60	4.5	-18.63	-14.03	-21.88	-15.78	-15.78	-12.60	-13.98	-5.25
KADD	+30	1.5	-1.26	-4.03	-6.33	-2.77	-2.77	-0.60	-1.28	-0.73
KADD	+30	3.0	-0.38	-6.39	-4.34	-1.74	-1.74	-6.05	-3.60	0.00
KADD	+30	4.5	-2.69	-14.68	-5.09	-6.08	-6.08	-10.87	-4.14	-0.66
KADD	0	1.5	-1.03	-3.19	-1.46	-1.43	0.00	-0.18	-0.98	-0.89
KADD	0	3.0	-1.17	-1.77	-0.30	-0.77	-0.95	-0.39	-3.25	-0.33
KADD	0	4.5	-2.85	-2.13	-2.89	-1.51	0.00	-0.36	-3.96	-0.13
KADD	-30	1.5	-0.07	-7.89	-1.64	-2.77	-1.37	-2.20	-1.04	-0.84
KADD	-30	3.0	-0.11	-10.49	-0.14	-2.99	-0.97	-1.90	-2.06	-1.88
KADD	-30	4.5	0.00	-4.07	0.00	0.00	0.00	-1.51	-1.40	-0.60
KADD	-60	1.5	0.00	-3.58	0.00	-0.73	-1.29	-2.77	-2.00	-0.28
KADD	-60	3.0	0.00	-0.40	0.00	0.00	-0.34	-0.27	-3.42	-0.90
KADD	-60	4.5	0.00	-3.76	0.00	0.00	0.00	0.00	0.00	-0.40

Hip moment	Turning direction	Running speed	Subject							
			1	2	3	4	5	6	7	8
HINTR	+60	1.5	3.10	8.08	2.01	3.40	4.14	4.16	1.31	1.12
HINTR	+60	3.0	2.24	3.06	0.00	1.68	1.63	0.30	0.00	0.00
HINTR	+60	4.5	2.88	0.58	0.00	0.00	1.78	0.44	0.00	0.00
HINTR	+30	1.5	6.42	4.29	6.31	4.07	0.29	5.58	2.21	1.18
HINTR	+30	3.0	4.02	4.59	0.34	0.24	0.00	0.97	0.45	0.66
HINTR	+30	4.5	6.96	3.20	2.04	2.79	0.00	1.57	1.21	0.15
HINTR	0	1.5	6.84	7.03	2.72	1.05	2.20	1.64	1.77	1.23
HINTR	0	3.0	3.56	4.69	6.12	0.73	0.67	0.83	3.26	0.91
HINTR	0	4.5	10.20	4.63	5.02	6.47	0.00	2.14	2.71	2.28
HINTR	-30	1.5	12.40	10.02	3.86	4.01	1.58	2.04	1.80	1.41
HINTR	-30	3.0	3.04	9.82	10.00	4.08	4.24	5.50	6.38	2.71
HINTR	-30	4.5	4.03	12.53	12.01	5.81	5.36	6.02	6.64	4.62
HINTR	-60	1.5	0.00	3.07	7.94	6.39	3.05	3.68	1.36	0.37
HINTR	-60	3.0	1.22	3.05	12.07	4.36	10.52	13.91	5.60	4.41
HINTR	-60	4.5	0.00	0.00	16.55	10.93	19.14	13.08	13.09	6.83
HEXTR	+60	1.5	-11.19	-28.45	-5.67	-0.65	-0.66	-4.06	-1.81	-5.05
HEXTR	+60	3.0	-21.94	-12.91	-12.52	-5.80	-5.89	-15.39	-8.95	-8.83
HEXTR	+60	4.5	-25.52	-12.92	-42.24	-31.86	-17.76	-23.09	-22.21	-18.45
HEXTR	+30	1.5	-15.08	-9.12	-4.47	-3.32	-3.12	-1.47	-2.32	-2.96
HEXTR	+30	3.0	-7.32	-11.28	-5.51	-9.35	-4.22	-7.91	-7.46	-5.85
HEXTR	+30	4.5	-30.96	-16.44	-9.97	-4.09	-14.83	-18.42	-9.36	-8.23
HEXTR	0	1.5	-9.15	-5.43	-1.87	-6.93	-4.07	-2.32	-1.42	-2.30
HEXTR	0	3.0	-11.58	-9.38	-1.80	-2.10	-2.89	-0.94	-1.74	-2.64
HEXTR	0	4.5	-22.31	-17.36	-0.47	-0.16	-1.50	-0.93	-3.71	-4.80
HEXTR	-30	1.5	-7.96	-26.18	-3.95	-6.37	-8.27	-3.96	-1.74	-3.35
HEXTR	-30	3.0	-12.82	-33.94	-0.28	-0.92	-0.48	-0.70	0.00	-3.19
HEXTR	-30	4.5	-12.17	-10.82	0.00	0.00	0.00	-0.26	0.00	-1.41
HEXTR	-60	1.5	-10.19	-8.24	-0.03	-3.58	-9.44	-3.08	-1.69	-3.10
HEXTR	-60	3.0	-10.42	-7.58	0.00	-0.04	0.00	-1.97	0.00	-1.64
HEXTR	-60	4.5	-19.62	-12.16	0.00	0.00	-0.47	0.00	0.00	-2.28
HFLEX	+60	1.5	3.10	8.08	3.24	0.89	0.89	0.45	1.10	0.00
HFLEX	+60	3.0	2.24	3.06	1.49	3.71	10.70	4.22	1.73	0.00
HFLEX	+60	4.5	2.88	0.58	1.36	2.71	4.82	6.32	0.89	0.00
HFLEX	+30	1.5	6.42	4.29	11.19	4.61	14.83	3.75	3.40	0.00
HFLEX	+30	3.0	4.02	4.59	6.59	6.84	6.73	6.65	4.76	0.00
HFLEX	+30	4.5	6.96	3.20	2.11	4.10	8.85	7.97	3.82	0.00
HFLEX	0	1.5	6.84	7.03	5.48	11.74	13.62	10.79	5.68	0.32
HFLEX	0	3.0	3.56	4.69	6.80	5.61	17.67	4.73	6.05	0.00
HFLEX	0	4.5	10.20	4.63	23.44	1.40	9.89	3.35	5.50	0.00
HFLEX	-30	1.5	12.40	10.02	9.09	5.84	14.59	2.96	5.89	0.00
HFLEX	-30	3.0	3.04	9.82	5.36	3.85	4.31	16.29	3.11	0.88
HFLEX	-30	4.5	4.03	12.53	17.23	2.93	6.24	11.52	5.72	0.16
HFLEX	-60	1.5	0.00	3.07	0.41	5.24	12.59	0.05	0.00	0.00
HFLEX	-60	3.0	1.22	3.05	3.90	3.30	7.49	6.75	1.94	0.00
HFLEX	-60	4.5	0.00	0.00	3.80	0.00	3.46	0.85	0.00	0.00
HEXTN	+60	1.5	-11.19	-28.45	-6.48	-12.80	-11.28	-14.89	-11.81	-13.13

HEXTN	+60	3.0	-21.94	-12.91	-13.48	-15.95	-39.15	-12.79	-19.48	-8.24
HEXTN	+60	4.5	-25.52	-12.92	-18.22	-17.49	-33.65	-19.18	-17.44	-5.48
HEXTN	+30	1.5	-15.08	-9.12	-5.46	-12.64	-3.76	-16.55	-15.17	-8.54
HEXTN	+30	3.0	-7.32	-11.28	-9.65	-19.06	-20.88	-13.47	-16.21	-10.18
HEXTN	+30	4.5	-30.96	-16.44	-22.15	-36.95	-48.66	-13.81	-33.35	-10.20
HEXTN	0	1.5	-9.15	-5.43	-7.39	-10.09	-10.64	-13.04	-15.44	-8.60
HEXTN	0	3.0	-11.58	-9.38	-10.22	-17.00	-19.88	-12.06	-9.61	-11.02
HEXTN	0	4.5	-22.31	-17.36	-9.37	-39.58	-34.74	-18.07	-27.92	-12.80
HEXTN	-30	1.5	-7.96	-26.18	-7.83	-13.04	-10.87	-18.18	-12.96	-7.00
HEXTN	-30	3.0	-12.82	-33.94	-5.48	-12.82	-18.51	-11.85	-9.60	-7.27
HEXTN	-30	4.5	-12.17	-10.82	-4.24	-42.48	-38.12	-13.33	-14.88	-10.56
HEXTN	-60	1.5	-10.19	-8.24	-9.73	-10.47	-7.46	-11.99	-16.35	-11.27
HEXTN	-60	3.0	-10.42	-7.58	-6.48	-16.66	-14.64	-14.82	-12.59	-10.36
HEXTN	-60	4.5	-19.62	-12.16	-15.04	-13.52	-15.72	-19.32	-10.17	-7.14
HABD	+60	1.5	3.10	0.16	0.00	0.34	4.46	0.50	0.00	0.00
HABD	+60	3.0	2.24	3.06	0.00	0.00	3.03	0.50	0.00	0.00
HABD	+60	4.5	2.88	0.58	0.00	0.00	1.66	0.74	0.00	0.00
HABD	+30	1.5	6.42	4.29	0.62	0.16	0.97	5.01	2.48	0.50
HABD	+30	3.0	4.02	4.59	0.35	0.00	0.00	0.00	0.00	0.00
HABD	+30	4.5	6.96	3.20	2.36	0.87	0.00	2.20	0.00	0.00
HABD	0	1.5	6.84	7.03	5.39	6.76	6.12	5.21	3.24	4.16
HABD	0	3.0	3.56	4.69	10.99	0.48	6.70	5.01	3.55	1.82
HABD	0	4.5	10.20	4.63	2.25	5.95	5.57	11.34	3.52	2.50
HABD	-30	1.5	12.40	10.02	16.52	13.74	21.29	12.98	9.95	12.66
HABD	-30	3.0	3.04	9.82	20.31	8.34	18.69	14.38	11.11	7.79
HABD	-30	4.5	4.03	12.53	29.18	4.16	19.24	22.34	11.58	10.43
HABD	-60	1.5	14.18	12.56	13.58	16.37	31.99	11.69	13.43	13.49
HABD	-60	3.0	15.11	16.18	24.79	6.07	38.03	25.90	8.65	18.75
HABD	-60	4.5	18.38	24.17	26.97	13.52	30.54	26.16	22.20	21.22
HADD	+60	1.5	-11.19	-14.07	-13.94	-11.45	-20.54	-11.49	-11.32	-12.53
HADD	+60	3.0	-21.94	-12.91	-16.51	-14.30	-13.42	-21.35	-13.42	-13.88
HADD	+60	4.5	-25.52	-12.92	-53.92	-47.42	-25.77	-32.02	-26.88	-25.17
HADD	+30	1.5	-15.08	-9.12	-10.06	-3.24	-8.89	-5.22	-5.94	-5.81
HADD	+30	3.0	-7.32	-11.28	-8.81	-24.35	-9.96	-20.48	-11.45	-9.78
HADD	+30	4.5	-30.96	-16.44	-13.13	-15.05	-37.41	-26.78	-15.08	-14.19
HADD	0	1.5	-9.15	-5.43	-3.58	-3.30	-4.93	-3.63	-2.60	-3.17
HADD	0	3.0	-11.58	-9.38	-2.39	-2.68	-1.98	-1.53	-4.73	-3.02
HADD	0	4.5	-22.31	-17.36	-4.92	-4.26	-0.60	-0.36	-5.51	-6.82
HADD	-30	1.5	-7.96	-26.18	-2.50	-1.01	-2.57	-4.86	-3.13	-3.80
HADD	-30	3.0	-12.82	-33.94	-0.58	-3.51	0.00	-3.48	-2.11	-3.33
HADD	-30	4.5	-12.17	-10.82	0.00	-8.05	-5.87	-1.21	0.00	-1.89
HADD	-60	1.5	0.00	-2.83	-1.05	0.00	0.00	-4.30	-2.31	-1.07
HADD	-60	3.0	0.00	-1.14	0.00	-2.23	0.00	-4.09	0.00	0.00
HADD	-60	4.5	0.00	0.00	-0.26	0.00	-2.35	0.00	0.00	0.00

APPENDIX D

Absolute maximum moments data

Ankle	DIR	SPEED	Subject							
			1	2	3	4	5	6	7	8
AINV	+60	1.5	-18.46	-0.10	-27.45	-32.82	-23.46	-61.50	-55.95	-22.65
AINV	+60	3.0	-23.33	-32.87	-35.30	-46.88	-10.51	-40.01	-73.15	-51.83
AINV	+60	4.5	-29.36	-51.66	-45.84	-40.50	-32.60	-60.02	-92.23	-34.49
AINV	+30	1.5	-37.43	-25.92	-32.80	-41.34	-21.61	-33.68	-61.38	-34.70
AINV	+30	3.0	-83.86	-41.64	-52.70	-62.14	-10.37	-60.40	-83.93	-56.27
AINV	+30	4.5	-56.17	-53.08	-20.50	-40.56	-19.09	-59.57	-84.06	-44.13
AINV	0	1.5	-24.88	-43.48	-34.08	-35.05	-25.86	-30.16	-55.18	-42.35
AINV	0	3.0	-67.99	-60.21	-72.19	-71.77	-60.99	-63.88	-118.58	-69.74
AINV	0	4.5	-103.43	-45.30	-95.96	-68.06	-65.48	-57.57	-109.50	-82.99
AINV	-30	1.5	-33.09	-37.57	-33.12	-37.22	-28.84	-47.04	-58.52	-44.66
AINV	-30	3.0	-91.45	-49.88	-75.69	-111.59	-87.72	-70.21	-138.08	-79.41
AINV	-30	4.5	-113.69	-68.10	-109.11	-125.12	-140.21	-87.85	-140.52	-110.54
AINV	-60	1.5	-33.93	-52.45	-40.83	-50.16	-24.63	-47.29	-64.95	-54.83
AINV	-60	3.0	-83.15	-89.40	-74.96	-88.03	-79.48	-112.56	-118.85	-135.40
AINV	-60	4.5	-100.16	-111.99	-150.93	-82.11	-95.97	-95.88	-125.08	-127.44
AEVE	+60	1.5	14.05	54.66	8.21	2.85	3.41	11.71	0.00	32.32
AEVE	+60	3.0	31.53	21.03	12.66	2.23	12.39	0.00	0.00	13.16
AEVE	+60	4.5	31.09	36.57	8.36	1.30	36.46	0.00	0.00	22.01
AEVE	+30	1.5	0.00	26.51	0.00	8.67	4.87	6.84	0.00	11.78
AEVE	+30	3.0	0.00	6.57	1.10	0.00	20.45	0.30	1.85	0.84
AEVE	+30	4.5	5.65	37.55	16.85	9.94	27.66	1.58	0.00	1.23
AEVE	0	1.5	0.00	2.08	0.00	0.00	0.00	0.00	0.00	0.00
AEVE	0	3.0	0.00	0.00	1.01	0.96	1.45	0.19	2.34	0.00
AEVE	0	4.5	1.17	2.40	1.82	0.00	0.00	0.97	0.00	0.00
AEVE	-30	1.5	1.61	0.00	0.00	0.00	0.00	0.00	0.00	0.00
AEVE	-30	3.0	0.94	0.20	1.49	0.22	0.00	1.01	0.00	0.00
AEVE	-30	4.5	0.47	0.00	2.01	0.00	0.73	0.44	2.54	1.24
AEVE	-60	1.5	0.00	0.00	0.00	0.00	0.00	0.00	0.00	0.00
AEVE	-60	3.0	0.00	0.17	0.28	0.00	1.09	0.89	0.00	0.65
AEVE	-60	4.5	0.00	0.00	3.46	0.00	1.94	1.11	0.05	0.00
AFLEX	+60	1.5	-14.39	0.00	-29.27	-2.85	-24.74	-2.91	-30.29	-9.96
AFLEX	+60	3.0	-13.63	-6.12	-34.86	-4.43	-5.10	-30.64	-12.18	-41.90
AFLEX	+60	4.5	-18.13	-25.49	-104.71	-39.01	-23.75	-45.96	-20.13	-23.67
AFLEX	+30	1.5	-8.29	-6.93	-31.88	-19.44	-36.91	-8.04	-31.70	-24.92
AFLEX	+30	3.0	-10.69	-20.57	-29.75	-16.04	-0.48	-14.58	-20.13	-39.73
AFLEX	+30	4.5	-1.34	-32.32	-37.29	-5.26	-22.27	-33.17	-7.11	-25.91
AFLEX	0	1.5	-11.27	-20.44	-20.28	-10.26	-25.26	-17.43	-20.29	-27.03
AFLEX	0	3.0	-12.36	-3.50	-21.48	-5.08	-4.98	-4.30	-19.27	-23.00
AFLEX	0	4.5	-13.21	-20.97	-37.04	-7.25	-1.30	-8.84	-19.76	-80.58
AFLEX	-30	1.5	-16.22	0.00	-16.79	-1.65	-19.31	-1.79	-27.27	-20.03
AFLEX	-30	3.0	-10.97	0.00	-24.90	-6.13	-20.41	-35.33	-27.47	-37.13

AFLEX	-30	4.5	-10.26	-21.19	-64.35	-1.95	-6.90	0.00	-29.74	-3.62
AFLEX	-60	1.5	-13.93	-21.70	-8.01	-23.39	-28.91	-17.92	-12.72	-22.58
AFLEX	-60	3.0	-12.74	-9.41	-25.44	-4.21	-10.06	-20.45	-16.85	-20.61
AFLEX	-60	4.5	-9.23	-5.66	-21.95	-7.71	-11.62	0.00	-17.67	-37.39
AEXTN	+60	1.5	73.58	138.33	57.32	69.48	69.37	90.78	68.07	91.00
AEXTN	+60	3.0	128.23	95.87	67.06	80.13	68.89	90.50	92.57	87.12
AEXTN	+60	4.5	135.86	77.76	71.94	81.00	81.99	135.75	104.97	85.79
AEXTN	+30	1.5	86.56	73.30	50.37	46.14	58.74	88.44	69.91	80.98
AEXTN	+30	3.0	79.48	91.84	79.24	93.60	90.05	101.44	83.40	76.02
AEXTN	+30	4.5	147.07	61.56	88.86	92.46	141.32	135.16	111.68	101.52
AEXTN	0	1.5	71.13	71.53	50.66	38.56	60.85	65.00	71.59	73.09
AEXTN	0	3.0	97.58	90.17	83.17	103.08	94.75	124.15	81.78	92.08
AEXTN	0	4.5	133.93	70.29	61.75	111.65	109.50	111.95	109.70	87.17
AEXTN	-30	1.5	63.32	166.48	50.58	44.92	48.34	65.63	59.65	73.15
AEXTN	-30	3.0	96.73	223.33	65.61	96.73	91.74	77.87	79.23	81.47
AEXTN	-30	4.5	90.60	84.58	69.57	129.89	97.58	65.97	63.37	91.38
AEXTN	-60	1.5	60.69	74.44	47.40	39.49	42.01	59.00	63.60	56.51
AEXTN	-60	3.0	62.39	99.27	55.50	87.25	58.29	97.24	69.53	67.49
AEXTN	-60	4.5	32.02	111.66	53.20	81.68	53.29	110.19	35.80	58.70
AABD	+60	1.5	25.05	80.83	16.07	48.74	25.72	39.06	35.97	38.70
AABD	+60	3.0	54.30	62.47	19.08	44.87	28.04	17.00	39.33	23.98
AABD	+60	4.5	63.66	57.24	21.76	54.00	53.75	25.50	53.69	33.51
AABD	+30	1.5	19.35	44.97	6.10	35.17	15.37	33.49	28.18	22.05
AABD	+30	3.0	3.42	52.92	6.10	44.49	28.73	19.73	23.42	10.07
AABD	+30	4.5	48.67	57.04	30.00	65.86	48.68	47.54	52.21	28.96
AABD	0	1.5	7.25	25.10	1.23	11.48	11.60	10.74	17.57	3.15
AABD	0	3.0	15.44	28.95	1.79	15.79	3.79	12.47	7.81	0.00
AABD	0	4.5	15.99	27.41	1.32	14.92	10.74	7.22	9.38	0.00
AABD	-30	1.5	5.05	40.14	0.57	12.49	3.84	34.50	5.45	0.00
AABD	-30	3.0	9.61	41.67	3.04	0.90	0.00	0.89	0.00	0.00
AABD	-30	4.5	15.48	0.26	11.47	15.54	23.26	3.57	1.11	8.34
AABD	-60	1.5	5.19	8.26	0.44	4.71	8.43	3.89	0.98	0.00
AABD	-60	3.0	4.83	2.58	5.22	10.56	0.47	9.18	0.41	0.28
AABD	-60	4.5	6.77	0.00	21.44	0.03	1.97	1.77	0.93	0.47
AADD	+60	1.5	-1.81	0.00	-13.80	-7.93	-9.25	-23.27	-30.94	-6.10
AADD	+60	3.0	-2.06	-11.61	-15.76	-3.93	-0.81	-22.73	-22.10	-20.87
AADD	+60	4.5	-8.90	-43.76	-62.64	-36.41	-53.55	-34.09	-61.08	-12.99
AADD	+30	1.5	-0.11	-8.03	-11.85	-26.01	-13.26	-13.48	-25.11	-10.55
AADD	+30	3.0	-30.57	-19.17	-12.58	-12.32	-0.67	-11.08	-24.02	-21.13
AADD	+30	4.5	0.00	-45.17	-15.16	-1.76	-15.14	-24.18	-15.28	-13.18
AADD	0	1.5	0.00	-18.94	-7.07	-15.17	-7.90	-9.26	-17.70	-11.36
AADD	0	3.0	-10.37	-7.26	-17.17	-6.16	-1.82	-0.25	-28.69	-23.56
AADD	0	4.5	-12.03	-22.91	-59.62	-1.86	0.00	-2.55	-15.11	-30.19
AADD	-30	1.5	-6.84	0.00	-10.06	-12.76	-9.01	-1.92	-17.82	-19.77
AADD	-30	3.0	-32.67	-0.07	-31.13	-24.62	-16.54	-26.78	-40.70	-52.09
AADD	-30	4.5	-45.63	-32.45	-57.73	-4.58	-10.35	-35.26	-66.51	-69.74
AADD	-60	1.5	-4.91	-16.47	-6.06	-30.12	-11.69	-25.77	-24.58	-26.45
AADD	-60	3.0	-31.72	-14.25	-32.23	-25.64	-32.98	-37.54	-47.13	-82.07
AADD	-60	4.5	-33.47	-26.85	-90.56	-46.63	-45.66	-31.08	-61.03	-90.46

Knee	DIR	SPEED	Subject							
			1	2	3	4	5	6	7	8
KINTR	+60	1.5	6.70	13.08	18.87	24.77	25.93	37.98	52.79	56.09
KINTR	+60	3.0	5.85	30.92	16.07	9.17	16.01	21.59	15.96	12.13
KINTR	+60	4.5	6.06	23.81	25.45	9.60	0.81	20.39	29.18	20.12
KINTR	+30	1.5	46.22	42.98	50.81	19.57	41.02	30.58	65.34	12.78
KINTR	+30	3.0	5.30	21.87	31.91	29.01	13.90	16.21	13.52	13.43
KINTR	+30	4.5	6.49	21.23	36.54	9.97	4.39	42.59	31.37	19.16
KINTR	0	1.5	11.46	49.55	8.62	13.28	14.73	23.80	27.88	11.74
KINTR	0	3.0	1.61	20.43	8.74	11.70	9.84	7.20	10.26	11.25
KINTR	0	4.5	13.36	19.30	15.16	7.80	1.66	1.14	47.96	7.55
KINTR	-30	1.5	22.89	20.03	50.75	21.80	0.57	0.00	34.99	18.58
KINTR	-30	3.0	4.00	49.60	10.56	10.11	7.19	9.14	11.11	11.66
KINTR	-30	4.5	5.52	64.40	13.60	12.45	22.77	26.72	42.28	25.85
KINTR	-60	1.5	2.44	42.98	25.95	6.90	2.72	17.30	52.11	14.05
KINTR	-60	3.0	4.36	21.62	9.50	28.36	12.19	10.07	7.67	16.10
KINTR	-60	4.5	3.32	20.75	11.13	20.59	27.31	17.41	40.08	24.58
KEXTR	+60	1.5	7.32	35.42	24.71	12.20	40.27	14.94	39.94	31.11
KEXTR	+60	3.0	-9.34	-48.55	-1.98	-23.10	-26.36	-15.10	-3.34	-25.73
KEXTR	+60	4.5	-4.11	-5.99	-3.58	-40.59	-72.19	-8.48	-2.90	-8.58
KEXTR	+30	1.5	-6.15	-6.67	-4.34	-46.82	-109.19	-12.72	-3.47	-19.42
KEXTR	+30	3.0	-8.24	-13.51	-0.97	-33.56	-30.62	-12.22	-8.72	-13.60
KEXTR	+30	4.5	-4.66	-0.62	-0.53	-44.09	-33.80	-5.95	-2.07	-3.46
KEXTR	0	1.5	-4.92	-3.14	-15.53	-60.69	-74.59	-4.24	0.00	-16.34
KEXTR	0	3.0	-11.49	-5.71	-0.94	-29.91	-19.09	-4.58	-6.69	-7.82
KEXTR	0	4.5	-7.69	-0.23	-2.04	-41.03	-21.63	-10.83	-1.24	0.00
KEXTR	-30	1.5	-2.21	-1.10	-1.13	-55.98	-36.70	-18.25	0.00	0.00
KEXTR	-30	3.0	-28.89	-26.98	-19.73	-17.75	-15.33	-9.29	-6.08	-6.89
KEXTR	-30	4.5	-5.68	-5.20	-9.45	-4.68	-15.87	-1.01	0.00	0.00
KEXTR	-60	1.5	-12.62	0.00	-4.09	-23.81	-37.70	-2.26	-0.83	-6.59
KEXTR	-60	3.0	-12.56	-8.06	-11.19	-5.84	-35.99	-10.89	-9.00	-11.01
KEXTR	-60	4.5	-10.27	-10.00	-21.07	-0.71	-24.61	-1.58	-1.81	0.00
KFLEX	+60	1.5	-19.34	-2.39	0.00	-3.03	-4.43	-5.76	0.00	0.00
KFLEX	+60	3.0	5.16	5.55	4.31	44.77	55.16	84.26	30.54	0.21
KFLEX	+60	4.5	8.69	0.03	2.22	1.15	0.00	18.26	12.82	40.10
KFLEX	+30	1.5	0.00	5.19	5.03	5.08	0.00	27.40	5.84	22.79
KFLEX	+30	3.0	16.83	0.00	1.76	13.93	16.96	58.24	24.94	32.15
KFLEX	+30	4.5	0.00	0.00	0.00	9.23	0.00	24.90	5.54	31.27
KFLEX	0	1.5	27.24	0.00	8.87	28.61	0.00	9.12	8.52	32.88
KFLEX	0	3.0	1.60	0.00	3.30	8.96	18.45	24.56	23.10	39.30
KFLEX	0	4.5	0.45	0.00	0.00	0.00	0.88	23.42	0.00	14.19
KFLEX	-30	1.5	13.00	0.00	6.92	3.41	6.97	0.93	7.59	20.50
KFLEX	-30	3.0	0.00	0.00	2.70	21.20	24.55	41.80	14.28	14.42
KFLEX	-30	4.5	0.00	0.00	1.07	5.60	0.00	7.91	0.00	0.33
KFLEX	-60	1.5	4.76	0.00	1.13	77.72	4.82	18.32	0.00	49.78
KFLEX	-60	3.0	29.40	0.00	25.30	27.06	20.41	35.48	34.44	23.81
KFLEX	-60	4.5	0.00	0.00	0.00	0.31	0.00	16.78	2.79	16.08
KEXTN	+60	1.5	2.50	14.98	11.13	8.02	4.93	51.31	2.97	15.21

KEXTN	+60	3.0	-96.17	-29.66	-125.24	-12.69	-18.08	-39.16	-75.13	-54.83
KEXTN	+60	4.5	-169.68	-194.54	-175.33	-123.85	-80.92	-200.62	-165.79	-123.67
KEXTN	+30	1.5	-266.27	-318.79	-205.92	-199.40	-212.89	-300.93	-293.24	-111.40
KEXTN	+30	3.0	-83.14	-166.74	-128.76	-59.51	-66.62	-10.26	-59.32	-5.61
KEXTN	+30	4.5	-151.12	-199.74	-173.66	-101.96	-79.78	-145.19	-182.53	-117.15
KEXTN	0	1.5	-134.62	-328.61	-209.22	-70.66	-106.77	-228.80	-150.60	-118.66
KEXTN	0	3.0	-78.83	-176.77	-81.12	-44.71	-40.56	-30.16	-15.69	-3.37
KEXTN	0	4.5	-137.75	-214.63	-144.01	-83.32	-71.26	-36.34	-181.93	-103.15
KEXTN	-30	1.5	-192.45	-279.75	-174.32	-53.13	-60.32	-153.75	-132.80	-149.66
KEXTN	-30	3.0	-75.50	-23.29	-72.09	-14.97	-28.97	-1.14	-37.96	-31.22
KEXTN	-30	4.5	-166.69	-38.56	-145.21	-75.58	-99.06	-158.97	-139.69	-123.60
KEXTN	-60	1.5	-186.91	-326.88	-249.74	0.00	-74.03	-164.45	-198.81	-32.13
KEXTN	-60	3.0	-43.13	-167.28	-31.28	-63.87	-45.33	-46.06	-6.69	-18.35
KEXTN	-60	4.5	-153.30	-231.32	-138.89	-111.13	-97.66	-133.64	-129.97	-67.96
KABD	+60	1.5	-66.88	-222.87	-115.77	-92.15	-154.81	-130.48	-166.88	-78.31
KABD	+60	3.0	28.60	49.39	0.35	75.36	18.27	71.57	18.83	57.14
KABD	+60	4.5	4.04	15.80	1.64	0.00	0.00	0.00	19.98	68.80
KABD	+30	1.5	0.00	5.80	0.00	0.00	0.00	0.00	0.00	9.18
KABD	+30	3.0	27.44	12.42	14.43	8.26	6.92	52.99	16.72	50.02
KABD	+30	4.5	52.55	19.23	17.61	23.20	19.43	5.82	9.99	81.05
KABD	0	1.5	11.06	0.00	22.89	6.83	5.72	3.99	19.43	89.00
KABD	0	3.0	20.97	14.03	24.71	17.39	25.86	26.48	7.99	39.02
KABD	0	4.5	34.07	17.76	24.84	22.64	36.35	44.13	0.49	64.20
KABD	-30	1.5	5.63	11.51	12.51	2.96	56.29	62.63	1.23	83.64
KABD	-30	3.0	58.79	27.23	40.79	33.37	25.15	17.83	14.68	23.72
KABD	-30	4.5	44.13	6.84	54.59	32.77	41.10	15.57	5.43	46.88
KABD	-60	1.5	87.77	40.62	113.62	75.24	101.05	51.89	24.18	69.55
KABD	-60	3.0	25.51	46.07	59.20	37.77	52.95	9.78	14.48	27.34
KABD	-60	4.5	86.14	105.62	135.14	102.67	83.00	68.25	12.63	69.71
KADD	+60	1.5	81.83	33.17	86.47	61.71	46.23	81.92	92.15	76.61
KADD	+60	3.0	-15.86	-40.33	-35.56	-5.39	-6.57	-4.56	-13.25	-2.31
KADD	+60	4.5	-27.10	-47.43	-40.23	-34.85	-29.18	-53.18	-29.41	-19.28
KADD	+30	1.5	-124.85	-91.80	-137.60	-97.73	-81.85	-79.77	-105.39	-36.83
KADD	+30	3.0	-8.45	-26.39	-39.78	-17.13	-14.35	-3.80	-9.65	-5.08
KADD	+30	4.5	-2.53	-41.77	-27.26	-10.77	-9.02	-38.28	-27.11	0.00
KADD	0	1.5	-18.03	-96.00	-32.01	-37.62	-31.51	-68.82	-31.22	-4.59
KADD	0	3.0	-6.88	-20.83	-9.15	-8.87	0.00	-1.16	-7.39	-6.20
KADD	0	4.5	-7.84	-11.58	-1.86	-4.75	-4.93	-2.47	-24.47	-2.31
KADD	-30	1.5	-19.07	-13.90	-18.17	-9.35	0.00	-2.30	-29.89	-0.89
KADD	-30	3.0	-0.47	-51.64	-10.33	-17.14	-7.12	-13.95	-7.82	-5.89
KADD	-30	4.5	-0.74	-68.59	-0.86	-18.50	-5.03	-12.03	-15.56	-13.20
KADD	-60	1.5	0.00	-26.62	0.00	0.00	0.00	-9.54	-10.53	-4.18
KADD	-60	3.0	0.00	-23.39	0.00	-4.51	-6.69	-17.54	-15.08	-1.96
KADD	-60	4.5	0.00	-2.62	0.00	0.00	-1.74	-1.71	-25.75	-6.29

Hip	DIR	SPEED	Subject							
			1	2	3	4	5	6	7	8
HINTR	+60	1.5	20.76	52.86	12.61	21.05	21.45	26.30	9.90	7.83
HINTR	+60	3.0	15.02	19.98	0.00	10.37	8.45	1.87	0.00	0.00
HINTR	+60	4.5	19.27	3.82	0.00	0.00	9.23	2.80	0.00	0.00
HINTR	+30	1.5	43.01	28.09	39.68	25.17	1.52	35.33	16.67	8.28
HINTR	+30	3.0	26.91	29.99	2.11	1.46	0.00	6.14	3.36	4.60
HINTR	+30	4.5	46.68	20.93	12.83	17.25	0.00	9.94	9.10	1.07
HINTR	0	1.5	45.88	45.97	17.07	6.52	11.39	10.40	13.37	8.64
HINTR	0	3.0	23.89	30.65	38.49	4.52	3.47	5.25	24.58	6.36
HINTR	0	4.5	68.37	30.27	31.57	40.07	0.00	13.57	20.46	16.01
HINTR	-30	1.5	83.10	65.57	24.27	24.81	8.21	12.89	13.55	9.89
HINTR	-30	3.0	20.40	64.24	62.91	25.27	21.96	34.82	48.14	19.01
HINTR	-30	4.5	26.99	81.96	75.55	35.98	27.77	38.09	50.07	32.39
HINTR	-60	1.5	0.00	20.05	49.93	39.55	15.82	23.27	10.23	2.58
HINTR	-60	3.0	8.19	19.95	75.90	27.00	54.53	88.06	42.23	30.90
HINTR	-60	4.5	0.00	0.00	104.08	67.65	99.24	82.78	98.71	47.87
HEXTR	+60	1.5	-75.01	-186.13	-35.63	-4.03	-3.44	-25.70	-13.67	-35.38
HEXTR	+60	3.0	-147.07	-84.45	-78.75	-35.89	-30.53	-97.43	-67.46	-61.88
HEXTR	+60	4.5	-171.05	-84.52	-265.63	-197.30	-92.11	-146.15	-167.49	-129.36
HEXTR	+30	1.5	-101.08	-59.66	-28.08	-20.56	-16.16	-9.31	-17.47	-20.75
HEXTR	+30	3.0	-49.07	-73.76	-34.65	-57.90	-21.87	-50.08	-56.22	-41.02
HEXTR	+30	4.5	-207.53	-107.51	-62.70	-25.33	-76.89	-116.61	-70.58	-57.70
HEXTR	0	1.5	-61.36	-35.49	-11.73	-42.89	-21.11	-14.71	-10.71	-16.14
HEXTR	0	3.0	-77.62	-61.33	-11.29	-13.00	-14.99	-5.95	-13.08	-18.50
HEXTR	0	4.5	-149.55	-113.58	-2.96	-0.99	-7.80	-5.91	-28.00	-33.66
HEXTR	-30	1.5	-53.34	-171.23	-24.86	-39.43	-42.91	-25.05	-13.12	-23.46
HEXTR	-30	3.0	-85.94	-221.99	-1.74	-5.67	-2.46	-4.43	0.00	-22.34
HEXTR	-30	4.5	-81.60	-70.78	0.00	0.00	0.00	-1.67	0.00	-9.89
HEXTR	-60	1.5	-68.31	-53.92	-0.19	-22.15	-48.96	-19.47	-12.77	-21.74
HEXTR	-60	3.0	-69.86	-49.56	0.00	-0.22	0.00	-12.47	0.00	-11.51
HEXTR	-60	4.5	-131.53	-79.54	0.00	0.00	-2.41	0.00	0.00	-15.97
HFLEX	+60	1.5	20.76	52.86	20.34	5.51	4.63	2.82	8.27	0.00
HFLEX	+60	3.0	15.02	19.98	9.37	22.95	55.51	26.68	13.01	0.00
HFLEX	+60	4.5	19.27	3.82	8.53	16.80	24.97	40.03	6.67	0.00
HFLEX	+30	1.5	43.01	28.09	70.34	28.52	76.93	23.74	25.64	0.00
HFLEX	+30	3.0	26.91	29.99	41.44	42.36	34.89	42.08	35.86	0.00
HFLEX	+30	4.5	46.68	20.93	13.27	25.36	45.90	50.46	28.78	0.00
HFLEX	0	1.5	45.88	45.97	34.46	72.72	70.64	68.29	42.83	2.21
HFLEX	0	3.0	23.89	30.65	42.76	34.74	91.64	29.94	45.62	0.00
HFLEX	0	4.5	68.37	30.27	147.41	8.67	51.31	21.23	41.48	0.00
HFLEX	-30	1.5	83.10	65.57	57.16	36.14	75.67	18.72	44.39	0.00
HFLEX	-30	3.0	20.40	64.24	33.73	23.81	22.35	103.13	23.43	6.15
HFLEX	-30	4.5	26.99	81.96	108.35	18.11	32.34	72.93	43.11	1.12
HFLEX	-60	1.5	0.00	20.05	2.58	32.43	65.29	0.28	0.00	0.00
HFLEX	-60	3.0	8.19	19.95	24.49	20.40	38.82	42.73	14.59	0.00
HFLEX	-60	4.5	0.00	0.00	23.90	0.00	17.92	5.35	0.00	0.00
HEXTN	+60	1.5	-75.01	-186.13	-40.75	-79.27	-58.50	-94.27	-89.04	-92.05

HEXTN	+60	3.0	-147.07	-84.45	-84.77	-98.80	-203.04	-80.94	-146.90	-57.79
HEXTN	+60	4.5	-171.05	-84.52	-114.55	-108.30	-174.51	-121.41	-131.48	-38.40
HEXTN	+30	1.5	-101.08	-59.66	-34.34	-78.24	-19.52	-104.77	-114.40	-59.87
HEXTN	+30	3.0	-49.07	-73.76	-60.69	-118.00	-108.29	-85.30	-122.24	-71.35
HEXTN	+30	4.5	-207.53	-107.51	-139.29	-228.79	-252.34	-87.43	-251.52	-71.51
HEXTN	0	1.5	-61.36	-35.49	-46.47	-62.48	-55.16	-82.55	-116.46	-60.29
HEXTN	0	3.0	-77.62	-61.33	-64.27	-105.27	-103.10	-76.35	-72.47	-77.26
HEXTN	0	4.5	-149.55	-113.58	-58.92	-245.10	-180.18	-114.40	-210.57	-89.74
HEXTN	-30	1.5	-53.34	-171.23	-49.22	-80.73	-56.39	-115.12	-97.76	-49.05
HEXTN	-30	3.0	-85.94	-221.99	-34.46	-79.36	-95.97	-75.02	-72.42	-50.97
HEXTN	-30	4.5	-81.60	-70.78	-26.64	-263.03	-197.70	-84.41	-112.19	-74.06
HEXTN	-60	1.5	-68.31	-53.92	-61.17	-64.84	-38.69	-75.87	-123.32	-79.01
HEXTN	-60	3.0	-69.86	-49.56	-40.72	-103.17	-75.90	-93.82	-94.94	-72.63
HEXTN	-60	4.5	-131.53	-79.54	-94.58	-83.72	-81.50	-122.31	-76.69	-50.06
HABD	+60	1.5	20.76	1.07	0.00	2.11	23.11	3.17	0.00	0.00
HABD	+60	3.0	15.02	19.98	0.00	0.00	15.71	3.13	0.00	0.00
HABD	+60	4.5	19.27	3.82	0.00	0.00	8.58	4.70	0.00	0.00
HABD	+30	1.5	43.01	28.09	3.87	0.99	5.01	31.72	18.73	3.50
HABD	+30	3.0	26.91	29.99	2.20	0.00	0.00	0.00	0.00	0.00
HABD	+30	4.5	46.68	20.93	14.84	5.39	0.00	13.93	0.00	0.00
HABD	0	1.5	45.88	45.97	33.90	41.84	31.76	32.98	24.46	29.16
HABD	0	3.0	23.89	30.65	69.11	2.97	34.75	31.72	26.73	12.74
HABD	0	4.5	68.37	30.27	14.15	36.85	28.90	71.79	26.57	17.50
HABD	-30	1.5	83.10	65.57	103.89	85.09	110.40	82.17	75.03	88.77
HABD	-30	3.0	20.40	64.24	127.72	51.65	96.93	91.04	83.81	54.61
HABD	-30	4.5	26.99	81.96	183.50	25.73	99.78	141.45	87.30	73.14
HABD	-60	1.5	95.06	82.16	85.38	101.35	165.91	73.98	101.30	94.58
HABD	-60	3.0	101.27	105.84	155.90	37.59	197.20	163.97	65.19	131.46
HABD	-60	4.5	123.20	158.13	169.61	83.72	158.39	165.61	167.44	148.77
HADD	+60	1.5	-75.01	-92.05	-87.66	-70.91	-106.51	-72.74	-85.34	-87.84
HADD	+60	3.0	-147.07	-84.45	-103.80	-88.52	-69.62	-135.13	-101.16	-97.32
HADD	+60	4.5	-171.05	-84.52	-339.08	-293.65	-133.62	-202.70	-202.67	-176.44
HADD	+30	1.5	-101.08	-59.66	-63.26	-20.06	-46.09	-33.05	-44.79	-40.73
HADD	+30	3.0	-49.07	-73.76	-55.40	-150.76	-51.67	-129.68	-86.35	-68.59
HADD	+30	4.5	-207.53	-107.51	-82.57	-93.17	-194.03	-169.54	-113.69	-99.48
HADD	0	1.5	-61.36	-35.49	-22.51	-20.44	-25.57	-22.98	-19.58	-22.23
HADD	0	3.0	-77.62	-61.33	-15.03	-16.57	-10.27	-9.69	-35.67	-21.17
HADD	0	4.5	-149.55	-113.58	-30.94	-26.38	-3.13	-2.30	-41.53	-47.79
HADD	-30	1.5	-53.34	-171.23	-15.72	-6.25	-13.33	-30.75	-23.58	-26.63
HADD	-30	3.0	-85.94	-221.99	-3.63	-21.74	0.00	-22.03	-15.89	-23.31
HADD	-30	4.5	-81.60	-70.78	0.00	-49.85	-30.42	-7.66	0.00	-13.26
HADD	-60	1.5	0.00	-18.50	-6.58	0.00	0.00	-27.19	-17.42	-7.47
HADD	-60	3.0	0.00	-7.42	0.00	-13.78	0.00	-25.89	0.00	0.00
HADD	-60	4.5	0.00	0.00	-1.64	0.00	-12.16	0.00	0.00	0.00